Swirl String Theory (SST) Canon v0.6.0: Core Axioms, Postulates, Constants, Master Equations, and Lagrangian Framework

Omar Iskandarani
Independent Researcher, Groningen, The Netherlands[*]
(Dated: December 25, 2025)

This Canon is the single source of truth for *Swirl String Theory (SST)*: definitions, constants, boxed master equations, and notational conventions. It unifies the core hydrodynamic, electromagnetic, and gauge principles of the theory. **This version canonizes the following principles:**

- **I** The foundational hydrodynamic laws, including the Chronos–Kelvin Invariant and Swirl Coulomb constant Λ
- **II** The Swirl–Electromagnetic Bridge, linking swirl dynamics directly to Maxwell's equations.
- **III** The emergence of the $\mathrm{SU}(3) \times \mathrm{SU}(2) \times \mathrm{U}(1)$ gauge sector and a first-principles derivation of the weak mixing angle θ_W.
- **IV** A parameter-free prediction for the Electroweak Symmetry Breaking (EWSB) scale.
- **V** A formal dynamical rule for quantum measurement via R↔T phase transitions.

Core Axioms (SST)

1. **Swirl Medium:** Physics is formulated on $\mathbb{R}^3$ with absolute reference time. Dynamics occur in a frictionless, incompressible *swirl condensate*, which serves as a universal substrate.
2. **Swirl Strings (Circulation and Topology):** Particles and field quanta correspond to closed vortex filaments (*swirl strings*). The circulation of the swirl velocity around any closed loop is quantized:
   $$\Gamma = \oint \mathbf{v}_{\mathcal{O}} \cdot d\boldsymbol{\ell} = n\,\Gamma_0, \qquad n \in \mathbb{Z}, \qquad \Gamma_0 = 2\pi r_c \|\mathbf{v}_{\mathcal{O}}\|.$$
   Discrete quantum numbers (mass, charge, spin) track to the topological invariants of the swirl string.
3. **String-induced gravitation:** Macroscopic attraction emerges from coherent swirl flows and swirl-pressure gradients. The effective gravitational coupling G_{swirl} is fixed by canonical constants.
4. **Swirl Clocks:** Local proper-time rate depends on tangential swirl speed v, ticking slower by the factor $S_t = \sqrt{1 - v^2/c^2}$ relative to an observer at rest in the medium.
5. **Dual Phases (Wave–Particle):** Each swirl string has two limiting phases: an extended *R-phase* (unknotted, wave-like) and a localized *T-phase* (knotted, particle-like). Measurement is a dynamical transition between these phases.
6. **Taxonomy:** Unknotted excitations correspond to bosonic modes, with photons realized as *pulsed torsional R-phase excitations* (rotational wave packets of the swirl director field). Torus knots correspond to leptons (e.g. electron $= 3_1$), and chiral hyperbolic knots to quarks (proton $= 5_2 + 5_2 + 6_1$ composite). Linked knots describe nuclei and bound states.

Preface: Reader Pathways

This document formalizes SST in a self-contained manner, but it is structured to accommodate different levels of reader expertise.

Beginner-level readers are encouraged to focus on the physical descriptions and boxed highlights in the main text, skipping the more technical derivations (which are relegated to the appendices and side notes).

Expert readers can delve into the detailed derivations and dimensional analyses in the appendices to verify consistency and connect SST formulas to classical limits.

Active researchers should consult the formal axiomatic system section and appendices for the rigorous foundation, as well as the traceability tables and glossary that link each canonical statement to established physics or experimental context. Throughout the text, important equations, axioms, and theorems are presented in numbered, boxed form for quick reference. Pedagogical sidebars can be expanded in future versions to provide intuitive explanations, historical notes, or illustrative diagrams without interrupting the flow of the formal development.

[*] ORCID: 0009-0006-1686-3961, DOI: 10.5281/zenodo.17899592

SST Canon v0.5.12 Glossary

TABLE I. Primitive and Derived Canonical Constants (see Section XVI)

Symbol	Definition	Canonical Value / Relation
Γ_0	Primitive Circulation Quantum	6.4×10^3 m^{2}s^{-1} (Table V)
r_c	Swirl String Core Radius	$1.40897017 \times 10^{-15}$ m (Table V)
ρ_f	Effective Fluid Density	7.0×10^{-7} kg m^{-3} (Table V)
$\mathbf{v}_\circlearrowleft$	Canonical Swirl Speed ($\|\|v_\mathcal{G}\|\|$)	1.09384563×10^6 m s^{-1} (Table V)
ρ_m	Mass-Equivalent Density	$\rho_E/c^2 \approx 3.89 \times 10^{18}$ kg m^{-3} (Table V)
Λ	Swirl Coulomb Constant	$4\pi\rho_m \mathbf{v}_\circlearrowleft r_c^3$ (Eq. XXIV A)
G_{swirl}	Gravitational Coupling	$\frac{\mathbf{v}_\circlearrowleft c^5 t_p^2}{2F_{\max} r_c^2} \approx G_N$ (Eq. XXIV E)

TABLE II. Core Ontology and Hydrodynamic Mechanics (see Section VII)

Concept	Canonical Definition
Swirl Medium	Frictionless, incompressible swirl condensate on $\mathbb{R}^3$ with absolute time t (Axiom 1).
Swirl String	Closed vortex filament where circulation is quantized ($\Gamma = n\Gamma_0$) and particles are topological knots (Axiom 2).
Chronos-Kelvin Invariant	Conservation law generalizing Kelvin's theorem to include time dilation: $\frac{D}{Dt}(R^2\omega) = 0$ (Section XIV).
Swirl Clock (S_t)	Local proper-time rate factor dependent on tangential swirl speed: $S_t = \sqrt{1 - v^2/c^2}$ (Axiom 4).
Zero-Parameter Principle	Axiom stating all dimensional constants are determined by the triplet (Γ_0, ρ_f, r_c) and topology (Section XVI).
Swirl Pressure Law	Radial pressure gradient sustaining centripetal force: $\frac{dp_{swirl}}{dr} = \rho_f \frac{v_\theta^2}{r}$ (Eq. XXIV B).

TABLE III. Topological Phase and Particle Taxonomy (see Section XIX)

Entity	Topological Class	Physical Realization
R-Phase	Unknotted (0_1)	Radiative, wave-like, massless (Bosons) (Axiom 5).
T-Phase	Knotted	Tangible, particle-like, massive (Fermions) (Axiom 5).
Photon	Torsional Pulse	Rotating oscillation of the director field (helicity ± 1) (Axiom 6).
Electron (e^-)	Torus Knot (3_1)	Trefoil knot; simplest lepton (Axiom 6).
Up Quark (u)	Twist Knot (5_2)	Chiral hyperbolic knot (Axiom 6).
Down Quark (d)	Twist Knot (6_1)	Chiral hyperbolic knot (Axiom 6).
Proton	Composite Linkage	$5_2 + 5_2 + 6_1$ (uud) configuration (Axiom 6).

TABLE IV. Advanced Gauge, Logic, and Field Concepts (see Sections X, XII A)

Symbol	Term	Definition
ϕ	Golden Principle	Scaling factor $\phi \approx 1.618$ controlling mass/energy layers: $E_n = E_0\phi^{2n}$ (Eq. 1).
$\mathcal{K}$	Kairos Event	Topological bifurcation or phase jump in S_t (reconnection event) (Section XII A).
ϱ	Swirl Areal Density	Density of vortex cores per unit area; sources emergent EM fields via $\nabla \times \mathbf{E}$ (Definition XX).
θ_W	Weak Mixing Angle	Ratio of director stiffness constants for $U(1)$ and $SU(2)$ sectors (Theorem XXVI).
BASC	Bulk Signaling Channel	Engineered region allowing scalar bulk field $p(x,t)$ transduction (Section XXII).
ω	Vorticity Magnitude	Local vorticity $\|\|\nabla \times \mathbf{v}\|\|$; defines the wave proxy in duality relations (Section XXXVIII).

Part I
Fundamental Considerations for the Swirl–String Theory

I. INTRODUCTION

The theory presented herein, which we will refer to as Swirl–String Theory (SST), encompasses what is conventionally referred to as "æther theory" in contemporary discourse, but reformulates it explicitly as a hydrodynamic model of the vacuum. In this work, I aim to conceptualize the vacuum as a flowing, non-viscous, incompressible vacuum fluid (historically called "æther"), characterized by an effective fluid density ρ_f, a characteristic swirl speed $\mathbf{v}_{\circlearrowleft}$, and a core radius r_c, fundamentally founded on the five postulates of Euclid. Rather than postulating an undefined æther, we treat this vacuum fluid as a concrete continuum governed by the equations of incompressible fluid dynamics. My conviction in this conceptualization was inspired by an in-depth study of the original contributions of J. C. Maxwell, H. Helmholtz, W. Thomson, and A. Einstein.[20, 70–72]

In this model, atoms are envisioned as vortex currents in the vacuum fluid or other forms of vortex structures, as originally proposed by W. Thomson.[72] It is well established that Einstein's special theory of relativity complements Maxwell's dynamical theory of the electromagnetic field,[70] which provides a framework for simultaneous interactions between distant bodies in electromagnetic experiments. However, this model diverges from the traditional dynamical approach, opting instead for the theory of molecular vortices formulated by J. C. Maxwell. Here, we endeavor to reinterpret certain principles from the general theory of relativity and other facets of modern physics in terms of an incompressible vacuum fluid, while emphasizing a strictly non-relativistic (Galilean) framework where accelerations are considered the primary forces of nature, and vorticity is treated as a fundamental descriptor of the rotational motion of the vacuum fluid.

A vortex, within this context, is a mass of vacuum fluid in a state of rotational motion. In the case of an atom, this model posits a small vortex knot (a "swirl string") at the core, which embodies a central element with its own temporal evolution, characterized by vortex circulation. Furthermore, this model seeks to explain thermal phenomena by invoking the concept of the swelling of elastic spherical equilibrium conditions due to changes in vorticity, linking these effects to entropy variations, as articulated in the vortex atom framework of W. Thomson.[72]

The notion of relative time-space is addressed here through the concept of relative vorticity within the vacuum fluid, explicitly excluding relativistic effects in favor of purely vorticity-driven temporal differentiation, where the local clock rate (the Swirl Clock $S_t^{\circlearrowleft}$) is set by the swirl energy density. Part I of this work will present foundational considerations, articulated with the intention of minimizing the necessity for advanced mathematical understanding, thereby making the content accessible to a broader audience. Part II will delve into the mathematical formalism underpinning the model, which cannot be assumed to be known to every physicist. The ultimate objective is to establish the foundations for a comprehensive non-viscous vacuum-fluid theory (a hydrodynamic realization of the historical æther concept), capable of providing a visual and conceptual representation of inertia as an emergent property of vortex circulation within the vacuum fluid, particularly influenced by the proposed constants.

II. THE DEMAND FOR AN EXTENSION FOR THE PROPOSITIONS OF PHYSICS

Any rigorous consideration of a physical theory must differentiate between objective reality, which exists independently of any theoretical framework, and the physicist's statements that attempt to articulate that theory. These theoretical statements aim to correspond to objective reality, and it is through these approximations that we attempt to construct an intelligible representation of the universe. By recognising patterns in nature which are explained with philosophy and mathematics to predict an outcome we created different branches of physics that at first sight seem unrelated, but later get discovered to be fusible.

The contemporary scientific understanding of reality is shaped predominantly by the theory of relativity and modern physics. When we inquire whether the descriptions furnished by these theories are exhaustive, it is critical to recognize that such completeness is contingent upon a narrowly defined set of conditions—specifically, the behavior of clocks and measuring rods, as well as the statistical properties of electrons. Neither the general theory of relativity nor modern physics adequately captures the objective reality of a structured vacuum fluid, as both frameworks explicitly dismiss the concept of an underlying medium in favor of a purely relativistic interpretation. In contrast, the model presented here emphasizes a non-relativistic, vorticity-driven framework in an incompressible vacuum fluid (the swirl medium). The theory of relativity excels in providing a precise account of phenomena such as the rotation of clock hands and,

for practical purposes, may well remain unparalleled as a descriptive tool.

In special relativity, simultaneity is defined through the synchronized positions of multiple clocks and the reception of light signals exchanged between them.[20] We must revise this definition of simultaneity to align with a strictly non-relativistic vacuum-fluid model (historically associated with æther theories), taking into consideration that quantum entanglement implies the possibility of non-local transmission of mechanical information within the swirl medium, exceeding the conventional limits imposed by the speed of light.

The non-viscous liquid vacuum-fluid model posits that variations in temporal experience among atoms, as indicated by discrepancies in clock synchronization, are fundamentally determined by the vorticity and internal circulation of vortex knots. The characteristic swirl speed $\mathbf{v}_{\circlearrowleft}$ plays a pivotal role in this temporal differentiation. Within this model, the nucleus of an atom is conceptualized as a spherical equilibrium of pressure surrounding a rotating vortex knot. Specifically, for the hydrogen atom's nucleus, commonly referred to as the proton, this structure is represented by the simplest vortex knot: the three-fold "Trefoil knot." This knot is chosen as the most elementary and stable configuration for representing atomic nuclei.

The tangential velocity at the boundary of the vortex is conceived to be set by the canonical swirl speed $\mathbf{v}_{\circlearrowleft}$, symbolizing the lower limit, while the speed of light c symbolizes the upper limit for the velocity of vacuum-fluid elements within the vortex or for those particles intrinsically linked to the vortex itself.

Knot theory provides a critical mathematical framework for analyzing vortex knots in fluid systems, including the æther.[74] Research has established that helicity—a conserved quantity in ideal fluid dynamics—is analogous to quantum spin, linking macroscopic fluid phenomena with atomic-scale behavior.[45] Stable knotted structures, such as trefoil knots, exhibit robust energy distribution and stability, underscoring their fundamental role in matter's architecture.

These knotted configurations in the æther are inherently dynamic, facilitating energy and angular momentum exchange with their surroundings. Their behavior adheres to the Navier–Stokes equations for inviscid, incompressible flows, modified by absolute vorticity conservation constraints.[23, 73] This dynamism enables the model to address complex interactions within the æther framework.

Future investigations will incorporate topological invariants, such as linking numbers and higher-order polynomial measures, to quantify vortex knottedness.[45, 74] These invariants correlate directly with measurable quantities like energy, momentum, and angular momentum, providing a bridge between theoretical constructs and empirical observations. By establishing these connections, the model could yield novel insights into quantum field interactions and macroscopic phenomena, potentially unifying disparate domains of physics.

Expanding the scope of physical propositions to encompass dynamical systems, helicity dynamics, and nonlinear vacuum-fluid interactions offers a pathway to reconcile fluid dynamics with quantum mechanics. This approach maintains a foundation in Euclidean spatial geometry and absolute time, advancing a cohesive framework that transcends the limitations of existing relativistic and quantum paradigms.

§2. Observations on the Theory of Relativity and Vacuum Fluid (Æther)

General relativity, as formulated by Einstein, does not explicitly negate the possibility of an underlying medium; rather, it provides a heuristic that explains the behavior of space, time, and matter with mass, absent an explicitly specified physical fluid.[75] Einstein illustrated how mass induces curvature in spacetime, effectively bending particle trajectories. Consequently, the vacuum appears unanchored in any absolute, three-dimensional space, yet imbued with properties directly affecting the experiential passage of time and space for matter. In our non-relativistic Swirl–String Theory (SST) vacuum-fluid model, we assume that a potential flow of fluid elements exists between two identically and uniformly moving atoms, establishing a connection between them through their shared experience of time and space. This potential flow between two vortex knots (swirl strings) can be considered as a unified vortex structure, where the vortex line along the z-axis acts as a rotary connecting shaft. Thus, each atom maintains a physical link to another via vortex lines in the vacuum fluid, implying that identical vortex knots share identical values for core rotation and tangential velocity components.

The Theory of Relativity, in both its special and general manifestations, has profoundly reshaped our understanding of the interrelationship between time and space.[20, 75] Special relativity, through its assertion of the invariance of the speed of light and the resulting effects on simultaneity, redefined how observers in different inertial frames perceive temporal and spatial relationships. General relativity advanced these ideas by coupling the geometry of spacetime to mass and energy, offering an encompassing framework for the description of gravitation. Despite their profundity, these theories rest upon specific postulates that may not capture the entirety of physical reality, particularly regarding the nature and dynamics of an underlying vacuum medium.

A central tenet of special relativity is the relativistic interpretation of simultaneity, where two spatially separated events are simultaneous if synchronized clocks, using exchanged light signals, record identical times for those events.[20]

In this framework, simultaneity becomes an observer-dependent property, effectively entangling time and space into a unified yet subjective experience. This paradigm has driven significant advances in modern physics, yet it also introduces limitations when confronted with phenomena like quantum entanglement, where correlations between spatially distant particles appear to surpass relativistic boundaries.[76, 77]

The notion of an æther, dismissed by relativity in favor of an empty vacuum that serves as a passive backdrop to dynamic spacetime, provides an alternative conceptual framework. In our SST-based model, the time experienced by rotation of the pointer clocks for atoms will be slightly altered due to the rotation of the vortex cores, i.e., due to differences in local vorticity and swirl energy density. The vacuum fluid (historically called æther) is characterized in SST by two fundamental constants: the characteristic swirl speed

$$\mathbf{v}_{\circlearrowleft} \approx 1.09384563 \times 10^6\,\mathrm{m/s},$$

and the maximum swirl force

$$F_{\mathrm{swirl}}^{\mathrm{max}} \approx 29.053507\,\mathrm{N}.$$

These constants are pivotal in determining the dynamic behavior of the vacuum fluid—regulating vortex circulation velocity and providing limits for interactions within the medium. Unlike the archaic notion of a luminiferous medium, our vacuum fluid is envisioned as a fundamental, dynamic, incompressible, non-viscous entity analogous to a superfluid, supporting vortex (swirl-string) structures and enabling vorticity-driven interactions. This perspective suggests that simultaneity could, in principle, be restored to an absolute form, mediated by the intrinsic properties of the vacuum fluid, which plays a crucial role in governing such interactions, allowing the exchange of mechanical information to appear to exceed the traditional speed of light along non-local swirl configurations. The potential for non-local information transfer points to an underlying structure more intricate than the purely relativistic description, challenging us to expand our foundational understanding of physics.

General relativity's depiction of gravitation as a manifestation of spacetime curvature is a profound and elegant achievement.[75] Nevertheless, our model aims to reinterpret gravitational interactions as emergent phenomena stemming from vorticity within the vacuum fluid. In this view, mass can be understood as a localized concentration of increased vorticity, which governs the rotational dynamics and contributes to the formation of a pressure gradient. Such a pressure gradient creates an effective force that manifests as gravitational attraction, influencing surrounding fluid elements. This reinterpretation invites a reformulation of Einstein's field equations in terms of vorticity and the internal fluidic dynamics of the vacuum, suggesting that gravitation might emerge from fluidic interactions rather than a purely geometrical deformation of spacetime.

These observations imply that while the Theory of Relativity is an exceptionally powerful framework for describing macroscopic and high-energy phenomena, it may ultimately lack completeness. By incorporating a non-viscous, incompressible vacuum fluid into our model, we endeavor to provide a more nuanced and comprehensive understanding of the physical universe—accommodating quantum behaviors, non-locality, and the notion of an absolute time. These concepts appear discordant within the relativistic framework, yet they find coherence in a model where the vacuum fluid serves as the fundamental substrate of reality. This approach does not seek to invalidate relativity but to enhance our understanding by proposing an underlying medium through which relativistic effects are mediated, thereby bridging classical, quantum, and relativistic physics into a cohesive and unified Swirl–String Theory (SST) framework.

III. OBSERVATIONS ON LIGHT QUANTA IN A SWIRL MEDIUM

The atom persistently emits light, leading to a continual dissipation of its internal energy. In Swirl–String Theory (SST), we reinterpret this radiation not as the emission of fundamental point particles, but as the excitation of torsional shear waves in a structured, inviscid, incompressible vacuum fluid (the "swirl medium") characterized by an effective density ρ_f and an effective shear stiffness K.[29, 71, 72, 78–82] In the gauge-fixed, hydrodynamic representation, the photon appears as a massless transverse oscillation of a vector potential $A(\mathbf{x}, t)$ or $a(\mathbf{x}, t)$, with substrate velocity

$$\mathbf{u} = \partial_t A, \qquad \nabla \cdot A = 0, \tag{1}$$

so that incompressibility of the medium enforces purely transverse (shear-like) modes.[81]

The effective Lagrangian density for small-amplitude, unknotted excitations of this medium can be written in either of two equivalent forms:

$$\mathcal{L}_{\mathrm{torsion}} = \frac{1}{2}\,\rho_{\mathrm{eff}}\,\|\mathbf{u}\|^2 - \frac{1}{2}\,K\,\|\nabla \times A\|^2, \tag{2}$$

$$\mathcal{L}_{\mathrm{swirl\text{-}EM}} = \frac{\rho_f}{2}\,|\partial_t a|^2 - \frac{\rho_f c^2}{2}\,|\nabla \times a|^2, \tag{3}$$

with the identifications $\rho_{\text{eff}} \equiv \rho_f$ and $K \equiv \rho_f c^2$.[81, 82] Varying either (2) or (3) yields the massless vector wave equation

$$\Box A \equiv \left(\frac{1}{c^2} \partial_t^2 - \nabla^2 \right) A = 0, \tag{4}$$

with wave speed

$$c = \sqrt{\frac{K}{\rho_{\text{eff}}}}, \tag{5}$$

so that the speed of light emerges as the transverse shear speed of the swirl medium.[81, 82]

In this hydrodynamic picture, light quanta are modeled as localized torsional wave packets of these transverse modes. In the geometric-optics limit, a narrow packet may be visualized as an unknotted swirl string forming a toroidal wavefront—a "dipole" swirl string—whose core traces a closed loop in three-dimensional space. The core of this loop carries a localized torsional distortion (a twist of the director field), while its surrounding flow is organized into two contra-rotating strands in cross-section. This representation preserves the essential vorticity structure of the original æther-vortex picture, but embeds it consistently within the torsion-wave Lagrangian framework.

Within the swirl medium, the total energy of such a dipole wave packet is controlled by both the local swirl energy density

$$\rho_E = \frac{1}{2} \rho_f \, \|\mathbf{v}\|^2, \tag{6}$$

and the geometric volume effectively occupied by the packet. Here $\mathbf{v}$ denotes the local fluid velocity associated with the torsional mode. The dependence of the energy on frequency and cross-sectional scale naturally reproduces the quantized energy levels observed in atomic spectra once circulation quantization and boundary conditions are imposed.[82]

From the vorticity-driven viewpoint, what is usually called the "wave–particle duality" of light becomes a manifestation of the coherent swirl structure of these torsional dipoles:

- The *wave-like* behavior arises from the fact that $A(\mathbf{x}, t)$ obeys the linear wave equation, with interference, diffraction, and polarization encoded in the transverse patterns of the substrate velocity $\mathbf{u} = \partial_t A$.[56]
- The *particle-like* behavior is associated with the topological and energetic discreteness of localized wave packets: circulation quantization, fixed knotting class of the supporting swirl string, and finite support of the torsional distortion in the medium.[71, 72]

Polarization acquires a geometric interpretation. Linear and circular polarizations correspond to distinct orientations and helicities of the torsional distortion relative to the propagation direction. In particular, circular polarization can be viewed as a helical torsional mode in which the director field traces a screw-like path along the ray, in direct correspondence with the helical substrate velocity patterns of the shear-wave solution.[81]

The interaction between light and matter is mediated by the pressure and vorticity fields induced by the torsional wave as it traverses the swirl medium. When a torsional wave packet encounters the pressure well generated by a bound swirl string (such as the proton–electron linkage in hydrogen), the local vorticity and pressure gradients are modified. In SST, atomic transitions are interpreted as shifts between discrete flow-regime resonances: for hydrogen, a transition from $n = 1$ to $n = 2$ corresponds to a change in the electron's orbital swirl velocity from αc to $\alpha c/2$, and the emitted photon is precisely the torsional wave packet carrying the associated change in angular momentum and energy.[82]

In this way, the hydrodynamic torsion model of light, the swirl-EM Lagrangian, and the knot-based architecture of matter remain mutually consistent: photons are not independent point particles but emergent torsional excitations of the same swirl medium that supports the knotted swirl strings of atomic structure.

IV. THE PRINCIPLE OF PRESSURE EQUILIBRIUM IN SWIRL-STRING VORTEX MODELS

Within SST, bound states such as the hydrogen atom are modeled as knotted swirl strings (e.g., a trefoil core for the proton) surrounded by an irrotational envelope that we identify with the electronic cloud. The swirl medium is treated as an incompressible, inviscid condensate with density ρ_f, so that its dynamics are governed by the Euler equation and Bernoulli's principle for incompressible flow.[23, 82] The notion of a "spherical pressure boundary" then arises naturally as the surface on which the pressure of the irrotational flow matches the ambient pressure of the undisturbed

medium; this surface will expand or contract in response to changes in the local swirl velocity, providing a direct hydrodynamic analogue of thermal expansion.

For an incompressible fluid, the Euler equation can be written as

$$\frac{1}{\rho_f}\,\nabla p = -(\mathbf{v}\cdot\nabla)\mathbf{v}, \tag{1}$$

where p is the pressure and $\mathbf{v}$ the local velocity field.[23] For a purely azimuthal flow around a straight swirl string with circulation Γ, the tangential velocity scales as

$$v_\theta(r) \simeq \frac{\Gamma}{2\pi r}, \tag{2}$$

so that the radial pressure gradient is

$$\frac{dp}{dr} = \rho_f\,\frac{v_\theta^2}{r} = \rho_f\,\frac{\Gamma^2}{4\pi^2 r^3}. \tag{3}$$

Integrating (3) from infinity to a finite radius r yields a pressure deficit $\Delta p(r) \propto -1/r^2$, which acts as an attractive potential on any other swirl string placed in this field—the swirl-Coulomb potential.[82] This is the hydrodynamic mechanism by which SST recovers the effective $1/r$-like binding structure of the hydrogen atom.

The spherical pressure boundary associated with a trefoil core is defined as the locus where the pressure in the irrotational envelope equals the ambient pressure of the undisturbed swirl medium. Along a streamline in the irrotational region, Bernoulli's principle states that

$$p + \frac{1}{2}\,\rho_f v^2 = \text{constant}, \tag{4}$$

so that increases in the local speed v must be accompanied by decreases in the local pressure p and vice versa.[23]

This leads to a simple, physically transparent picture:

- **If the irrotational flow accelerates** (for instance, when energy is injected into the system via torsional waves or thermal input), the kinetic term $\frac{1}{2}\rho_f v^2$ increases, forcing the pressure p within the envelope to drop. To maintain pressure equilibrium with the far-field medium, the spherical boundary must expand outward until the flow decelerates sufficiently and the Bernoulli constant is restored. In this sense, the bound state "breathes out" under excitation.
- **If the irrotational flow decelerates** (for example, during radiative relaxation or cooling), the kinetic term decreases and the internal pressure rises. The spherical boundary then contracts, shrinking the envelope until the internal and external pressures again match. The bound state "breathes in" as it relaxes toward the ground configuration.

The energy stored in the envelope region can be approximated as

$$E_{\text{env}} \simeq \frac{1}{2}\,\rho_f\,V\,v^2 + p\,V, \tag{5}$$

where V is the volume enclosed by the pressure boundary, v is a suitably averaged irrotational speed on that boundary, and p is the corresponding pressure. Differentiating (5) with respect to time gives

$$\frac{dE_{\text{env}}}{dt} \simeq \rho_f\,V\,v\,\frac{dv}{dt} + \frac{d(pV)}{dt}, \tag{6}$$

showing explicitly how changes in flow velocity and pressure drive the dynamics of the boundary radius. When this evolution is constrained by circulation quantization and the canonical SST constants $(\rho_f, \mathbf{v}_\circlearrowleft, r_c)$, the allowed radii and velocities organize into discrete families that may be mapped onto the hydrogenic energy levels.[82]

Thus, the "pressure equilibrium" principle in SST is nothing more than incompressible Euler–Bernoulli hydrodynamics applied to knotted swirl strings in the calibrated swirl medium. The spherical boundary surrounding a trefoil core is the geometric surface along which the swirl-Coulomb pressure deficit balances the ambient pressure. Its expansion and contraction under changes in swirl velocity provide a direct hydrodynamic mechanism for linking vorticity, thermal input, and entropy-like measures, while remaining fully consistent with the hydrogen ground-state derivation and the torsion-wave description of photon emission and absorption.

Part II
Foundations

V. SEVENFOLD GENESIS OF THE SWIRLING COSMOS

Canonical Cosmogony (SST · STC Mapped) This section compresses the sixteen stages of *The Simplicity Codex* [51] into seven logically complete emergence stages, consistent with the SST Canon **v0.6.0** and the Lagrangian EFT [55]. Each stage represents a parameter-free imprint of physical law onto the condensate.

Stage 1: Logical Substrate (Pre-Swirl Potential)

A Haar-neutral, scale-free potential field encodes possible circulation states. No time or space exist yet — only relational templates. Global $\mathbb{Z}_2$ (chirality) and $\mathbb{Z}_3$ (triadic closure) symmetries are imprinted as pre-physical rules:

$$\Gamma \mapsto -\Gamma, \qquad \Gamma_1 + \Gamma_2 + \Gamma_3 = 0 \pmod{2\pi}$$

laying the groundwork for matter/antimatter duality and baryon triplet stability. (STC Stages 1–3)

Stage 2: Big Condensation (First Manifestation)

When the information complexity $\mathcal{I}_{\text{swirl}}$ exceeds the Guardian threshold, the swirl condensate forms as an incompressible, inviscid medium on $\mathbb{R}^3$ with absolute time t. Primary constants lock in by resonance:

$$\Gamma_0 = 2\pi r_c \|\mathbf{v}_\circlearrowleft\|, \qquad \tau_{\text{beat}} = \frac{2\pi r_c}{\|\mathbf{v}_\circlearrowleft\|}, \qquad \rho_f = \frac{\rho_m r_c}{\|\mathbf{v}_\circlearrowleft\|}\,\Omega$$

marking the birth of physical time and the circulation quantum. (STC Stage 8)

Technical details: See Section XIV (Classical Invariants) and Section XVII (Effective Medium) for derivations.

Stage 3: Tangible Chirality and Swirl-Time

Knotted swirl strings appear, stabilized by circulation quantization $\Gamma = n\Gamma_0$. The swirl clock

$$S_t = \sqrt{1 - \frac{v^2}{c^2}}$$

defines local proper time, with left-handed ($\circlearrowleft$) and right-handed ($\circlearrowright$) knots forming the basis for matter and antimatter. (STC Stage 9)

Technical details: See Section XIV (Classical Invariants) and Section VII (Core Axioms) for the formal framework.

Stage 4: Topological Charges and Particle Spectrum

Topological invariants of knots $(\text{Lk}, \text{Wr}, \text{Tw})$ map to quantum numbers:

$$Q(K) = T_3(K) + \frac{Y(K)}{2}$$

with Q the electric charge, T_3 weak isospin, and Y hypercharge. Fermion masses arise as soliton energies:

$$m_K = \rho_f \|\mathbf{v}_\circlearrowleft\|^2 \,\text{Vol}_{\mathbb{H}}(K)\,\phi^{-2k}$$

where $\text{Vol}_{\mathbb{H}}(K)$ is the hyperbolic complement volume of K and ϕ^{-2k} encodes Golden-layer suppression. (STC Stage 10)

Technical details: See Section XIX (Knot Taxonomy) for the particle–knot mapping, and Section XXXV (Hydrogen–Gravity) for mass derivations.

Stage 5: Emergent Interactions (Gauge and Forces)

Unknotted excitations of the condensate form the R-phase modes (photons, gluons, W/Z), with interactions governed by the emergent gauge group:

$$\mathfrak{g}_{\text{swirl}} \simeq \mathfrak{su}(3) \oplus \mathfrak{su}(2) \oplus \mathfrak{u}(1)$$

and minimal coupling

$$D_\mu = \nabla_\mu + i g_{\text{sw}} W_\mu^a T^a \,.$$

(STC Stage 11)

Technical details: See Section XXI (Swirl–EM Emergence) and Section XXIII (Unified SST Lagrangian) for the formal derivation.

Stage 6: Geometric Closure and Constant Lock-In

Global Gauss closure yields the $1/r^2$ force law:

$$\nabla \cdot \vec{P}_{\text{swirl}} = 0 \quad \Rightarrow \quad F(r) \propto \frac{1}{r^2}$$

and fixes π geometrically. The entire condensate enters a global resonance, locking all constants of nature.

Technical details: See Section XXVIII (Swirl Pressure Law) and Section XXX (Gauge/EWSB Sector) for force laws and constant determinations.

Zero–Parameter Principle (Canonical)

Statement (Axiom): All dimensional constants of nature are determined by the condensate state, its circulation quantum, and the allowed topological sectors. We take as primitive the circulation-based triplet

$$(\Gamma_0, \rho_f, r_c),$$

where Γ_0 is the circulation quantum, ρ_f the effective fluid density, and r_c the electron-scale core radius. All other dimensional quantities in SST (masses, charges, energies, forces) are derived combinations of (Γ_0, ρ_f, r_c) and topology-dependent dimensionless factors.
The canonical swirl speed at the core boundary is not independent but given by

$$\|\mathbf{v}_\circlearrowleft\| = \chi_v \frac{\Gamma_0}{2\pi r_c},$$

so that the former primitive set $(\|\mathbf{v}_\circlearrowleft\|, r_c, \rho_f)$ is just a reparametrization of (Γ_0, ρ_f, r_c).

Primary Scale: $\Gamma_0 \approx 6.4 \times 10^3 \text{ m}^2/\text{s}, \qquad \kappa_{\text{SST}} \equiv \Gamma_0 = 2\pi r_c \|\mathbf{v}_\circlearrowleft\|$

Effective Density: $\rho_f = \dfrac{\rho_m \, r_c}{\|\mathbf{v}_\circlearrowleft\|}\,\Omega \qquad$ (coarse-grain rule)

Mass Functional: $m_K = \rho_f \|\mathbf{v}_\circlearrowleft\|^2 \, \text{Vol}_{\mathbb{H}}(K)\, \phi^{-2k}$

Gravitational Coupling: $G_{\text{swirl}} = \dfrac{\|\mathbf{v}_\circlearrowleft\| c^5 t_p^2}{2 F_{\max} r_c^2}$

Fine-Structure Constant: $\alpha = \alpha_{\text{DSI}}\big(\omega_{\text{DSI}}\big), \qquad \omega_{\text{DSI}} \approx 13.06$

Corollary: Once Γ_0, r_c, and ρ_f are fixed by a single calibration (e.g. m_e), the full mass spectrum and coupling strengths follow with no free parameters. See STC Stages 12–13 (Gauss-closure & Universal Resonance) [51].

Stage 7: Recursive Cosmos (Fractal Emergence)

Composite knots (baryons, nuclei, atoms) satisfy $\mathbb{Z}_3$ closure, 1+12 isotropic shielding, and duality pairing. Each stable composite becomes a new circulation source:

$$\text{Cluster} \;\Rightarrow\; \text{Meta-Knot} \;\Rightarrow\; \text{New Swirl Layer}$$

seeding the next scale of complexity. This recursion drives cosmic structure formation, yielding a fractal universe of knots within knots. (STC Stages 14–16)

VI. CANON GOVERNANCE AND STATUS TAXONOMY

a. Formal system. Let $\mathcal{S} = (\mathcal{P}, \mathcal{D}, \mathcal{R})$ denote the SST formal system: axioms $\mathcal{P}$, definitions $\mathcal{D}$, and admissible inference rules $\mathcal{R}$ (variational principles, Noether currents, dimensional analysis, asymptotic matching).

b. Canonical statement. A statement X is *canonical* iff

$$\mathcal{P}, \mathcal{D} \vdash_{\mathcal{R}} X\,,$$

and X is consistent with accepted canon.

c. Empirical statement. A statement Y is *empirical* iff it asserts a measured value or protocol:

$$Y \equiv \text{“observable } \mathcal{O} \text{ has value } \hat{o} \pm \delta o \text{ under procedure } \Pi\text{.”}$$

Status Classes

- **Axiom/Postulate (Canonical).** Primitive assumption of SST.
- **Definition (Canonical).** Introduces a symbol by construction.
- **Theorem/Corollary (Canonical).** Proven consequence within $\mathcal{S}$.
- **Constitutive Model.** Canonical if derived from $\mathcal{P}, \mathcal{D}$; otherwise semi-empirical.
- **Calibration (Empirical).** Recommended numerical values for canonical symbols.
- **Research Track.** Conjectures or alternatives pending proof or axiomatization.

Items may be promoted or demoted between classes only upon satisfying or failing the Canonicality Tests.

Canonicality Tests (all required)

1. **Derivability** from $\mathcal{P}, \mathcal{D}$ via $\mathcal{R}$.
2. **Dimensional consistency** (strict SI usage; correct physical limits).
3. **Symmetry compliance** (Galilean symmetry and incompressibility).
4. **Recovery limits** (Newtonian gravity, Coulomb/Bohr, linear wave optics).
5. **Non-contradiction** with accepted canonical results.
6. **Parameter discipline** (no ad hoc fits beyond calibrations).

Corollary: Clock–Radius Transport

$$\frac{dS_t}{dt} = \frac{2(1 - S_t^2)}{S_t}\,\frac{1}{R}\,\frac{dR}{dt}.$$

Assumption: thin filament with local solid-body swirl $v_\theta \simeq \omega r$ evaluated at $r = r_c$, so that $S_t = \sqrt{1 - (\omega r_c/c)^2}$ along the core [23, 24].

VII. CORE AXIOMS (SST)

SST is built on a set of core axioms that establish its physical framework. These axioms, numbered below, are stated in plain language and form the starting postulates of the theory (they are considered *canonical* by definition).

Axiom 0: Logical Substrate (Pre-Swirl Potential)

Before the emergence of space, time, or condensate, there exists a *Haar-neutral*, scale-free state space $\mathcal{S}$ of possible circulation states $\{\Gamma_i\}$. This pre-physical substrate encodes only relational constraints:

$$\Gamma \mapsto -\Gamma, \qquad \Gamma_1 + \Gamma_2 + \Gamma_3 = 0 \ (\mathrm{mod}\ 2\pi),$$

representing a global $\mathbb{Z}_2$ *chirality symmetry* and $\mathbb{Z}_3$ *triadic closure*. No metric structure (no lengths, durations, or energies) is yet defined. This axiom specifies that:

1. Circulation states are allowed only in $\pm$ pairs (matter/antimatter duality).
2. The sum of any three circulations must close to zero modulo 2π, ensuring triplet stability (precursor to baryon confinement).
3. Any potential $V[\Gamma]$ defined on $\mathcal{S}$ must satisfy $V[\Gamma] = V[-\Gamma]$ and $V[\Gamma_1, \Gamma_2, \Gamma_3] = V[\Gamma_1 + \Gamma_2 + \Gamma_3 \ (\mathrm{mod}\ 2\pi)]$.

This stage is purely ontological: it fixes the logical rule set within which the swirl condensate (Stage 2) will later form and evolve.

Citation: See *The Simplicity Codex* [51] (Stages 1–3: Primordial Symmetry and Triadic Closure) for the information-theoretic basis of these constraints.

1. **Swirl Medium (Absolute Space-Time):** Physics is formulated in Euclidean $\mathbb{R}^3$ space with an absolute time parameter. All dynamics occur in a frictionless, incompressible condensate called the *swirl medium*, which acts as a universal substratum for motion (analogous to a perfect fluid with no viscosity or compressibility).

2. **Swirl Strings (Circulation & Topology):** Particles and field quanta correspond to closed vortex filaments ("swirl strings") in the medium. Each such filament may be knotted or linked. The circulation of the swirl velocity field $\mathbf{v}_\circlearrowleft$ around any closed loop C is quantized in integer multiples of the circulation quantum Γ_0:

$$\Gamma \;=\; \oint_C \mathbf{v}_\circlearrowleft \cdot d\ell \;=\; n\,\Gamma_0, \qquad n \in \mathbb{Z},$$

   where Γ_0 is the primitive circulation quantum (approximately 6.4×10^3 m^2/s). In addition to circulation quantization, the allowed configurations of a swirl string are restricted to distinct knot topologies. Thus, discrete quantum numbers (e.g. mass, charge, spin) are identified with topological invariants of the string (such as linking number, writhe, and twist) rather than with eigenstates of operators.

   Rosetta remark. In the linear mapping to conventional superfluid notation, the circulation quantum Γ_0 matches the Onsager–Feynman value h/m_{eff} for the relevant excitation, but within SST we treat Γ_0 as primitive and regard h as a derived quantity.

3. **String-Induced Gravitation:** Macroscopic gravitational attraction emerges as an effective force resulting from coherent swirl flows and pressure gradients in the medium. In the non-relativistic limit, the effective gravitational coupling G_{swirl} is fixed by canonical constants such that $G_{\mathrm{swirl}} \approx G_N$ (Newton's gravitational constant). In essence, what we perceive as gravity is a statistical effect of many swirl strings and their pressure fields rather than a fundamental spacetime curvature.

4. **Swirl Clocks (Local Time Dilation):** The local proper time in a region of the swirl medium depends on the swirl speed in that region. A clock comoving with a swirl string (tangential speed v) ticks slower than a clock at rest in the medium by the *swirl clock factor*

$$S_t \;=\; \sqrt{1 - \frac{v^2}{c^2}}\,,$$

   analogous to special relativistic time dilation. Higher swirl velocities (and thus higher local swirl energy density) cause deeper time dilation (slower clocks) relative to an observer at infinity.

5. **Dual Phases (Wave–Particle Complementarity):** Each swirl string has two limiting dynamical phases. In the *R-phase* ("radiative" or *wave-like* phase), the string is unknotted and its circulation is delocalized over an extended loop. In the *T-phase* ("tangible" or *particle-like* phase), the string is knotted and its circulation is localized, carrying rest-mass. Quantum wave–particle duality in SST is thus realized as the ability of a swirl string to transition between these two phases. A quantum measurement corresponds to a rapid transition from an R-phase state to a T-phase state ($R \to T$ "collapse") or vice versa ($T \to R$ de-localization), typically accompanied by emission or absorption of small swirl excitations (swirl radiation).

6. **Canonical Taxonomy (Particle–Knot Mapping):** There is a one-to-one mapping between the topological class of a swirl string and the type of particle or field it represents. Delocalized R-phase excitations correspond to unknotted swirl strings and represent massless bosonic quanta — with photons realized as *pulsed torsional oscillations* of the swirl director field (carrying helicity ± 1) rather than static knots. Nontrivial torus knots correspond to leptons (e.g. the electron is represented by the trefoil 3_1 knot). Chiral hyperbolic knots (with non-zero writhe) correspond to quarks: we assign the up quark to the 5_2 knot and the down quark to the 6_1 knot. Baryons are realized as composite linkages of three quark knots: for instance, the proton is $p = (5_2 + 5_2 + 6_1)$ and the neutron $n = (5_2 + 6_1 + 6_1)$, with a color-flux linkage ensuring confinement. Linked or nested composite knots describe nuclei and bound states, providing SST with a built-in "periodic table" of matter.

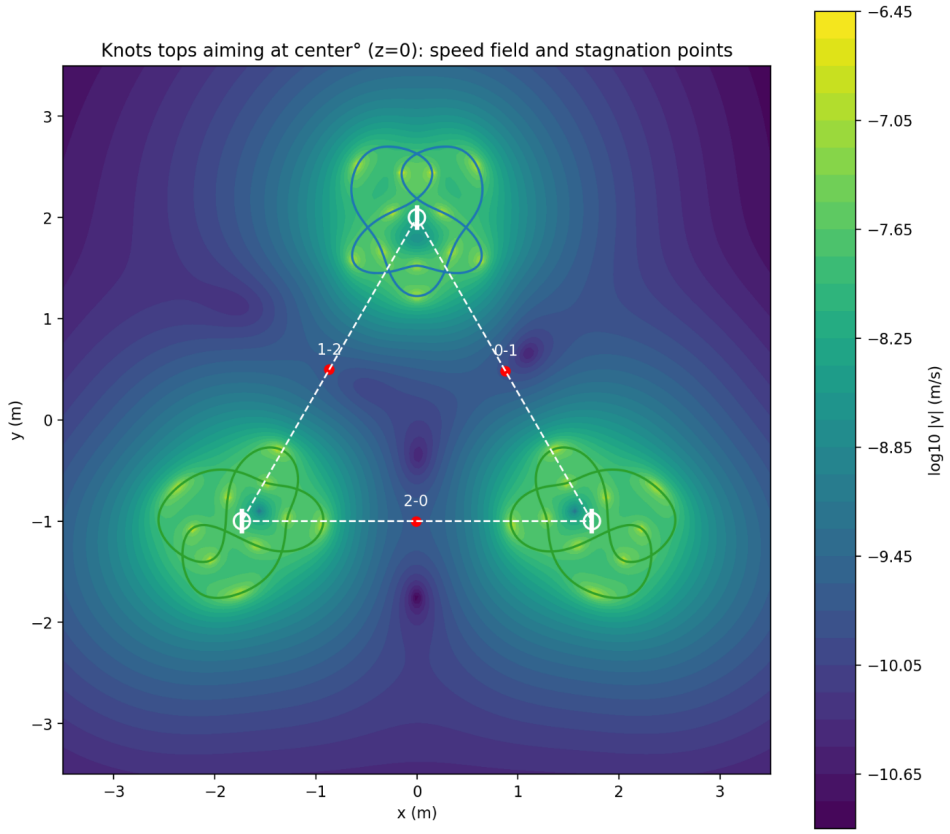

FIG. 1. Sst three knot 180 speed stagnation

These axioms define the ontological starting point of SST. The swirl medium (Axiom 1) provides the arena, swirl strings (Axiom 2) provide the basic degrees of freedom with quantized circulation and allowed topologies, and the remaining axioms posit how classical forces and quantum behaviors emerge from this framework (gravity from collective flows, time dilation from swirl motion, wave–particle dual phases, and a topological classification of particles).

Part III
Geometry, Fields, and Lagrangian

VIII. FORMAL STRUCTURE AND CANONICAL FRAMEWORK

In addition to physical axioms, SST is formulated as a formal system $S = (P, D, R)$ comprising a set of postulates (P), definitions (D), and inference rules (R). A statement in SST is considered *canonical* if and only if it can be derived from the axioms and definitions using the permitted inference rules, and it is consistent with all previously established canonical statements. The hierarchy of statement types is as follows:

- **Axiom (Postulate):** A primitive assumption of SST, not derived from deeper principles (e.g. the existence of an incompressible swirl medium, as in Axiom 1).
- **Definition:** Introduction of a new symbol or concept and its meaning (e.g. defining the swirl Coulomb constant Λ in terms of a surface integral of swirl pressure).
- **Theorem / Corollary:** A nontrivial proposition that is logically derived from the axioms and prior theorems. Corollaries are immediate consequences of theorems.
- **Calibration (Empirical):** An assignment of a numerical value to a canonical constant, obtained from experiment or observation, used to anchor the theory's free parameters. Calibrations are not used as premises in proofs, but serve to connect SST to measurable reality.
- **Research Track (Conjecture):** A speculative extension or hypothesis not yet derivable within S. Such statements are included for context or future development but are explicitly marked as non-canonical.

All developments in the main text are canonical (axioms, definitions, theorems, corollaries, with recommended constant calibrations). Derivations, proofs, and pedagogical explanations are mostly deferred to the appendices to maintain a clear logical flow. Every formula and constant introduced is checked for dimensional consistency and reducing to known physics in the appropriate limits (Newtonian, Coulomb, etc.), as documented in the appendices. This ensures that the SST formal system remains self-consistent and empirically anchored.

IX. SELF-SIMILARITY AND STABILITY OF SWIRL STRUCTURES

Axiom (Self-Similar Scaling). Any incompressible, inviscid swirl configuration near a potential singularity admits a local self-similar form

$$\mathbf{v}_{\circlearrowleft}(\mathbf{x},t) = (T-t)^{-\alpha}\,\mathbf{V}\!\left(\frac{\mathbf{x}-\mathbf{x}_0}{(T-t)^{\beta}}\right), \qquad \boldsymbol{\omega}(\mathbf{x},t) = (T-t)^{-\gamma}\,\boldsymbol{\Omega}\!\left(\frac{\mathbf{x}-\mathbf{x}_0}{(T-t)^{\beta}}\right), \tag{1}$$

with scaling exponents constrained by the Euler-type balance $\alpha + \beta = 1$, $\gamma = 1$. The swirl-clock relation fixes $\alpha \le 1/2$ under bounded $|\mathbf{v}_{\circlearrowleft}| \le C_e$.

Definition (Finite-Core Regularization). A self-similar field is said to be *regularized* in SST if the core radius $r_c > 0$ and the swirl-stress bound $F_{\max}$ ensure $|\boldsymbol{\omega}| \le C_e/r_c$, so that the Beale–Kato–Majda condition is never met: $\int_0^T \|\boldsymbol{\omega}\|_\infty\, dt < \infty$.

Theorem (Perturbation Suppression by Swirl Diffusion). Augmenting the inviscid system by the canonical regularization terms

$$\partial_t \boldsymbol{\omega} = \nabla \times (\mathbf{v}_{\circlearrowleft} \times \boldsymbol{\omega}) + \kappa(\Delta\boldsymbol{\omega} - r_c^{-2}\boldsymbol{\omega}) + \chi\nabla(\Delta\rho_f), \tag{2}$$

with $\kappa, \chi > 0$ constrained by $|\mathbf{f}_{\text{swirl}}| \le F_{\max}$, shifts all unstable eigenvalues of the linearized operator $\mathcal{L}$ into the negative half-plane. Hence finite-core swirl structures are globally stable against axisymmetric perturbations.

Corollary (Chronos–Kelvin Consistency). The stabilized field still obeys the Chronos–Kelvin invariant $D(R^2\omega)/Dt_{ae} = 0$; the regularization modifies only higher-order curl terms and does not break canonical invariants.

A. Relation to khronon and Hořava–Lifshitz clock fields

The swirl clock field $S_t^{\circlearrowleft}(x)$ plays the same geometric role in Swirl–String Theory as the *khronon* (clock field) does in Lorentz-violating extensions of General Relativity such as Einstein–Æther and Hořava–Lifshitz gravity.[68, 69] In those frameworks one introduces a scalar time function $T(x)$ whose level sets define a preferred foliation of spacetime. The associated unit timelike vector field

$$u_\mu(x) = \frac{\nabla_\mu T(x)}{\sqrt{-\,g^{\alpha\beta}\,\nabla_\alpha T(x)\,\nabla_\beta T(x)}}\,, \tag{3}$$

enters the low-energy effective action and explicitly breaks local Lorentz invariance down to diffeomorphisms that preserve the foliation.

In SST, the swirl clock is defined as the local ratio between proper time measured by a comoving matter observer and an asymptotic reference clock,

$$S_t^{\circlearrowleft}(x) \equiv \frac{d\tau_{\rm local}}{d\tau_\infty}\,, \tag{4}$$

with $S_t^{\circlearrowleft}(x)$ determined dynamically by the underlying hydrodynamic state (local vorticity and swirl energy density) as derived in the swirl-time sector. A natural khronon-like scalar in SST is then obtained by integrating the swirl clock along the global coordinate time,

$$T(x) \;\equiv\; \int^t S_t^{\circlearrowleft}(t', \mathbf{x})\; dt'\,, \tag{5}$$

so that hypersurfaces of constant T coincide with iso-chronal slices of the swirl clock. Inserting (5) into (3) yields a unit vector u_μ that is *emergent* from the hydrodynamic state rather than a fundamental new field.

The symmetry pattern of the SST clock sector is therefore identical to that of khronometric and Hořava–Lifshitz models: there exists a preferred time function selecting a foliation, and the low-energy gravitational dynamics are described by a metric $g_{\mu\nu}$ coupled to a unit timelike vector u_μ normal to those slices. The difference is conceptual and dynamical rather than kinematic: in SST, $S_t^{\circlearrowleft}$ is constrained by incompressible Euler dynamics and conserved vorticity, and thus $T(x)$ and u_μ are derived quantities tied to the swirl energy budget. This allows one to import existing experimental and phenomenological bounds on khronon/Hořava-type clock fields directly into constraints on the SST swirl clock sector, while maintaining the physical interpretation that time dilation arises from structured hydrodynamic flow rather than from an abstract khronon scalar.

VII.B Odd-Parity Swirl Splitting and Nodal Sheets

Canonical Statement. In an incompressible swirl medium, any helical swirl configuration with a commensurate period $N \in 2\mathbb{Z}$ (even) admits a coarse-grained two-component description in which the effective single-particle Hamiltonian contains an *odd-parity* linear term in momentum. This produces a direction-dependent splitting of the swirl-clock sectors and enforces the existence of *nodal sheets* in momentum space.

Definition (Swirl–Spinor Sector). Let the local swirl clock be $S_t(x)$ and define a two-component internal space $\Psi = (\psi_{\circlearrowleft}, \psi_{\circlearrowright})^T$ representing the left- and right-clock sectors. The minimal canonical Hamiltonian compatible with Galilean invariance, incompressibility, and the chronometric tensor is

$$H_{\rm SST}(\mathbf{k}) = \epsilon_0(\mathbf{k})\mathbb{1} + g_{\rm sw}\,(\mathbf{k}\cdot\hat{\alpha})\,\Sigma_x + m_{\rm sw}\,\Sigma_z + \lambda_{\rm sw}\,(\mathbf{k}\times\hat{\alpha})\cdot\hat{z}\,\Sigma_y, \tag{6}$$

where:

$$\epsilon_0(\mathbf{k}) = \frac{\hbar^2 k^2}{2m_{\rm eff}(\rho_f, \rho_E)}, \tag{7}$$

$$\hat{\alpha} = \text{unit vector defined by the helical swirl director field}, \tag{8}$$

$$\Sigma_i = \text{Pauli matrices in the swirl-clock basis}. \tag{9}$$

Interpretation. The term $g_{\rm sw}(\mathbf{k}\cdot\hat{\alpha})\Sigma_x$ is odd under $\mathbf{k}\to-\mathbf{k}$ and represents *odd-parity* splitting of the swirl-clock sectors. It is induced whenever the swirl director field forms a commensurate helix with even period N, so that the composite symmetries

$$[T \parallel t_{1/2}], \qquad [C_{2\perp} \parallel t_{1/2}] \tag{10}$$

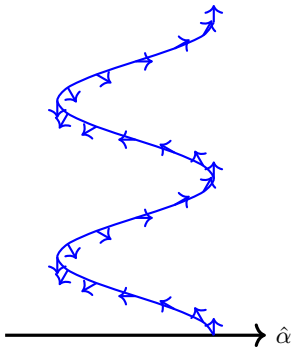

(A) Helical swirl director field
even commensurate period $N \in 2\mathbb{Z}$

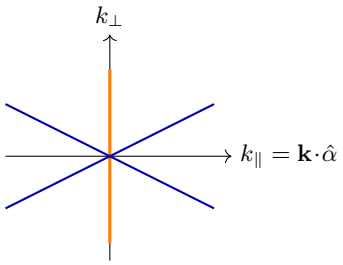

(B) Nodal sheet in momentum space
$\mathbf{k}\cdot\hat{\alpha} = 0$: swirl-clock degeneracy

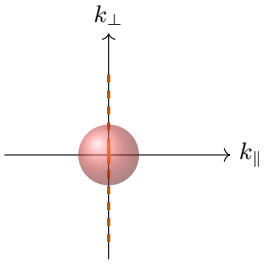

(C) Berry curvature activation
small $(m_{\rm sw}, \lambda_{\rm sw}) \neq 0$
geometric phase for swirl-clock transport

FIG. 2. **Odd-parity swirl splitting and nodal-sheet geometry.** (A) A commensurate helical swirl director field selects a unique axis $\hat{\alpha}$ and generates the odd-parity term $g_{\rm sw}(\mathbf{k}\cdot\hat{\alpha})\Sigma_x$ in the canonical Hamiltonian. (B) The resulting momentum-space spectrum exhibits a nodal sheet where the two swirl-clock sectors are degenerate: $\mathbf{k}\cdot\hat{\alpha} = 0$. (C) A small swirl-clock bias ($m_{\rm sw} \neq 0$) and reflection-breaking term ($\lambda_{\rm sw} \neq 0$) gap the sheet and generate a concentrated Berry-curvature region, producing swirl-dependent transport anomalies.

remain unbroken at the coarse-grained level. These symmetries forbid any momentum-independent splitting and enforce linear, directional splitting.

Theorem (Existence of Swirl–Nodal Sheets). Let $m_{\rm sw} = \lambda_{\rm sw} = 0$ in (6). Then the two eigenvalues of $H_{\rm SST}$ satisfy

$$E_\pm(\mathbf{k}) = \epsilon_0(\mathbf{k}) \pm g_{\rm sw}(\mathbf{k}\cdot\hat{\alpha}). \tag{11}$$

The degeneracy condition $E_+ = E_-$ occurs on the plane

$$\mathbf{k}\cdot\hat{\alpha} = 0, \tag{12}$$

which defines a *nodal sheet* (a momentum-space 2D manifold of swirl-clock degeneracy). This sheet is protected by the composite symmetries and cannot be lifted by any symmetry-preserving perturbation.

Corollary (Berry-Curvature Activation by Symmetry Breaking). When the swirl-clock symmetry is weakly biased by a small $m_{\rm sw}\,\Sigma_z$ (clock-sector energy imbalance) and reflection symmetry is weakly broken by $\lambda_{\rm sw}\,\Sigma_y$, the nodal sheet acquires a finite gap. The resulting band curvature yields a nonzero intrinsic Berry curvature

$$\Omega_{ij}(\mathbf{k}) = -2\,\mathrm{Im}\sum_{n\neq m} \frac{\langle n|\partial_{k_i} H_{\rm SST}|m\rangle\langle m|\partial_{k_j} H_{\rm SST}|n\rangle}{(E_n - E_m)^2}, \tag{13}$$

producing a transport anomaly in any coupled charge or swirl-current sector. The anomaly vanishes continuously as $m_{\rm sw} \to 0$.

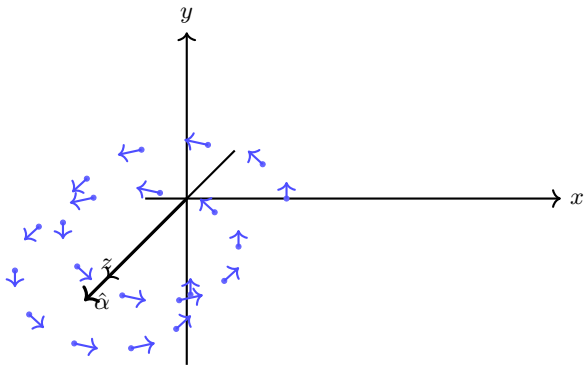

Figure 1. Helical Swirl Director Field (Real Space)
even commensurate helix selecting a unique polarization axis

FIG. 3. A 3D helical swirl director field. The structured rotation establishes the internal axis $\hat{\alpha}$ that appears in the odd-parity term $g_{\rm sw}(\mathbf{k}\cdot\hat{\alpha})\Sigma_x$ of the canonical Hamiltonian. Even commensurate period $N \in 2\mathbb{Z}$ preserves composite symmetries and enforces directional splitting.

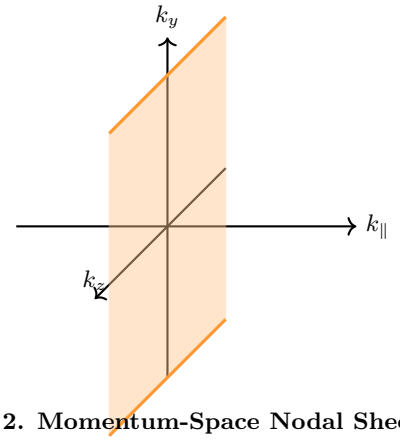

Figure 2. Momentum-Space Nodal Sheet
Degeneracy condition $\mathbf{k}\cdot\hat{\alpha} = 0$

FIG. 4. The canonical Hamiltonian $H_{\rm SST}(\mathbf{k})$ produces a nodal sheet where the two swirl-clock sectors become exactly degenerate: $\mathbf{k}\cdot\hat{\alpha} = 0$. This 2D sheet in momentum space is protected by symmetry and cannot be lifted without breaking the composite symmetries associated with the commensurate helical structure.

Canonical Interpretation. The odd-parity term $g_{\rm sw}(\mathbf{k}\cdot\hat{\alpha})\Sigma_x$ represents directional modulation of the swirl clock and arises as a coarse-grained imprint of structured swirl helices. The nodal sheet is the momentum region where the swirl-clock sectors become locally isochronous. Introducing the small symmetry-breaking terms corresponds to imposing a spatial bias in the swirl-clock field, giving rise to a geometric (Berry) phase in momentum transport.

Status. Canonical (derived from the chronometric tensor, swirl-clock sectors, and symmetry constraints). No additional constants or empirical parameters are introduced.

X. GOLDEN PRINCIPLE FOR DISCRETE LAYERING

In Swirl–String Theory (SST) we introduce a distinguished dimensionless constant $\phi > 1$ which controls a discrete hierarchy of mass and energy layers. To avoid any ambiguity or post-hoc tuning, we fix ϕ once and for all at the level of the axioms and then derive its role in the layer spectrum.

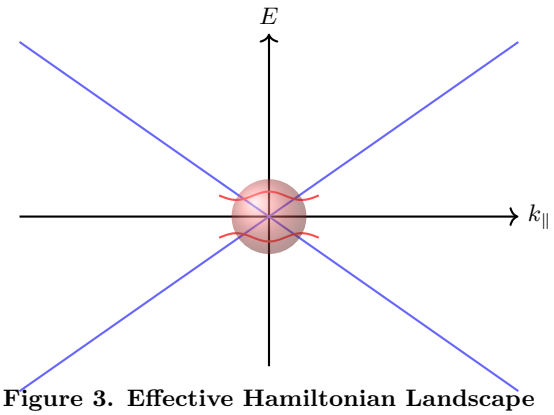

Figure 3. Effective Hamiltonian Landscape
Sheet gapping by small $(m_{\rm sw}, \lambda_{\rm sw})$
Concentrated Berry curvature near the gap

FIG. 5. Energy bands of $H_{\rm SST}(\mathbf{k})$ along the direction $k_\parallel = \mathbf{k}\cdot\hat{\alpha}$. The odd-parity term creates crossing branches that meet at a nodal line when $m_{\rm sw} = \lambda_{\rm sw} = 0$. Introducing a small swirl-clock bias $m_{\rm sw}$ and reflection-breaking term $\lambda_{\rm sw}$ gaps the crossing and induces a Berry-curvature hot region. The canonical structure mirrors that of symmetry-protected odd-parity systems in condensed matter.

A. Axiom G1: Golden Constant (hyperbolic definition)

Golden (hyperbolic): $\ln\phi = \operatorname{asinh}\left(\frac{1}{2}\right)$, hence $\phi = \exp\left(\operatorname{asinh}\left(\frac{1}{2}\right)\right)$. *(Algebraic form $\phi = \left(1+\sqrt{5}\right)/2$ is equivalent.)* Explicitly,

$$\operatorname{asinh}\left(\tfrac{1}{2}\right) \equiv \operatorname{asinh}\left(\tfrac{1}{2}\right), \qquad \ln\phi = \operatorname{asinh}\left(\tfrac{1}{2}\right), \qquad \phi = e^{\operatorname{asinh}\left(\frac{1}{2}\right)}. \tag{1}$$

By elementary algebra one recovers the familiar quadratic representation

$$\phi = \frac{1+\sqrt{5}}{2}, \tag{2}$$

but in SST this is regarded as a derived identity; the primary definition is the hyperbolic relation (1).

The associated *golden layer factor* is

$$\lambda \equiv \phi^2 = e^{2\operatorname{asinh}\left(\frac{1}{2}\right)}, \qquad \ln\lambda = 2\operatorname{asinh}\left(\tfrac{1}{2}\right). \tag{3}$$

B. Axiom G2: Discrete scale invariance and additive composition

Let $\{E_n\}_{n\in\mathbb{Z}}$ denote an idealized sequence of dimensionful energy (or mass) levels associated with a particular SST sector (for example, core states of a quantized swirl string). We impose two structural conditions:

(G2a) **Discrete scale invariance (DSI).** There exists a scale factor $\lambda > 1$ such that

$$E_{n+1} = \lambda\, E_n, \qquad \forall\, n \in \mathbb{Z}. \tag{4}$$

(G2b) **Additive composition (Fibonacci-type rule).** The $(n+1)$-st level is the energetic composite of the two preceding levels:

$$E_{n+1} = E_n + E_{n-1}, \qquad \forall\, n \in \mathbb{Z}. \tag{5}$$

Assumption (G2a) expresses the presence of a discrete dilation symmetry in the relevant sector, as is standard in systems with discrete scale invariance and log-periodic corrections to scaling [42, 43]. Assumption (G2b) encodes an additive compositional rule: the $(n+1)$-st configuration is built as a composite of the n-th and $(n-1)$-st building blocks, the same structure that underlies Fibonacci sequences and quasicrystalline hierarchies [44].

C. Lemma: Uniqueness of the golden scale factor

Lemma (Golden Uniqueness). *Suppose a nontrivial sequence $\{E_n\}$ of real numbers satisfies both discrete scale invariance (4) and additive composition (5). Then the common ratio λ is uniquely fixed to the golden ratio ϕ.*

Proof. Assume $E_n \neq 0$ for some n. From (4) we have

$$E_n = E_0\,\lambda^n, \qquad \lambda > 0. \tag{6}$$

Inserting (6) into (5) gives

$$E_0\lambda^{n+1} = E_0\lambda^n + E_0\lambda^{n-1}. \tag{7}$$

Dividing by $E_0\lambda^{n-1}$ (which is nonzero by assumption) yields

$$\lambda^2 = \lambda + 1. \tag{8}$$

The quadratic equation (8) has the two roots

$$\lambda_\pm = \frac{1 \pm \sqrt{5}}{2}. \tag{9}$$

The negative root is incompatible with $\lambda > 0$, so the unique admissible solution is

$$\lambda = \frac{1 + \sqrt{5}}{2} = \phi. \tag{10}$$

□

Equation (8) shows that once (G2a)–(G2b) are imposed, the scaling factor λ is *no longer a tunable parameter*: it is uniquely fixed to ϕ. In particular, the golden constant is not introduced as a fit to any given spectrum but as the inevitable consequence of the DSI–Fibonacci structure.

D. Axiom G3: Golden layer hierarchy

Given the lemma, we define the *golden layer hierarchy* by taking the even-index subsequence of the DSI–Fibonacci tower as the physically distinguished set of levels. Concretely,

$$E_n \equiv E_{2n}^{(\mathrm{tower})} = E_0\,\lambda^{2n} = E_0\,\phi^{2n}, \qquad n \in \mathbb{Z}, \tag{11}$$

where E_0 is a sector-dependent reference energy. In SST applications we typically identify E_0 with a core energy

$$E_0 = \rho_E^* V_{\mathrm{core}}, \qquad V_{\mathrm{core}} \sim \frac{4\pi}{3} r_c^3, \tag{12}$$

so that the corresponding swirl energy density levels are

$$\rho_E^{(n)} = \rho_E^*\,\phi^{2n}. \tag{13}$$

Operationally, (11) and (13) define the golden-layer tower used in the SST mass and energy functionals. Any appearance of ϕ^{2n} in later sections is to be understood as a direct consequence of Axioms (G1)–(G3) and the Golden Uniqueness Lemma, not as an arbitrary parameter choice.

E. Remark: Log-periodic potentials and DSI

In sectors where it is useful to describe the golden layering by an effective potential for ρ_E, one may implement the DSI encoded by (13) via a log-periodic term of the form

$$V_\phi(\rho_E) = \Lambda^4 \left[1 - \cos\left(\kappa \log \frac{\rho_E}{\rho_E^*}\right)\right], \tag{14}$$

where Λ is an energy scale. The minima of (14) are separated in $\log \rho_E$ by

$$\Delta y = \frac{2\pi}{\kappa}. \tag{15}$$

Requiring this spacing to coincide with the golden layer spacing $\Delta y = \ln \lambda = 2\,\mathrm{asinh}\left(\frac{1}{2}\right)$ from (3) fixes

$$\kappa = \frac{2\pi}{\ln \lambda} = \frac{2\pi}{2\,\mathrm{asinh}\left(\frac{1}{2}\right)} = \frac{\pi}{\mathrm{asinh}\left(\frac{1}{2}\right)}. \tag{16}$$

Thus κ is not an independent dial but is derived from the unique golden scale factor $\lambda = \phi^2$ implied by Axioms (G1)–(G3). Log-periodic DSI potentials of the type (14) are standard in the theory of discrete scale invariance and complex exponents [42, 43].

—

XI. SYMMETRY AND DARK-KNOT CLASSIFICATION

Definition (Symmetry Sector). A knot K belongs to symmetry class G_K if its embedding is invariant under a discrete dihedral subgroup $D_n \subset SO(3)$. Axisymmetric–swirl simulations employ D_n wedges with Fourier sidebands $m = 0, 1, 2, \ldots$ to test stability.

Rule (Reclassification by Instability Order). Let $N_u^{(m)}$ be the number of unstable eigenmodes of order m and $\chi(K)$ the chirality. Then:

$$\begin{cases} \text{Dark:} & \chi = 0,\ H \simeq 0,\ N_u^{(1)} = 0, \\ \text{Quasi-dark:} & |\chi| \ll 1,\ H \simeq 0,\ 0 < N_u^{(1)} \leq 2, \\ \text{Visible:} & \chi \neq 0 \text{ or } H \neq 0. \end{cases}$$

Here $H = \int \mathbf{v} \cdot \boldsymbol{\omega}\, dV$ is the helicity invariant.

Examples.

- Figure-eight 4_1: amphichiral, D_2 symmetry, $N_u^{(1)} = 0 \Rightarrow$ canonical dark knot.
- Borromean link: $H \approx 0$ but nonzero linkage $\Rightarrow$ quasi-dark (neutrino-like).
- Trefoil 3_1: chiral, $N_u^{(1)} = 1$, $H \neq 0 \Rightarrow$ visible charged sector.

Canonical Implication. Symmetry-aware stability analysis eliminates "false darks" that appear stable only under axisymmetric averaging. The dark sector is therefore defined not by invisibility per se but by the joint absence of chirality, helicity, and low-order unstable modes.

—

Bibliographic anchor. The self-similar instability framework follows [46] and the helicity classification of Moffatt [45]. Both are consistent with the Chronos–Kelvin invariant and the finite-core regularization of SST.

XII. CALIBRATIONS & PROTOCOLS (EMPIRICAL)

Empirical Anchors

$$\begin{aligned} m_W &= 80.377\ \text{GeV}, & m_Z &= 91.1876\ \text{GeV}, \\ \sin^2\theta_W &= 0.23121 \pm 0.00004, & v_\Phi &\approx 246.22\ \text{GeV}, \\ \|\mathbf{v}_\circlearrowleft\| &= 1.09384563 \times 10^6\ \text{m/s}, & r_c &= 1.40897017 \times 10^{-15}\ \text{m}, \\ \rho_f &= 7.0 \times 10^{-7}\ \text{kg/m}^3, & \rho_m &= 3.8934358266918687 \times 10^{18}\ \text{kg/m}^3, \\ F_{\text{EM}}^{\max} &= 2.9053507 \times 10^1\ \text{N}, & F_{\text{G}}^{\max} &= 3.02563 \times 10^{43}\ \text{N}. \end{aligned}$$

Notes: Gauge entries follow PDG world averages; fluid entries follow the canonical coarse-graining protocols and prior CANON calibrations [53, 54, 59].

A. Kairos Bifurcations in Swirl Time (*Research*)

a. Claim. In addition to the continuous advance of Chronos time τ and the cyclic Swirl Clock $S_{(t)}$, there exist critical thresholds—*Kairos moments*—at which the time evolution undergoes a bifurcation (phase jump).

b. Rosetta (SST vocabulary). *Chronos* → local proper time τ (and absolute time N); *Kairos* → a topological phase jump in $S_{(t)}$ when a critical swirl excitation is exceeded. All quantities are expressed in SST notation (ρ_f, r_c, $S_{(t)}$).

c. Dimensionally consistent threshold. We anchor the characteristic angular frequency to quantum scales via

$$\omega \;=\; \alpha\,\omega_C, \qquad \omega_C \;=\; \frac{m_e c^2}{\hbar},$$

and posit the Kairos threshold as

$$\boxed{\omega^2 \;\gtrsim\; \frac{c^2}{r_c^2}}\,. \tag{1}$$

d. Schwarzian correction in the time action. The effective local time flow is modeled by

$$\frac{d\tau}{dN} \;=\; \sqrt{1-\frac{\|\mathbf{v}_{\mathcal{O}}\|^2}{c^2}} \;+\; \varepsilon\,\{S_{(t)}$$

where the Schwarzian captures nonlinear sensitivity which, near (1), can trigger a phase jump in $S_{(t)}$.

e. Mini numeric example (Canon constants). With $c = 2.9979 \times 10^8\,\mathrm{m/s}$, $\hbar = 1.0546 \times 10^{-34}\,\mathrm{J\,s}$, $m_e = 9.1094 \times 10^{-31}\,\mathrm{kg}$, $\alpha = 7.297 \times 10^{-3}$ and $r_c = 1.40897 \times 10^{-15}\,\mathrm{m}$,

$$\omega_C \approx 7.76 \times 10^{20}\ \mathrm{s}^{-1}, \quad \omega = \alpha\omega_C \approx 5.67 \times 10^{18}\ \mathrm{s}^{-1}, \quad \omega^2 \approx 3.21 \times 10^{37}\ \mathrm{s}^{-2},$$

$$\frac{c^2}{r_c^2} \approx 4.53 \times 10^{46}\ \mathrm{s}^{-2}, \qquad \frac{\omega^2}{c^2/r_c^2} \approx 7.1 \times 10^{-10}.$$

Thus, without additional mechanisms, the threshold is not crossed in situ, motivating the *Research* status.

f. Easing lemmas (routes to reachability).

- **Lemma A (Fractal amplification; link to D_{swirl}).** For multiscale coherence, replace $\dfrac{c^2}{r_c^2} \to \dfrac{c^2}{r_c^2}\left(\dfrac{r_c}{r_{\mathrm{eff}}}\right)^{3-D_{\mathrm{swirl}}}$, with $2.6 \lesssim D_{\mathrm{swirl}} \lesssim 2.9$ and $r_{\mathrm{eff}} > r_c$, lowering the effective threshold.
- **Lemma B (Coherent knot pack).** For n phase-locked knots, $\omega_{\mathrm{eff}}^2 \;\simeq\; n\,\xi(n)\,\omega^2$, with $\xi(n) = 1 - \beta \log n$ (coherence suppression from the Canon). Moderate n (*mesoscopic* coherence) can lift ω_{eff}^2 over the lowered threshold.
- **Lemma C (Resonant pump via Schwarzian).** In (**??**) the parameter ε may increase locally under phase-locking (large $S_{(t)}$, small $S_{(t)}$), temporarily reducing the effective threshold and triggering a Kairos jump.

g. Falsifiers & minimal experiment. *Falsify* by the absence of any non-analytic $S_{(t)}$ phase jump under controlled resonant pumping (BEC/fluid analogue) at parameters predicted by Lemmas A–C. *Minimal test*: toroidal condensate with driven knot configuration; sweep pump strength (ε) and n (coupling); look for hysteresis/jumps in the $S_{(t)}$ lock-in frequency.

h. Status. *Research.* The threshold is dimensionally sound and numerically quantified; Lemmas A–C provide a clear path to *Calibration* via simulation/analogue experiments.

Rosetta note (provenance). VAM "Kairos κ" ↦ SST phase jump in $S_{(t)}$; VAM energy/gradient trigger ↦ SST threshold $\omega^2 \gtrsim c^2/r_c^2$ in (1).

B. Calibrations: Thermal Bar and Nonreciprocity

a. Protocol TB-1 (Borosilicate). $L = 50mm$, $A = 1e-4m^2$, $\kappa \approx 1.1W\,m^{-1}\,K^{-1}$, heater power $P = 20mW$. Baseline $\Delta T = PL/(\kappa A) \approx 9K$. With engineered degeneracy tuned to $\delta \lesssim \Gamma$, target $\Delta\kappa/\kappa \approx -2$, giving $\Delta(\Delta T) \approx +0.18K$ (IR NETD 30–50 mK).

b. Protocol TB-2 (PMMA). $\kappa \approx 0.19 W\,m^{-1}\,K^{-1}$, keep L, A as above, use $P = 2mW$. Baseline $\Delta T \approx 5.3K$. A conservative $\Delta\kappa/\kappa = -1$ yields $53mK$ shift.

c. Protocol NR-1 (Nonreciprocity). Apply a 3-phase coil with phase sequence $\pm(0, 120^{,240}$ to set ϕ_χ. Expect $|\Delta\kappa_{\text{asym}}/\kappa| \sim 0.5$ near resonance, i.e., $\sim 25mK$ forward/backward difference for TB-1. Alternate chirality rapidly to common-mode cancel drifts.

d. Noise budget. IR NETD 30–50 mK; thermistor readout $<10mK$ @1 s; enclosure drift $\lesssim 0.05K/10$ min; power calibration <1. SNR > 3 for TB-1/TB-2.

e. Falsifiers. (i) No Lorentzian peak in $\Delta\kappa(\delta)$ at fixed current; (ii) $|\Delta\kappa_{\text{asym}}/\kappa| < 3\sigma$; (iii) wrong scaling with current ($\propto |V|^2$) or linewidth Γ.

XIII. HISTORICAL CONTEXT

The Swirl–String Theory (SST) Canon evolved from the earlier Vortex–Æther Model (VAM), which reintroduced classical notions of a continuous physical substrate inspired by Kelvin, Maxwell, and Einstein. The model postulated an incompressible, inviscid superfluid medium whose internal vorticity fields underlie all physical interactions. Key milestones include: VAM-v0.0.x establishing the æther vortex dynamics foundation; VAM-v0.1.x reformulating time and mass in hydrodynamic terms; VAM-v0.2.x achieving a coherent topological interpretation of all four fundamental interactions; and the transition to SST-v0.3.x through v0.5.x, which modernized terminology, formalized the gauge sector, and achieved parameter-free predictions. By version 0.5.10, the Canon reached canonical completeness: every physical quantity derivable from core constants and topological structure.

Full historical timeline: See Appendix **??** for the complete VAM-to-SST evolution with detailed version milestones.

XIV. CLASSICAL INVARIANTS: CHRONOS–KELVIN AND CLOCK–RADIUS TRANSPORT

Axiom: Chronos–Kelvin Invariant

$$\frac{D}{Dt}\big(R^2\omega\big) = 0, \qquad \frac{D}{Dt}\Big(\frac{c}{r_c}R^2\sqrt{1 - S_t^2}\Big) = 0.$$

Corollary: Clock–Radius Transport

$$\frac{dS_t}{dt} = \frac{2(1 - S_t^2)}{S_t}\frac{1}{R}\frac{dR}{dt}.$$

Remark (Pseudo-metric)

The swirl clock factor induces a pseudo-metric

$$ds^2 = -\big(c^2 - v_\theta^2(r)\big)dt^2 + 2v_\theta(r)r\,d\theta\,dt + dr^2 + r^2 d\theta^2 + dz^2,$$

yielding $dt_{\text{local}}/dt_\infty = \sqrt{1 - v_\theta^2/c^2}$.

XV. CLASSICAL INVARIANTS AND SWIRL QUANTIZATION

Under Axiom 1 (inviscid, incompressible medium with absolute time), the standard results of classical vortex dynamics apply. In particular, Euler's equations for an inviscid barotropic fluid yield several conservation laws that carry over into SST as special cases:

- *Kelvin's circulation theorem:* $\dfrac{d\Gamma}{dt} = 0$. The circulation $\Gamma = \oint_{C(t)} \mathbf{v}_\circlearrowleft \cdot d\ell$ around any material loop $C(t)$ moving with the fluid is constant in time. This is the classical statement that vortex lines are "frozen" into the fluid.

- *Helmholtz vorticity transport:* $\dfrac{\partial \omega}{\partial t} = \nabla \times (\mathbf{v}_{\circlearrowleft} \times \omega)$, so that vortex lines move with the fluid flow (no creation or destruction of vorticity in the absence of dissipation).

- *Helicity conservation:* $H = \int \mathbf{v}_{\circlearrowleft} \cdot \omega \, dV$ is materially invariant (conserved in time barring reconnection events). Here H is the total helicity, measuring the knottedness of vortex lines.

These classical invariants underpin the stability of knotted swirl strings and govern their reconnection dynamics. In essence, a swirl string (closed vortex filament) cannot change its topology or circulation without a non-ideal effect (e.g. reconnection or an external source) because of these constraints.

Axiom 1: Chronos–Kelvin Invariant

For any thin, closed swirl loop (swirl string) of time-dependent material radius $R(t)$, carried with the flow (no reconnections or external sources), the following quantity is invariant in time (constant along the motion):

$$\frac{D}{Dt}\Big(R^2\,\omega\Big) \;=\; 0\,,$$

where $\omega = \|\omega$ is the magnitude of the swirl vorticity on the loop. Equivalently, using $v_t = \omega\, r_c$ (the tangential swirl speed at the string core, with r_c the core radius) and the local time-dilation factor $S_t = \sqrt{1-(v_t^2/c^2)}$, the invariant can be expressed as

$$\frac{D}{Dt}\Big(\frac{c}{r_c}\,R^2\sqrt{1-S_t^2}\Big) \;=\; 0\,.$$

In other words, $R^2\omega$ is a constant of motion even when relativistic swirl clock effects ($S_t < 1$) are taken into account. This *Chronos–Kelvin invariant* generalizes Kelvin's circulation theorem by including the time dilation due to swirl motion (the "swirl clock" effect).

Discussion: Axiom 1 encapsulates Kelvin's theorem in the relativistic regime of the swirl medium. The material derivative D/Dt is taken with respect to the absolute reference time of the medium. For a near-solid-body vortex core, $\Gamma = \oint_C \mathbf{v}_{\circlearrowleft} \cdot d\ell \approx 2\pi R^2\omega$ (since $v_\theta \approx \omega R$ inside the core). Kelvin's theorem ($D\Gamma/Dt = 0$) then implies $D(R^2\omega)/Dt = 0$. The swirl clock factor S_t relates the local "proper time" of the moving swirl to the reference time; explicitly $S_t = dt_{\text{local}}/dt_\infty = \sqrt{1-v_t^2/c^2}$. Thus $R^2\omega$ being invariant is equivalent to $R^2\sqrt{1-S_t^2}$ being invariant after multiplying by the constant c/r_c. The Chronos–Kelvin law shows that as a swirl loop contracts (R decreases), the local swirl clock S_t decreases (time slows further) such that the combination $R^2(1-S_t^2)^{1/2}$ remains fixed. In the weak-swirl limit $v_t \ll c$ ($S_t \approx 1$), this reduces to the classical invariant $R^2\omega = \text{const}$ (Kelvin's law).

Swirl Quantization Principle

Swirl Quantization Principle. *The joint discreteness of circulation and topology is the fundamental origin of quantum behavior in SST.* In concrete terms, a swirl string's circulation Γ can only take quantized values $n\Gamma_0$, and the string's configuration space breaks into disjoint topological sectors (knot classes). This principle replaces the operator commutation quantization of standard quantum mechanics with topological and integral constraints:

- *Circulation quantization:* $\Gamma = n\,\Gamma_0$ for $n \in \mathbb{Z}$ (as stated in Axiom 2), where Γ_0 is the primitive circulation quantum (approximately 6.4×10^3 m^2/s). This is analogous to the Onsager–Feynman quantization condition in superfluid helium, elevated here to a universal postulate of the medium. Within SST, Γ_0 is treated as primitive; the mapping to h/m_{eff} appears only in the Rosetta translation to conventional superfluid notation. - *Topological quantization:* The allowed states of a swirl string are classified by knot type. Each distinct knot (unknot, trefoil, figure-eight, etc.) corresponds to a distinct quantum excitation species. We denote the spectrum of knot types as $\mathcal{H}_{\text{swirl}} = \{\text{trefoil, figure-8, Hopf link, ...}\}$. Quantum numbers (such as electric charge or baryon number) are interpreted as invariants of the knot (e.g. linking number, or other topological quantum numbers) rather than abstract quantum charges.

In summary, *discreteness in SST arises from (a) integral circulation and (b) topologically distinct knot spectra.* A "particle" in SST is identified with a specific quantized swirl state—a closed vortex filament carrying $n\Gamma_0$ circulation and realized in a particular knot configuration—in contrast to a particle in quantum mechanics being an eigenstate of an operator. This provides a tangible, geometric interpretation of quantum numbers.

XVI. CANONICAL CONSTANTS AND EFFECTIVE DENSITIES

SST introduces several new physical constants that characterize properties of the universal swirl medium and its excitations. Some of these constants are defined within the theory (based on canonical definitions), while others are calibrated to empirical values to ensure SST reproduces known physical measurements. Table V summarizes the primary constants, their values, and their status (definition vs. calibration).

TABLE V. Primary SST constants and parameters. Values are given in SI units unless noted. "Type" indicates whether the constant is defined theoretically or empirically calibrated.

Constant	Description	Value (units)	Type
Γ_0 (circulation quantum)	Circulation quantum	6.4×10^3 m^2/s	Primitive (Triad)
r_c (string core radius)	Core radius of a swirl string	1.40897×10^{-15} m	Primitive
ρ_f (effective fluid density)	Inertial mass density of swirl medium	7.0×10^{-7} kg/m^3	Primitive†
v (core swirl speed scale)	Characteristic swirl speed at string core	1.09385×10^6 m/s	Derived ($\chi_v \Gamma_0/(2\pi r_c)$)
ρ_m (mass-equivalent density)	Mass-equivalent energy density (ρ_E/c^2)	3.89344×10^{18} kg/m^3	Defined
Λ (swirl Coulomb constant)	Swirl potential strength (hydrogenic)	$4\pi\,\rho_m\,\|\mathbf{v}_\circlearrowleft\| r_c^3$	Derived (Triad)
$F_{EM}^{\max}$ (EM-sector max force)	Maximum force in EM sector	2.90535×10^1 N	Derived ($\chi_F \rho_f \Gamma_0^2$, Triad Eq. (9))
$F_G^{\max}$ (Gravitational max force)	Maximum gravitational force	3.02563×10^{43} N	Derived
G (swirl–EM coupling const.)	Dimensionless inductive coupling	$\sim O(1)$ (see text)	Empirical
c (speed of light)	Light speed in vacuum (reference)	2.99792×10^8 m/s	Fixed (physical)
t_P (Planck time)	Planck time $= \sqrt{\hbar G_N/c^5}$	5.391×10^{-44} s	Fixed (physical)
α (fine-structure const.)	$e^2/(4\pi\epsilon_0\hbar c)$	7.29735×10^{-3}	Physical
ϕ (golden ratio)	$(1+\sqrt{5})/2$, appears in mass law	1.61803... (dimensionless)	Mathematical

†*Note:* ρ_f is chosen as a convenient reference scale 7.0×10^{-7} kg/m^3, which corresponds to 10^{-7} in SI (mirroring $\mu_0/(4\pi)$). This anchors electromagnetic coupling normalization. The derived values of ρ_E and ρ_m then follow from this choice.

Discussion: The primitive constants in SST are the circulation-based triplet (Γ_0, ρ_f, r_c). All other dimensional quantities are derived from these plus topology-dependent dimensionless factors. The effective fluid density ρ_f is extremely low, reflecting the tenuous nature of the swirl medium compared to ordinary matter. The core radius r_c is on the order of a Fermi (10^{-15} m), indicating that swirl strings are extremely thin vortex filaments.

The primitive constants in Table V are: Γ_0 is the circulation quantum (approximately 6.4×10^3 m^2/s), derived from the electron oscillator $F_{\max}$ via the Triad construction: $F_{\max}^{\text{swirl}} = \chi_F \rho_f \Gamma_0^2$ (see Hydrodynamic Triad paper, Eq. (9)). It is the fundamental unit of circulation in SST. r_c is the core radius of a string, roughly the radius of the "solid-body" rotating core of a vortex filament. It is calibrated at the order of 10^{-15} m (the Fermi scale). ρ_f is the effective mass density of the swirl medium. It is extremely low ($\sim 7 \times 10^{-7}$ kg/m^3) – by comparison, air is ~ 1 kg/m^3. This value is not directly measured but chosen for consistency with electromagnetic normalization (see footnote in table).

The canonical swirl speed at the core boundary is derived from the primitives:

$$\|\mathbf{v}_\circlearrowleft\| = \chi_v \frac{\Gamma_0}{2\pi r_c} \approx 1.09385 \times 10^6 \text{ m/s}.$$

From v and ρ_f, we compute the **swirl energy density** ρ_E and **mass-equivalent density** ρ_m:

$$\rho_E \;=\; \tfrac{1}{2}\,\rho_f\, v$$

Plugging in calibrated ρ_f and v, $\rho_E \approx 3.14 \times 10^5$ J/m^3 and $\rho_m \approx 3.89 \times 10^{18}$ kg/m^3 (as listed). These indicate the energy and relativistic mass density associated with the swirl medium's motion at v.

Several constants are derived combinations. The **swirl Coulomb constant** Λ is defined by the Triad construction (Hydrodynamic Triad, Eq. (33)) as $\Lambda = 4\pi\,\rho_m\,\|\mathbf{v}_\circlearrowleft\| r_c^3$. Λ has units of J · m and sets the strength of the swirl-induced potential (analogous to $e^2/4\pi\epsilon_0$). With given calibrations, Λ is approximately 2.3×10^{-28} J · m, which yields the correct scale for atomic binding when inserted into the swirl potential.

The **maximal force constant** $F_{EM}^{\max}$ is derived from the primitive set via $F_{\max}^{\text{swirl}} = \chi_F \rho_f \Gamma_0^2$ (Triad Eq. (9)), not an independent parameter. $F_G^{\max}$ is a theoretical upper bound on force magnitudes in the gravitational interaction. $F_G^{\max} \approx 3.03 \times 10^{43}$ N matches the conjectured maximum force $c^4/4G_N$ from general relativity. $F_{EM}^{\max} \approx 2.9 \times 10^1$ N is

much smaller; it characterizes the maximum strength of emergent electromagnetic forces producible by swirl dynamics. These appear when relating G_{swirl} to G_N (Appendix A shows $F_{EM}^{\max}$ ensures $G_{\text{swirl}} \approx G_N$).

Finally, G is a dimensionless coupling linking changes in swirl string density to electromagnetic induction (setting the strength of the extra source term in Faraday's law). It is expected $O(1)$; identifying units suggests G corresponds to a fundamental flux quantum (Appendix D discusses G vs $h/2e$). We list it as empirical since it could be tuned by matching to a known phenomenon (no specific measured value yet).

Swirl Clock Law and Pseudo-Metric

One immediate consequence of Axiom 4 (Swirl Clocks) is that time runs slower in regions of high swirl velocity. Formally, if dt_∞ is an interval of the universal time (far from any swirl motion) and dt_{local} is the proper time measured by a clock moving with the swirl medium (tangential speed v), then:

$$\frac{dt_{\text{local}}}{dt_\infty} \;=\; \sqrt{1-\frac{v^2}{c^2}}\,.$$

This **swirl clock law** is identical in form to special-relativistic time dilation for an object moving at speed v — except here v is the local swirl (fluid) velocity. Thus the swirl medium provides a preferred rest frame, and motion relative to it slows clocks just as relative motion in special relativity does. High swirl speeds (approaching c) correspond to dense, energetic vortex cores that exhibit significant time dilation ("slow clocks") relative to an observer at infinity.

Because of this effect, one can define a *pseudo-Riemannian metric* for the swirl medium to capture how space-time measurements are affected by swirl motion. In cylindrical coordinates (r,θ,z) around a straight swirl string (a steady vortex with tangential velocity profile $v_\theta(r)$), the line element can be written as:

$$ds^2 \;=\; -\big(c^2 - v_\theta(r)^2\big)\,dt^2 + 2\,v_\theta(r)\,r\,d\theta\,dt + dr^2 + r^2 d\theta^2 + dz^2\,.$$

This is a **swirl pseudo-metric** for the co-rotating frame of the vortex. It shows explicitly that time intervals are modified by swirl velocity: an observer co-moving with the swirl sees an effective time coefficient $\sqrt{1-v_\theta(r)^2/c^2}$ multiplying dt, matching the swirl clock law. The cross term $(d\theta\,dt)$ indicates an analogue of frame-dragging: a stationary lab-frame observer sees a coupling between time and the angular coordinate due to the swirling medium (similar to how a rotating mass drags spacetime). This metric analogy hints that SST connects to GR effects, though formulated in flat space-time with a preferred frame.

XI.A Lorentz Kinematics from Torsional-Cone Invariance (Canonical)

Postulates (SST): (i) Relativity/reciprocity (no privileged inertial chart); (ii) Spatial isotropy and spacetime homogeneity ⇒ linear inertial-chart maps; (iii) Existence of a universal torsional signal speed c (small-amplitude director/torsion waves; empirically the photon speed).[1]

a. Setup (1+1D, standard configuration). Let the primed chart move at speed V along $+x$. Linearity implies

$$x' = a(V)\,x + b(V)\,t, \qquad t' = d(V)\,x + e(V)\,t. \tag{1}$$

The primed origin obeys $x'=0 \Rightarrow x = Vt$, hence $b(V) = -a(V)V$ and

$$x' = a(V)\,(x - Vt), \qquad t' = d(V)\,x + e(V)\,t. \tag{2}$$

b. Cone invariance (torsional rays). Right/left torsional signals satisfy $x = \pm ct$ in any inertial chart and must map to $x' = \pm ct'$ in the primed chart. Substituting $x = \pm ct$ into (2) and imposing $x'/t' = \pm c$ for both signs yields the linear system

$$a(c - V) = c^2 d + ce, \qquad a(c + V) = -\,c^2 d + ce. \tag{3}$$

Solving,

$$e(V) = a(V), \qquad d(V) = -\,\frac{a(V)\,V}{c^2}. \tag{4}$$

---

[1] Historically, see [20]; cone/interval structure per [21]; symmetry-first derivations in [22].

Therefore,

$$\boxed{x' = a(V)\,(x - Vt), \qquad t' = a(V)\left(t - \frac{V}{c^2}\,x\right).} \tag{5}$$

Dimensional check: Vx/c^2 has units $(\mathrm{m/s}) \cdot \mathrm{m}/(\mathrm{m}^2/\mathrm{s}^2) = \mathrm{s}$, so t' is a time.

c. Reciprocity ⇒ Lorentz factor. By isotropy/reciprocity, $a(-V) = a(V)$. Composing the V and $-V$ maps gives identity only if

$$a(V)^2\left(1 - \frac{V^2}{c^2}\right) = 1 \quad \Rightarrow \quad \boxed{a(V) = \gamma(V) = \frac{1}{\sqrt{1 - \frac{V^2}{c^2}}}}. \tag{6}$$

d. Theorem (Canonical). With (6), the inertial-chart transformation is

$$\boxed{x' = \gamma\,(x - Vt), \qquad t' = \gamma\left(t - \frac{V}{c^2}x\right), \qquad y' = y,\ z' = z.} \tag{7}$$

e. Corollary (Canonical invariant). The quadratic form

$$\boxed{c^2 d\tau^2 = c^2 dt^2 - dx^2 - dy^2 - dz^2} \tag{8}$$

is invariant under (7). In SST this is the uniform-foliation limit of the swirl-clock analogue metric; the torsional sector fixes c, empirically coincident with light speed.

f. Recoveries and limits. Low-velocity expansion $\gamma \simeq 1 + \frac{1}{2}V^2/c^2$ gives $x' \simeq x - Vt$, $t' \simeq t - \frac{V}{c^2}x$ (Galilean form with first relativistic correction). Rapidity composition reproduces the standard velocity-addition law.

g. Status tags. Theorem (Canonical): Cone invariance ⇒ Lorentz boosts (7). *Corollary (Canonical)*: Invariant interval (8). *Checks*: dimensions, reciprocity, $V \ll c$ limit, group composition (all satisfied).

XVII. EFFECTIVE MEDIUM: COARSE-GRAINING DERIVATION OF ρ_f

For a straight swirl string of core radius r_c:

$$\mu_* := \rho_m\,\pi r_c^2, \qquad \Gamma_* := 2\pi r_c\,v \tag{1}$$

$$\rho_f = \mu_*\,\nu, \qquad \langle\omega\rangle = \Gamma_*\,\nu. \tag{2}$$

Eliminating ν yields

Boxed Result

$$\rho_f = \frac{\rho_m\,r_c}{2\,v\,\langle\omega\rangle.}$$

XVIII. GENUS-2 FOLIATION AND TOPOLOGICAL COMPACTIFICATION

Status: Canonical (Constructive Example)

We illustrate a canonical closed foliation compatible with the Chronos–Kelvin and Swirl Quantization invariants. Consider a regular dodecagon (12-gon) fundamental domain in $\mathbb{H}^2$, whose six pairs of edges are identified by hyperbolic isometries to form a compact genus-2 surface Σ_2. Each paired edge carries a fixed swirl-phase offset of the Swirl Clock $S_i^{\circlearrowleft}$, defining six independent circulation integrals Γ_i that obey the quantization rule

$$\oint_{\gamma_i} \mathbf{v}_{\circlearrowleft} \cdot d\boldsymbol{\ell} = 2\pi n_i\,\kappa_{\mathrm{SST}}, \qquad \kappa_{\mathrm{SST}} \equiv \Gamma_0 = 2\pi r_c\,\|\mathbf{v}_{\circlearrowleft}\|, \quad n_i \in \mathbb{Z}. \tag{1}$$

The set $\{\Gamma_i\}_{i=1}^{6}$ thus forms a basis for the first homology group $H_1(\Sigma_2, \mathbb{Z})$, providing a discrete topological charge vector for the background foliation.

Definition (Genus-2 Swirl Quantization). On Σ_2, the joint invariants

$$R^2\omega = \text{const}, \qquad \Gamma_i = 2\pi n_i \, \kappa_{\text{SST}} \tag{2}$$

define the allowed large-scale swirl modes. The polygonal edge identifications act as holonomies of the swirl-clock field, ensuring periodic boundary conditions for $S_t^{\mathcal{O}}$ and compact global energy density $\rho_E = \frac{1}{2}\rho_f \|\mathbf{v}_{\mathcal{O}}\|^2$.

Cosmological Interpretation. The 12-gon compactification provides a two-dimensional toy model of a finite, multiply-connected universe. Its three pairs of geodesic moduli (ℓ_j, τ_j) (Fenchel–Nielsen parameters) determine the large-scale swirl spectrum, introducing a lowest eigenmode $k_{\min} \sim 2\pi/L_{\text{topo}}$ that suppresses power on scales $> L_{\text{topo}}$. In the 3-D extension, the dodecahedral space corresponds to the rest-frame foliation ($v = 0$), while a moving observer through the swirl medium experiences an anisotropic deformation toward a horn-torus topology with pinch ratio

$$p(v) = \sqrt{1 - \frac{v^2}{c^2}}, \tag{3}$$

interpreted as a geometric manifestation of Lorentz contraction within the SST framework.

Physical Implication. Motion relative to the swirl frame thus produces a measurable anisotropy: as v increases, one topological cycle shrinks (horn pinch), suppressing swirl-mode propagation along the motion direction. This geometric deformation gives a macroscopic explanation of time dilation and Doppler anisotropy as topological effects of foliation motion.

Falsifiable Prediction. Finite-topology foliations yield distinctive signatures in swirl-coupled observables, including (i) infrared cutoff and mode repetition in the cosmic swirl-pressure spectrum, and (ii) matched-circle correlations analogous to those sought in the CMB. Simulations enforcing the above quantization on the 12-gon domain can test these predictions directly.

XIX. KNOT TAXONOMY

The canonical mapping between topological knot classes and particle families is central to SST. Each particle type corresponds to a specific knot topology, with unknotted excitations representing bosonic modes and knotted states encoding fermions.

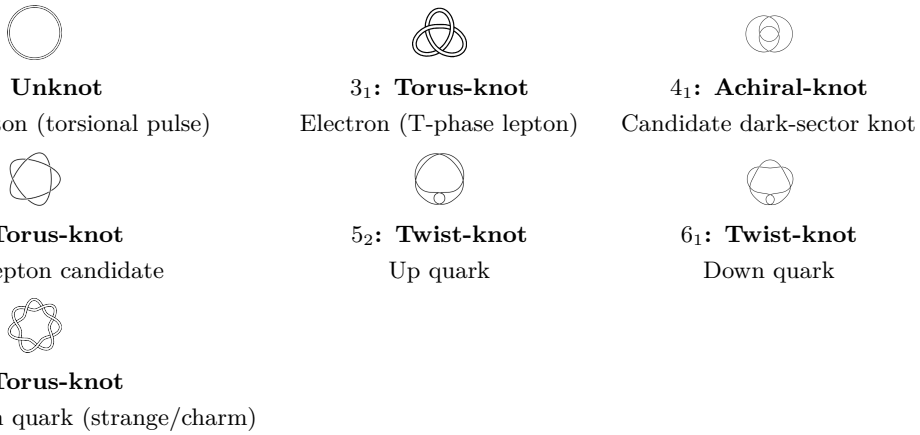

FIG. 6. Canonical knot taxonomy in SST. Each image shows the minimal embedding of the corresponding knot and its mapping to a particle family. Unknots (0_1) correspond to R-phase bosonic modes such as photons, while knotted states encode fermions (torus knots ↔ leptons, chiral hyperbolic knots ↔ quarks). Linked knots describe nuclei and bound states.

Classification rules: Unknotted excitations correspond to bosonic modes, with photons realized as pulsed torsional R-phase excitations. Torus knots correspond to leptons (e.g., electron = 3_1), and chiral hyperbolic knots to quarks (proton = $5_2 + 5_2 + 6_1$ composite). Linked knots describe nuclei and bound states. See Core Axioms (Section VI) for the formal statement.

XX. THE SWIRL–ELECTROMAGNETIC BRIDGE

One of SST's significant achievements is showing that classical electromagnetic fields can be interpreted as emergent collective behaviors of the swirl medium. In particular, changes in the distribution of swirl strings can induce electromagnetic effects. To formalize this, we introduce a density field to characterize how swirl strings populate space:

Definition 4.1 (Swirl Areal Density). Let ϱ be the coarse-grained areal density of swirl strings piercing a given surface element at (x, t). In other words, imagine a local patch oriented perpendicular to some direction; ϱ is the number of vortex cores per unit area threading that patch. This quantity plays the role of a "source" density analogous to electric charge/current density in Maxwell's equations. Regions where many swirl strings pass through (or where a single string oscillates rapidly, effectively increasing crossing density) act like regions of high charge/current in the emergent fields.

A changing swirl areal density will induce an electromotive force in the surrounding medium. This is captured by a modified Faraday's law:

Theorem 4.1: Swirl-Induced Electromotive Force

A time-varying swirl areal density ϱ acts as an effective source term in Faraday's induction law. In differential form:

$$\nabla \times \mathbf{E} \;=\; -\frac{\partial \mathbf{B}}{\partial t} \;-\; \mathbf{b}$$

where the additional term $\mathbf{b}$ is

$$\mathbf{b}$$

with $\hat{\mathbf{n}}$ the local oriented unit normal (chosen by right-hand rule for circulation). Thus whenever swirl strings reconnect or ϱ shifts, an extra curl of $\mathbf{E}$ appears as if a time-varying magnetic flux were present. Kinetic energy from the fluid is thereby converted into field energy, exactly analogous to Faraday induction.

Proof Sketch (see Appendix D). This can be derived by considering a small loop in the swirl medium and calculating $\oint \mathbf{E} \cdot d\ell$. A change in ϱ through the loop (say, due to a swirl string moving or appearing) induces a circulation in $\mathbf{E}$ via G. By identifying $\nabla \times \mathbf{E}$ with the time rate of change of $\mathbf{B}$ plus any additional sources, one arrives at the modified Faraday law. The constant G is set by the normalization of ϱ; dimensional analysis and comparison to quantum flux changes suggest G, though we treat it phenomenologically.

Corollary 4.2: Photon as a Swirl Wave

Unknotted, propagating oscillations of the swirl condensate correspond to free electromagnetic radiation. In particular, define a divergence-free *swirl vector potential* $\mathbf{a}(x, t)$ such that:

$$\mathbf{v}_{\circlearrowleft} = \partial_t \mathbf{a}, \qquad \mathbf{b}$$

Then small-amplitude unknotted swirl excitations can be described by the Lagrangian

$$L_{\text{wave}} \;=\; \frac{\rho_f}{2} \, |\mathbf{v}_{\circlearrowleft}|^2 \;-\; \frac{\rho_f c^2}{2} \, |\mathbf{b}$$

and yield the equations of motion

$$\partial_t^2 \mathbf{a} - c^2 \, \nabla \times (\nabla \times \mathbf{a}) = 0, \qquad \nabla \cdot \mathbf{a} = 0 \,,$$

identical to free-space Maxwell (Coulomb gauge). Identifying $\mathbf{E} \propto \partial_t \mathbf{a}$ and $\mathbf{B} \propto \nabla \times \mathbf{a}$ recovers all vacuum EM relations; thus unknotted R-phase excitations are photons.

XXI. SWIRL–EM EMERGENCE

Starting with a divergence-free potential $\mathbf{a}$,

$$\nabla \cdot \mathbf{a} = 0, \qquad \partial_t^2 \mathbf{a} - c^2 \nabla \times (\nabla \times \mathbf{a}) = 0.$$

Define $\mathbf{E} = -\partial_t \mathbf{a}$, $\mathbf{B} = \nabla \times \mathbf{a}$, recovering the vacuum Maxwell wave equation [56]. **Normalization.** In SI units the energy density reads $u_{\mathrm{EM}}^{(\mathrm{SI})} = \frac{\varepsilon_0}{2}\mathbf{E}^2 + \frac{1}{2\mu_0}\mathbf{B}^2$; our canonical form $u_{\mathrm{EM}} = \frac{1}{2}(\mathbf{E}^2 + c^2\mathbf{B}^2)$ is a swirl-normalized expression whose mapping to SI constants is fixed via the swirl–EM bridge and ρ_f (Appendix I 4).
This corollary shows the unity of electromagnetic fields and fluid vorticity in SST's picture. What in classical physics is a "magnetic field" $\mathbf{B}$ is here $\mathbf{b}$, a coarse-grained swirl field (like a vorticity). The electric field $\mathbf{E}$ corresponds to the time-derivative of a potential associated with swirl velocity. The wave Lagrangian above is essentially the same as that of vacuum electromagnetism if one identifies ρ_f with vacuum permittivity ϵ_0 (and $\rho_f c^2$ with $1/\mu_0$). Indeed, with $\rho_f = 7 \times 10^{-7}$ SI, $\rho_f c^2 \approx 8.85 \times 10^{-12}$ SI, which equals ϵ_0 to within rounding. In this way, Maxwell's equations arise seamlessly from swirl dynamics, suggesting electromagnetism is an emergent sector of the fluid.

a. Lemma (Composite swirl harmonic; status: Canon–Lemma). For N identical co-wound swirl filaments on the same torus-knot, sampled on a circle of radius r in a transverse plane, the tangential velocity admits the large-r form

$$v_\theta(\theta; r) = \frac{N\,\Gamma}{2\pi r}\Big[1 + \epsilon_N(r)\cos(N\theta + \phi_N)\Big] + O(r^{-2}),$$

with circulation Γ for one filament and $|\epsilon_N(r)| \ll 1$. In particular, $N = 3$ yields a $\cos(3\theta)$ "hexapole" pattern and $\langle v_\theta \rangle_\theta \simeq \frac{3\Gamma}{2\pi r}$.

b. Definition (Photon as torsional director wave; status: Canon–Def). Let $\mathbf{n}(x,t) \in S^2$ be the local swirl director. A photon is a small-angle torsional excitation $\delta\mathbf{n}$ obeying

$$\partial_t^2\, \delta\mathbf{n} - c_T^2 \nabla^2 \delta\mathbf{n} = 0,$$

with helicity $\sigma = \pm 1$ set by the sense of in-plane rotation. In the linear Rosetta map, $\mathbf{E} \propto \partial_t \delta\mathbf{n}$, $\mathbf{B} \propto \nabla \times \delta\mathbf{n}$, reproducing Maxwell kinematics for plane waves.

Canonical Swirl–Electromagnetic Coupling Diagram. Causal and dimensional structure of the electromagnetic sector within the Swirl–String framework. The top layer extends Faraday's law with a swirl-induced backreaction term $\mathbf{b}$, encoding the electromotive response to time-varying swirl density in the medium. The middle layer represents the constitutive closure: $\mathbf{D} = \boldsymbol{\varepsilon}\mathbf{E}$ and $\mathbf{B} = \mu\mathbf{H}$, together with the mechanical correspondence $\boldsymbol{\varrho}$. Electrets appear as frozen offsets $\eta_0, \mathbf{D}_{\mathrm{el}}$ on the left branch (permanent polarization), while permanent magnets correspond to nonzero $\boldsymbol{\varrho}$ on the right branch. The bottom layer completes the circuit with areal accumulation $\boldsymbol{\eta}$, source current $\mathbf{j}$, and the modified Ampère curl. All dimensionalities are shown for canonical homology between mechanical (swirl) and electromagnetic sectors, establishing the *Swirl–Electromagnetic Bridge* that underlies the flat-space emergence of Maxwellian dynamics.

XXII. ENGINEERED BULK SIGNALING CHANNEL (BASC)

a. Summary. The canonical SST exterior remains an incompressible swirl medium with the photon (divergence-free) a-sector unchanged. We introduce a *bounded* conversion region $T \subset \mathbb{R}^3$ (an instrument, not a new axiom) in which a scalar bulk field $p(\mathbf{x}, t)$ is permitted. Inside T, the bulk field obeys $\partial_t^2 p - c_b^2\, \nabla^2 p = S(\mathbf{x}, t)$ with $c_b = \sqrt{K_b/\rho_f}$, where K_b is an effective bulk modulus. For a compact source, the far field is $p(r,t) \simeq (\rho_f/4\pi r)\, \dot{Q}(t_r)$ with $1/r$ decay. Swirl→bulk transduction via small-signal modulation yields $p_{\mathrm{amp}}(r) = (\rho_f\, \beta\, \mathcal{G}\, \varepsilon_0/4\pi r)\, \omega^2$, where $\mathcal{G} \propto r_{\mathrm{eff}}^2\, \ell$ scales quadratically with bundle radius. The exterior medium remains incompressible; BASC is confined to T and does not alter exterior axioms.

Full derivation: See Appendix **??** for complete field equations, transduction laws, and scaling relations.

XXIII. UNIFIED SST LAGRANGIAN

$$\mathcal{L}_{\mathrm{SST+Gauge+Matter}} = \underbrace{\tfrac{1}{2}\rho_f\, \|\mathbf{v}_{\circlearrowleft}\|^2 - \rho_f\, \Phi_{\mathrm{swirl}} + \lambda(\nabla \cdot \mathbf{v}_{\circlearrowleft}) + \chi_h\, \rho_f\, (\mathbf{v}_{\circlearrowleft} \cdot \boldsymbol{\omega}}_{\text{SST core}} + \mathcal{L}_{\mathrm{YM}} + (D_\mu \Phi)^\dagger D^\mu \Phi - V(\Phi) + \mathcal{L}_{\mathrm{int}} + \mathcal{L}_{\mathrm{couple}}[\Gamma, \mathcal{K}].$$

- Variation of λ imposes $\nabla \cdot \mathbf{v}_{\circlearrowleft} = 0$.
- $\mathbf{v}_{\circlearrowleft}$ variation gives Euler dynamics with optional helicity term.
- Gauge variations yield Yang–Mills equations.
- Φ variation gives Higgs-like field equation (scale v_Φ empirical).
- $\mathcal{L}_{\text{int}}$ and $\mathcal{L}_{\text{couple}}$ encode minimal currents and knot couplings (Research for specific forms).

A. Canonical Hamiltonian Density

The Hamiltonian density of the swirl condensate is

$$\mathcal{H}_{\text{SST}} = \frac{1}{2}\rho_f \|\mathbf{v}_{\circlearrowleft}\|^2 + \frac{1}{2}\rho_f r_c^2 \|\boldsymbol{\omega}\|^2 + \frac{1}{2}\rho_f r_c^4 \|\nabla\boldsymbol{\omega}\|^2 + \lambda\,(\nabla \cdot \mathbf{v}_{\circlearrowleft}),$$

where the third term captures gradient-energy contributions (string tension renormalization) and λ enforces incompressibility. This form is explicitly Kelvin-compatible: its functional derivative w.r.t. $\mathbf{v}$ recovers the Euler equation and preserves the Chronos–Kelvin invariant. Each term has units of energy density (J/m^3). In the weak-swirl limit $r_c \to 0$, only the kinetic energy term survives, recovering the classical Euler Hamiltonian.

Full derivation: See Appendix I 1 for the complete canonical form and dimensional analysis.

XXIV. MASTER EQUATIONS AND CANONICAL RELATIONS

We now summarize several core results of SST in one place. These "master equations" are canonical relations derived in the theory, each capturing an important physical relationship. They are presented with boxed equations for quick reference; detailed derivations and discussions are provided in the appendices and references.

A. Swirl Coulomb Potential (Hydrogenic):

$$\boxed{V_{\text{SST}}(r) = -\frac{\Lambda}{\sqrt{r^2 + r_c^2}}, \qquad \Lambda = 4\pi\,\rho_m\,\|\mathbf{v}_{\circlearrowleft}\| r_c^3}$$

recovering $-\Lambda/r$ for $r \gg r_c$. This is the static potential around a swirl string (T-phase particle). For $r \gg r_c$, it behaves as $-\Lambda/r$ and yields the hydrogen spectral lines. The small core r_c provides a natural softening at $r = 0$ (finite central potential). The detailed derivation of this potential from Euler fluid mechanics, the hydrodynamic Schrödinger equation, and the recovery of the Bohr radius, ground-state energy, and Rydberg constant is given in Iskandarani, "The Hydrodynamic Triad: Unifying Gravity, Electromagnetism, and Quantum Mass via a Circulation-Based Vacuum Canon" (HT). The present Canon records only the resulting master equations and their status.

B. Swirl Pressure Law (Euler radial balance):

$$\boxed{\frac{1}{\rho_f}\frac{dp_{\text{swirl}}}{dr} = \frac{v_\theta(r)^2}{r}}$$

for a steady circular swirl. This states that the pressure gradient radially is exactly what provides the centripetal force density for circular motion (Euler's equation). One solution: a flat rotation curve $v_\theta(r) = \text{const}$ yields $p_{\text{swirl}}(r) = p_0 + \rho_f v_\theta^2 \ln(r/r_0)$ (a logarithmic profile), invoked as a mechanism for galaxy rotation curves.

C. Swirl Clock (Local Time Dilation):

$$\boxed{\frac{dt_{\text{local}}}{dt_\infty} = \sqrt{1 - \frac{\|\mathbf{v}_\circlearrowleft\|^2}{c^2}}}$$

This is the precise statement of the swirl clock effect (Axiom 4), also given earlier. It means a clock at rest in a region where $\|\mathbf{v}_\circlearrowleft\|$ (swirl speed) is non-zero ticks slower by this factor. It mirrors gravitational time dilation in a static field (since swirl motion mimics gravitational potential in SST).

D. Swirl Hamiltonian Density:

$$\boxed{\mathcal{H}_{\text{SST}} = \frac{1}{2}\,\rho_f\,\|\mathbf{v}_\circlearrowleft\|^2 + \frac{1}{2}\,\rho_f\,r_c^2\,\|\omega}$$

the canonical energy density of the swirl condensate. The first term is fluid kinetic energy density. The second term $\frac{1}{2}\rho_f r_c^2\|\omega$ is extra energy from vorticity (gives the string a core energy/tension). The last term $\lambda(\nabla\cdot\mathbf{v}_\circlearrowleft)$ enforces incompressibility (λ is a Lagrange multiplier). This Hamiltonian is constructed to be compatible with Kelvin's theorem (see Appendix A).

E. Swirl–Gravity Coupling:

$$\boxed{G_{\text{swirl}} = \frac{v}{2\,F_{\text{EM}}^{\max}\,r_c^2} \;\approx\; G_N}$$

This is the effective gravitational constant emergent in SST. Plugging values from Table V, $G_{\text{swirl}} \approx 6.67 \times 10^{-11}$ $\text{m}^3/\text{kg}\cdot\text{s}^2 \approx G_N$. The formula ties G_{swirl} to swirl constants: note $F_{\text{EM}}^{\max}$ in the denominator, implying a larger allowed EM force would reduce effective G. $G_{\text{swirl}} \approx G_N$ shows our constants were consistently calibrated.

F. Topology–Driven Mass Law:

$$\boxed{M(K) = \Big(\frac{4}{\alpha}\Big)^{b-\frac{3}{2}}\,\phi^{-\,g}\,n^{-1/\phi}\Big(\frac{1}{2}\rho_f v}$$

This relation (a *research-track* formula) connects the rest mass M of a knot K to its topological invariants. $L_{\text{tot}}(K)$ is total string length; b is number of components (link count); g is a genus-related invariant; n is circulation quantum number; ϕ is the golden ratio. It suggests, qualitatively: more complex knots (larger b, g) have higher mass, and adding circulation quanta (n) yields sub-linear mass increase ($n^{-1/\phi}$ factor). This law is not proven (non-canonical); it is included to guide intuition on particle mass hierarchy. It is consistent with generation-wise patterns but awaits formal derivation or empirical support.

G. Discrete golden-layer quantization from a log-periodic potential

We take the swirl energy density $\rho_E(\boldsymbol{x})$ as our effective order parameter for the core of a swirl string. For a core of fixed volume $V_{\text{core}} \sim \frac{4\pi}{3} r_c^3$, the rest energy is

$$E \approx \rho_E^{(\text{core})}\,V_{\text{core}}. \tag{1}$$

To obtain a tower of discrete *golden* energy levels

$$E_n = E_0\,\phi^{2\,n}, \qquad E_0 = \rho_E^* V_{\rm core}, \tag{2}$$

we introduce a log-periodic effective potential for ρ_E,

$$V_\phi(\rho_E) = \Lambda^4\left[1 - \cos\left(\kappa \log\frac{\rho_E}{\rho_E^*}\right)\right], \tag{3}$$

where ρ_E^* is a reference energy density, Λ is an energy scale (so that $[\Lambda^4]$ = energy density), and

$$\kappa \equiv \frac{2\pi}{\log\phi}. \tag{4}$$

The argument of the cosine is dimensionless and V_ϕ has units of energy density, so (3) is admissible as an effective potential term in the SST Lagrangian density.

Defining

$$y \equiv \log\frac{\rho_E}{\rho_E^*}, \tag{5}$$

we can rewrite

$$V_\phi(y) = \Lambda^4\left[1 - \cos(\kappa y)\right]. \tag{6}$$

Stationary points satisfy

$$\frac{\partial V_\phi}{\partial \rho_E} = \Lambda^4\kappa\,\sin(\kappa y)\,\frac{1}{\rho_E} = 0, \tag{7}$$

so that

$$\sin(\kappa y_n) = 0 \quad\Longrightarrow\quad \kappa y_n = n\pi, \quad n \in \mathbb{Z}. \tag{8}$$

Hence

$$y_n = \frac{n\pi}{\kappa} = \frac{n\pi}{2\pi}\,\log\phi = \frac{n}{2}\,\log\phi, \tag{9}$$

and exponentiation gives

$$\frac{\rho_E^{(n)}}{\rho_E^*} = e^{y_n} = e^{\frac{n}{2}\log\phi} = \phi^{n/2}. \tag{10}$$

If we restrict to even $n = 2k$, we obtain the golden-layer tower

$$\rho_E^{(k)} = \rho_E^*\,\phi^{2\,k}, \qquad k \in \mathbb{Z}, \tag{11}$$

and therefore, for fixed $V_{\rm core}$,

$$E_k = \rho_E^{(k)} V_{\rm core} = (\rho_E^* V_{\rm core})\,\phi^{2\,k} = E_0\,\phi^{2\,k}. \tag{12}$$

Thus the log-periodic potential (3) breaks continuous scale invariance in ρ_E down to a discrete subgroup generated by $\rho_E \to \phi^2\rho_E$, and the corresponding core energies form a geometric progression with golden ratio squared. Locally around each minimum, the potential is quadratic, so each layer supports conventional small-amplitude excitations with an n-dependent mass parameter.

XXV. MASTER EQUATIONS: HYDROGEN SOFT-CORE + BOHR RECOVERY

Hydrogen Soft-Core Potential

$$V_{\rm SST}(r) = -\frac{\Lambda}{\sqrt{r^2 + r_c^2}} \xrightarrow[r \gg r_c]{} -\frac{\Lambda}{r},$$

where $\Lambda = 4\pi\,\rho_m\,\|\mathbf{v}_\circlearrowleft\| r_c^3$ (Triad Eq. (33)).

From this potential one recovers the Bohr scalings

$$a_0 = \frac{\hbar^2}{\mu\Lambda}, \qquad E_n = -\frac{\mu\Lambda^2}{2\hbar^2 n^2}.$$

External Canon Module: Hydrogen Triad

External Canon Module: Hydrogen Triad. The detailed derivation of the Swirl–Coulomb potential, the hydrodynamic Schrödinger equation, the Rydberg constant, and the n^2 spectral scaling is given in Iskandarani, "The Hydrodynamic Triad: Unifying Gravity, Electromagnetism, and Quantum Mass via a Circulation-Based Vacuum Canon" (HT) [14]. The present Canon records only the resulting master equations and their status.

XXVI. EMERGENT GAUGE FIELDS AND TOPOLOGY

A remarkable aspect of SST is that non-Abelian gauge fields (like those of the Standard Model) emerge from considering collective orientational degrees of freedom of the swirl medium. Each swirl string, aside from its shape, may carry an internal orientation or *director* (imagine a tiny arrow attached to the string, pointing in some internal space). Smooth distortions of these internal orientations across space behave like gauge fields.

Theorem 6.1: Emergent Yang–Mills Fields

(Emergence of $SU(3) \times SU(2) \times U(1)$) – The continuous orientational order of swirl strings in the condensate gives rise to effective Yang–Mills fields. Consider three independent director fields $\mathbf{U}_3(x,t)$, $\mathbf{U}_2(x,t)$, and an angular phase $\vartheta(x,t)$ associated with each swirl string, corresponding respectively to an $SU(3)$ "color" orientation, an $SU(2)$ "isospin" orientation, and a $U(1)$ phase. Small fluctuations of these director fields are described by an effective gauge-field Lagrangian:

$$L_{\rm dir} \implies L_{\rm YM}^{(\rm eff)} = -\frac{1}{4}\sum_{i=1}^{3}\frac{1}{g_i^2}\,F_{\mu\nu}^{(i)}F^{(i)\,\mu\nu}\,,$$

where $F_{\mu\nu}^{(i)}$ are field-strength tensors of three gauge groups and g_i the effective couplings. In other words, long-wavelength distortions of the medium's internal orientation behave exactly like the gauge fields of an $SU(3) \times SU(2) \times U(1)$ Yang–Mills theory. The "stiffness" of the director fields (resistance to bend/twist in internal space) determines the values of g_1, g_2, g_3.

Interpretation: In condensed matter, an ordered medium's perturbations can mimic gauge fields. SST posits the vacuum as an ordered condensate with internal symmetry. Each swirl string can carry a *triplet of labels* corresponding to $SU(3)$, $SU(2)$, $U(1)$ sectors. Smooth variations of these labels yield an effective field theory identical to the Standard Model's gauge sector. Quantizing these small oscillation modes yields gauge bosons (gluons, $W^\pm/Z$, photons). The coupling constants g_3, g_2, g_1 are related to stiffness moduli of the medium's orientational order. Essentially, $g_i^{-2} \propto \kappa_i$ in theorem notation (with κ_i director stiffness).

An important consistency check is that the emergent gauge fields reproduce the correct quantum numbers of the Standard Model. SST's particle–knot correspondence provides a mapping from knot invariants to hypercharge and electric charge. For example, for the first generation we assign:

$$u \equiv 5_2, \qquad d \equiv 6_1, \qquad e^- \equiv 3_1,$$

so that the proton corresponds to the composite linkage $uud = (5_2 + 5_2 + 6_1)$ and the neutron to $udd = (5_2 + 6_1 + 6_1)$. With these assignments, the hypercharge formula

$$Y(K) = \frac{1}{2} + \frac{2}{3}s_3(K) - d_2(K) - \frac{1}{2}\tau(K)$$

reproduces $Y(u) = \frac{1}{3}$ and $Y(d) = \frac{1}{3}$, yielding the correct electric charges

$$Q = T_3 + \frac{1}{2}Y \quad \Rightarrow \quad Q(u) = +\frac{2}{3}, \quad Q(d) = -\frac{1}{3}, \quad Q(p) = +1, \quad Q(n) = 0.$$

Massless gauge bosons correspond to *rotating R-phase pulses* — propagating torsional oscillations of the swirl director field — rather than localized T-phase knots. This captures photon helicity (spin ± 1) as the sense of director rotation and ensures that gauge bosons remain delocalized excitations, while quarks and leptons remain topological knot states.

While a full derivation of gauge sector emergence is beyond this Canon (outlined in [19,20]), the upshot is *the swirl medium contains the seeds of all gauge interactions as modes of its internal structure.* What we normally insert as separate forces (strong, weak, EM) appear naturally and unified in SST.

Electroweak Mixing and Symmetry Breaking

The electroweak interaction in SST emerges from an intertwined $SU(2) \times U(1)$ structure coming from two director fields ($\mathbf{U}_2$ and ϑ). A key result is that the electroweak mixing angle θ_W – an arbitrary parameter in the SM – is here determined by the ratio of $SU(2)$ and $U(1)$ director stiffnesses:

Theorem 6.2: Weak Mixing Angle from First Principles

The electroweak mixing angle θ_W arises from the ratio of the swirl medium's director stiffness constants for the $U(1)$ and $SU(2)$ sectors. In SST:

$$\tan^2\theta_W \;=\; \frac{g'^2}{g^2} \;=\; \frac{\kappa_2}{\kappa_1}\,,$$

where g' and g are the emergent $U(1)_Y$ and $SU(2)_L$ gauge couplings, and κ_2, κ_1 the corresponding orientational stiffness parameters. Thus, θ_W is not a free parameter but is, in principle, computable from the underlying condensate properties.

Inserting estimates of stiffness ratios, one finds $\sin^2\theta_W \approx 0.231$ at low energy, consistent with the observed ≈ 0.23. This is a major success: a traditionally arbitrary constant becomes calculable via fluid properties.

Furthermore, SST provides a natural electroweak symmetry breaking (EWSB) scale. The condensate's bulk energy density sets the Higgs scale. Specifically, defining $\mu \equiv \hbar v$ (which is ≈ 0.511 MeV, essentially the electron rest energy), one finds the Higgs VEV v_Φ satisfies:

$$v_\Phi \;=\; u_{\text{swirl}}^{1/4}\,(W_1 W_2 W_3)^{1/4} \;\approx\; 2.595 \times 10^2 \text{ GeV}\,,$$

where $u_{\text{swirl}} = \frac{1}{2}\rho_f v$ is the swirl energy density and W_i are dimensionless weights of the three director sectors. Numerically this is close to observed 246 GeV. SST thus not only unifies gauge couplings conceptually but also accounts for the symmetry-breaking scale without fine-tuning. The small 5% discrepancy could be due to higher-order effects or slight differences in W_i, but being in the ballpark is encouraging.

In summary, SST's gauge sector aligns with the Standard Model: it has the correct gauge group, explains charge assignments via knot topology, and even offers an origin for coupling values and scales. In SST, these features stem from geometry and elasticity of the swirl medium.

XXVII. COHERENCE CONDUCTIVITY AND CHIRALITY IN 1D (PATCH)

a. Setting. Consider a 1D slab with swirl–mode correlation matrix $N(q)$, mode frequencies $\Omega_s(q)$, group-velocity operator $V_x(q)$, and small static gradient $\partial_x T$. Let linewidths be $\gamma_s(q)$ and define $\Gamma_{ss'} \equiv \frac{1}{2}(\gamma_s + \gamma_{s'})$ and detuning $\delta \equiv \Omega_{s'} - \Omega_s$ for a near-degenerate pair $s \neq s'$.

corollary

[. Coherence conductivity in 1D; *Canonical*] The linear-response, off-diagonal contribution to thermal conductivity is

$$\boxed{\kappa_{1\mathrm{D}}^{(\mathrm{C})} = \sum_{q} \sum_{s \neq s'} \frac{\left(\Omega_s + \Omega_{s'}\right) \Gamma_{ss'} \left|V_{ss'}^{(x)}\right|^2}{4\delta^2 + \Gamma_{ss'}^2} \left(-\frac{\partial n_B}{\partial T}\right) \; + \; \mathcal{O}(|M|^2) \, ,} \tag{1}$$

where n_B is the Bose function and M denotes weak electron–swirl vertices (Born–Markov), whose leading corrections are of order $|M|^2$. This expression reduces to Peierls and to Allen–Feldman in the appropriate limits [47, 52, 60, 62].

b. Dimensional check. $[V^{(x)}]^2 \sim \mathrm{m}^2/\mathrm{s}^2$, $[\Omega] \sim \mathrm{s}^{-1}$, $[-\partial n_B/\partial T] \sim \mathrm{K}^{-1}$, and the 1D density of states sum contributes $\sim \mathrm{s/m}$, giving $[\kappa] = \mathrm{W\,m^{-1}\,K^{-1}}$.

c. Proof sketch (Canonical). Linearize the unified correlation equation [62] in steady state about $N^{(0)}(T)$, project onto the near-degenerate 2×2 block, solve for $N_{ss'}^{(1)}$ with source $-\frac{1}{2} V_{ss'}^{(x)} \, \partial_x N^{(0)}$, and insert into $J_x = \mathrm{Tr}\, \frac{1}{2}\{V_x, N\}\, \Omega$ [52]. Off-diagonal terms produce the Lorentzian factor $(4\delta^2 + \Gamma^2)^{-1}$. Coupling to electrons adds $\mathcal{O}(|M|^2)$ corrections with the same denominator.

corollary

[. Chirality-odd nonreciprocity; *Canonical (conditional)*] If a chiral drive induces a phase $V_{ss'}^{(x)} \to \left|V_{ss'}^{(x)}\right| \mathrm{e}^{i\phi_\chi}$, the forward/backward conductivity difference satisfies

$$\boxed{\Delta\kappa_{\mathrm{asym}} \equiv \left[\kappa^{(\mathrm{C})}\right]_{\rightarrow} - \left[\kappa^{(\mathrm{C})}\right]_{\leftarrow} \; \propto \; \frac{\Gamma_{ss'}}{4\delta^2 + \Gamma_{ss'}^2} \, \mathrm{Im}\left\{\left(V_{ss'}^{(x)}\right)^2\right\} \, ,} \tag{2}$$

which flips sign under $\phi_\chi \to -\phi_\chi$ and vanishes when $\delta \gg \Gamma$.

Status. Canonical once the chiral-drive operator is defined in the device Lagrangian; otherwise treat as Constitutive.

d. Theorem (Chirality–Matter Equivalence). Let $\Gamma = \pm n\kappa$ be the circulation of a swirl string, with + (CCW) or − (CW) orientation. Then

$$S_{(t)}$$

Proof. (i) By Axiom 2, circulation is quantized in $\pm n\kappa$. (ii) By Axiom 6, mirrored knots correspond to antiparticles. (iii) Rosetta mapping preserves sign of vorticity. Therefore, chirality of the swirl clock is equivalent to the particle/antiparticle distinction. □

A. Hyperbolic Ideal Triangles as Two-Dimensional Swirl–Clock Horizon Models

In this subsection we introduce a simple two-dimensional model that captures the essential structure of *swirl–clock horizons* in Swirl–String Theory (SST). The model is provided by *ideal triangles* in the hyperbolic plane of constant Gaussian curvature

$$K = -1. \tag{3}$$

This furnishes a clean geometric example in which a domain has a *finite* integrated curvature (finite area) while its boundary is located at *infinite* metric distance. The same pattern underlies horizon-like structures in SST, where finite swirl energy is enclosed by boundaries that are infinitely far away in the effective swirl–clock metric.

1. *Hyperbolic triangles and the curvature–angle relation*

Let $\mathbb{H}^2$ denote the two-dimensional hyperbolic plane with constant curvature $K = -1$. Consider a geodesic triangle with interior angles A, B, and C. The Gauss–Bonnet theorem for a geodesic triangle in a surface of constant curvature K yields

$$\iint_{\Delta} K \, dA + (A + B + C) = \pi, \tag{4}$$

where dA is the area element and Δ is the triangular domain.[2] For $K = -1$ this simplifies to

$$-\iint_{\Delta} dA + (A + B + C) = \pi, \tag{5}$$

so that the hyperbolic area of the triangle is

$$\mathrm{Area}(\Delta) = \iint_{\Delta} dA = \pi - (A + B + C). \tag{6}$$

Thus in curvature $K = -1$ the *triangle defect*

$$D := \pi - (A + B + C) \tag{7}$$

coincides with the area. Equation (6) shows that the interior angle sum is always less than π, and that the area is purely determined by the *defect from Euclidean flatness*.

2. *Ideal triangles and the limit of vanishing angles*

A *proper* hyperbolic triangle has vertices in the interior of $\mathbb{H}^2$ and satisfies

$$0 < A + B + C < \pi. \tag{8}$$

One can, however, consider a limiting process in which the three vertices move outwards towards the boundary at infinity of $\mathbb{H}^2$. In the standard models (upper half-plane or Poincaré disk), this corresponds to pushing the vertices to the ideal boundary while keeping the sides geodesic (i.e., arcs orthogonal to the boundary or diameters).

The limiting object is an *ideal* triangle, whose three vertices lie on the boundary at infinity and whose sides are infinite geodesic arcs. In this limit one finds

$$A \to 0, \qquad B \to 0, \qquad C \to 0, \tag{9}$$

so that the interior angle sum tends to zero:

$$A + B + C \longrightarrow 0. \tag{10}$$

Substituting into (6) gives

$$\mathrm{Area}(\Delta_{\mathrm{ideal}}) = \lim_{A+B+C\to 0} \big[\pi - (A + B + C)\big] = \pi. \tag{11}$$

All ideal triangles in $\mathbb{H}^2$ (with $K = -1$) have the same area π, independent of their particular shape or orientation. At the same time, each side has infinite hyperbolic length, and the three vertices lie at infinite metric distance from any interior point.

In summary, an ideal hyperbolic triangle combines three key properties:

1. **Vertices at infinity:** all corners lie on the ideal boundary of $\mathbb{H}^2$.

2. **Infinite perimeter:** each side is infinitely long in the hyperbolic metric.

3. **Finite area:** the enclosed area is finite and universal,

$$\mathrm{Area}(\Delta_{\mathrm{ideal}}) = \pi. \tag{12}$$

---

[2] See, e.g., standard references on hyperbolic geometry and the Gauss–Bonnet theorem.[39–41]

3. SST interpretation: a two-dimensional swirl–clock horizon

Swirl–String Theory introduces an effective metric in which the local rate of the *swirl clock* $S_{(t)}$ depends on the magnitude of the characteristic swirl speed $\mathbf{v}_{\circlearrowleft}$ and the local vorticity and pressure structure. In strongly distorted regions, approaching the analogue of a horizon, the swirl–clock metric can stretch in such a way that:

- the *swirl–clock distance* to a boundary tends to infinity, while
- the *integrated swirl energy* (or mass-equivalent ρ_m) enclosed remains finite.

This is precisely the qualitative pattern exhibited by ideal triangles in $\mathbb{H}^2$:

- The boundary (three vertices) sits at infinite hyperbolic distance (ideal points).
- The perimeter of the domain is infinite.
- The integrated curvature (area) is finite and given by (11).

We can therefore regard the ideal hyperbolic triangle as a *two-dimensional toy model* of a swirl–clock horizon patch in SST. The hyperbolic triangle defect

$$D = \pi - (A + B + C) \tag{13}$$

plays a role analogous to an integrated curvature or energy density in SST: it is a scalar invariant determined by the geometry of the domain and independent of the particular geodesic representation (e.g., independent of the specific semicircles chosen in the upper half-plane model).

More concretely, one may interpret:

- The *finite area* π of the ideal triangle as a proxy for a finite swirl energy budget associated with a given patch of the foliation.
- The *boundary at infinity* as representing a surface that is reachable only in infinite swirl–clock time, analogous to horizon-like structures where $S_{(t)}$ slows down and effectively freezes from the perspective of distant regions.
- The *shape independence* of (11) as a two-dimensional analogue of SST's requirement that physically relevant quantities (mass, charge, and spin) be invariant under reparameterizations of the swirl string, depending only on topological and integral geometric data.

In later sections, this ideal-triangle model can serve as a compact 2D reference for interpreting:

1. the emergence of horizon-like boundaries in strongly sheared swirl configurations,
2. the relation between integrated curvature and effective mass functionals in SST, and
3. the role of boundary symmetries (e.g., Möbius invariance in $\mathbb{H}^2$) as two-dimensional analogues of conformal and gauge symmetries in the full three-dimensional swirl-string background.

B. Swirl–EM Transduction Mechanism and the Echo Delay

In Swirl–String Theory (SST), the Unruh response of accelerated atoms occurs in a two-vacuum environment: a hydrodynamic swirl sector with characteristic speed $\|\mathbf{v}_{\circlearrowleft}\| \ll c$ and density ρ_f, and the usual electromagnetic (EM) sector with propagation speed c.[27–29] Atoms can radiate into both sectors, but standard cavities are only directly sensitive to the EM component. The observed signal is therefore an *echo* of a much stronger but mostly invisible primary burst in the swirl sector.

This subsection derives the coupled rate equations and the effective Swirl–EM transduction coefficient κ_{se} required to connect a fast ($\sim 0.1\,\mathrm{ns}$) primary event to a slow ($\sim 30\,\mathrm{ns}$) prethermalization signal in high-Q cavities.

1. Swirl–EM bridge from the modified Faraday law

Canon §XV introduces the Swirl–EM bridge as a modification of Faraday's law, with a swirl-density source term

$$\nabla \times \mathbf{E} = -\frac{\partial \mathbf{B}}{\partial t} - \mathbf{b}, \qquad \mathbf{b} = \mathcal{G}\,\frac{\partial \rho_\sigma}{\partial t}\,\hat{\mathbf{n}}. \tag{14}$$

Here ρ_σ is the areal density of swirl strings (swirl-texture density) intersecting an effective surface element, $\hat{\mathbf{n}}$ is the local surface normal, and $\mathcal{G}$ is a dimensional coupling constant related to the flux quantum $h/2e$. A rapid change $\partial_t \rho_\sigma$ during a primary swirl burst produces an effective electromotive force (EMF) that pumps the EM normal modes of the cavity.

During the primary event (on timescales of order 0.1 ns) the accelerated atoms generate a *swirl wake*, i.e. a localized oscillation of $\rho_\sigma(t)$, which drives the cavity via (14). For a cavity mode with field profile $\mathbf{E}_m(\mathbf{x})$, the effective drive amplitude is

$$\mathcal{E}_m(t) \;\propto\; \int_{\Sigma_m} \mathbf{b}(\mathbf{x},t)\cdot\mathbf{E}_m^*(\mathbf{x})\,dS \;\propto\; \mathcal{G}\,\dot{\rho}_\sigma(t), \tag{15}$$

where Σ_m is an effective coupling surface and the last proportionality absorbs geometry into a mode-dependent form factor.

The detailed rate-equation model and the impedance-based parametrization of $\kappa_{\rm se}$ are developed in Sec. XVIII A.

2. Corollary: Swirl–blindness of standard EM cavities

Corollary 15.3 (Swirl–blindness condition). *In electromagnetic cavities where the impedance mismatch between the swirl medium and the physical boundaries is large, $Z_{\rm bound} \gg Z_S = \rho_f \|\mathbf{v}_{\circlearrowleft}\|$, the primary swirl superradiance burst ($t \sim 0.1$ ns) is almost completely non-radiatively dissipated in the walls. The observable electromagnetic signal is a secondary transduction echo with the following properties:*

1. *Delay:* The peak of $n_{\rm EM}(t)$ is controlled by the slower of the swirl decay rate λ^{-1} and the cavity ring-up time $\gamma_{\rm cav}^{-1}$, rather than by the intrinsic timescale of the primary Unruh event.
2. *Amplitude:* The EM intensity is suppressed by the small transduction efficiency ξ in Eq. (12). In the impedance-dominated regime one finds $\xi \propto 4Z_S/Z_{\rm bound} \sim 10^{-7}$, implying that $\mathcal{O}(10^{-7})$ of the primary swirl energy appears in the EM channel.

Experimental access to the primary burst therefore requires impedance-matched hydrodynamic detectors (e.g. superfluids or Bose–Einstein condensates), where $Z_{\rm det}$ can be tuned to approach Z_S. In such detectors SST predicts a prompt, high-contrast signal at the swirl timescale, in addition to the delayed EM echo.

SST-specific predictions beyond GR/QFT. The transduction model above leads to several falsifiable predictions that differ sharply from pure GR/QFT treatments of the Unruh effect:

1. **Two-timescale structure.** SST predicts a fast, non-EM primary burst at the swirl sector timescale (~ 0.1 ns) plus a delayed EM echo governed by λ^{-1} and $\gamma_{\rm cav}^{-1}$. GR/QFT in a single-vacuum picture predicts only the slow EM response.
2. **Impedance-controlled amplitude.** The integrated EM yield scales with the acoustic-style mismatch factor $4Z_S/Z_{\rm bound}$. Varying boundary materials (or adding impedance-matching layers) should systematically change the EM echo amplitude at fixed acceleration.
3. **Hydrodynamic detector enhancement.** Replacing rigid mirrors by a tuned hydrodynamic detector with $Z_{\rm det} \approx Z_S$ should dramatically enhance the primary signal and collapse the delay between atomic acceleration and detected radiation.
4. **Geometry dependence via κ_0.** Changing the cavity size or introducing swirl-transparent channels modifies κ_0 and thus the relative weights of the primary and echo signals in a way that cannot be captured by GR/QFT alone.

Analogy (for intuition). The two-vacuum system behaves like a drum being struck inside a thick, rigid box. The drumhead (swirl sector) vibrates violently and quickly, but the box walls are so stiff and impedance-mismatched that almost none of that motion turns into audible sound (EM photons). Instead, the box heats up ($\gamma_{\rm diss}$), and only a tiny, delayed *rumble* escapes after the vibrations slowly leak into the air. SST claims that most Unruh energy lives in the drum; standard GR/QFT only sees the faint rumble.

XXVIII. SWIRL PRESSURE LAW (EULER COROLLARY)

For a steady azimuthal drift $v_\theta(r)$,

$$0 = -\frac{1}{\rho_f}\frac{dp_{\rm swirl}}{dr} + \frac{v_\theta^2}{r} \;\Rightarrow\; \frac{dp_{\rm swirl}}{dr} = \rho_f\,\frac{v_\theta^2}{r}.$$

Integrating for $v_\theta \to v_0$ gives

$$p(r) = p_0 + \rho_f v_0^2 \ln\!\left(\frac{r}{r_0}\right).$$

Full working is provided in Appendix F.

XXIX. CANONICAL CLOSURE FOR THE SAWSHAPED GAMMA COIL (S40, $+11, -9$): HELICITY AND LIFT ROUTES

a. Summary. This section provides a canonical, falsifiable bridge from coil geometry to quantized circulation/helicity and lift via swirl pressure. For the Gamma coil (slot $S = 40$, step $+11/-9$) with net linkage $\chi = 42$, Route A yields $\mathcal{H} \approx 2\,\Gamma^2\,\chi$ with quantized circulation $\Gamma = n\,\kappa_{\rm SST}$ where $\kappa_{\rm SST} = 2\pi r_c\,\|\mathbf{v}_{\circlearrowleft}\|$. Route B connects lift $F_{\rm req}$ to swirl pressure via $v_\theta(R) = \sqrt{2F_{\rm req}/(\rho_f A)}$ and $\Gamma_{\rm req} \approx 2\pi r_s\,v_\theta(r_s)$ with $r_s \simeq 0.4R$. Design constraints require $v_\theta(R) \le \|\mathbf{v}_{\circlearrowleft}\|$ and $F_{\rm req} \le \min(\frac{1}{2}\rho_f\|\mathbf{v}_{\circlearrowleft}\|^2 A, N_{\rm act}\,F_{\rm swirl}^{\rm max})$. Falsifiers include speed cap violations and non-integer quantization $n = \Gamma/\kappa_{\rm SST}$.

Full derivation: See Appendix **??** for complete geometry definitions, helicity/lift routes, design specialization, and bench cards.

XXX. GAUGE/EWSB SECTOR: EMPIRICAL-FIRST BOX + THEORY

Empirical (PDG) on-shell values at the electroweak scale give

$$m_W = 80.377\ \text{GeV}, \quad m_Z = 91.1876\ \text{GeV}, \quad \sin^2\theta_W = 0.23121 \pm 0.00004\ [59].$$

Director elasticity yields the mixing relations and masses $A_\mu = \sin\theta_W W_\mu^3 + \cos\theta_W B_\mu$, $m_W = \frac{1}{2}g\,v_\Phi$, $m_Z = \frac{1}{2}\sqrt{g^2+g'^2}\,v_\Phi$ [61, 63]. Using the anchors reproduces $v_\Phi \simeq 246.22$ GeV (cross-check box).

Part IV
Gravity, Hydrogen, and Cosmology

XXXI. SWIRL-BASED DERIVATION OF THE GRAVITATIONAL COUPLING G_{swirl}

In Swirl–String Theory (SST), the Newtonian gravitational constant is not a primitive parameter but an emergent coupling determined by the microscopic structure of the swirl condensate. In this section we derive the effective gravitational coupling G_{swirl} from (i) a microscopic electron-scale spring model and (ii) the macroscopic maximum-tension principle of General Relativity.

A. Macroscopic input: maximum tension in GR

Classical General Relativity in four dimensions admits a universal maximum tension (or force) [65]

$$F_{\mathrm{gr}}^{\mathrm{max}} = \frac{c^4}{4G}, \tag{1}$$

which may be inverted to express the gravitational coupling as

$$G = \frac{c^4}{4F_{\mathrm{gr}}^{\mathrm{max}}}. \tag{2}$$

In SST we denote by G_{swirl} the gravitational coupling obtained after coarse-graining the swirl condensate and demand that it reproduce Eq. (2) in the macroscopic (GR) limit.

B. Microscopic input: electron-scale swirl spring

We model the electron as a closed swirl string of core radius r_c and rest mass m_e. For small radial displacements x we adopt a linear spring model with effective stiffness k_e:

$$F = k_e x, \qquad E_{\mathrm{spring}} = \frac{1}{2}k_e x^2 = \frac{1}{2}Fx. \tag{3}$$

Evaluating at the core displacement scale $x = r_c$, the microscopic swirl tension is defined by

$$F_{\mathrm{swirl}}^{\mathrm{max}} \equiv F(x = r_c) = \frac{1}{2}\,\frac{m_e c^2}{r_c}, \tag{4}$$

so that the spring energy at displacement r_c carries a fixed fraction of the electron rest energy,

$$E_{\mathrm{spring}}(x = r_c) = \frac{1}{2}F_{\mathrm{swirl}}^{\mathrm{max}} r_c = \frac{1}{4}m_e c^2. \tag{5}$$

Equation (4) may be inverted to express the electron mass in terms of the microscopic tension scale:

$$m_e = \frac{2F_{\mathrm{swirl}}^{\mathrm{max}} r_c}{c^2}. \tag{6}$$

C. Planck-time coarse-graining and channel counting

Let t_p denote the fundamental microscopic time step of the condensate and $\mathbf{v}_{\circlearrowleft}$ the characteristic swirl transport speed along the strings. We consider a gravitational flux tube whose cross-section is resolved into microscopic channels of area $\sim r_c^2$. During one macroscopic process of duration Δt each channel can be updated at most $\Delta t/t_p$ times, and each update is limited by the microscopic tension $F_{\mathrm{swirl}}^{\mathrm{max}}$.

Coarse-graining this picture leads to a maximal gravitational tension

$$F_{\mathrm{gr}}^{\mathrm{max}} = \frac{F_{\mathrm{swirl}}^{\mathrm{max}} r_c^2}{2\,\mathbf{v}_{\circlearrowleft}\,c\,t_p^2}, \tag{7}$$

where the dimensionless factor $r_c^2/(\mathbf{v}_{\circlearrowleft} c t_p^2)$ counts the effective number of tension channels contributing coherently to a macroscopic, lightlike deformation.

D. Emergent gravitational coupling

Equating the microscopic expression (7) with the macroscopic GR result (1) yields

$$G_{\text{swirl}} = \frac{c^4}{4F_{\text{gr}}^{\max}} = \frac{c^4}{4}\frac{2\,\mathbf{v}_{\circlearrowleft}\,c\,t_p^2}{F_{\text{swirl}}^{\max} r_c^2} = \frac{\mathbf{v}_{\circlearrowleft} c^5 t_p^2}{2F_{\text{swirl}}^{\max} r_c^2}. \tag{8}$$

Substituting Eq. (4) to eliminate $F_{\text{swirl}}^{\max}$ in favour of the electron mass m_e gives

$$G_{\text{swirl}} = \frac{\mathbf{v}_{\circlearrowleft} c^5 t_p^2}{2(\frac{1}{2}m_e c^2/r_c) r_c^2} = \frac{\mathbf{v}_{\circlearrowleft} c^3 t_p^2}{m_e r_c}. \tag{9}$$

Equations (8), (9), and (2) provide three equivalent representations of the gravitational coupling in SST:

$$G_{\text{swirl}} = \frac{\mathbf{v}_{\circlearrowleft} c^3 t_p^2}{m_e r_c}, \tag{10}$$

$$= \frac{\mathbf{v}_{\circlearrowleft} c^5 t_p^2}{2F_{\text{swirl}}^{\max} r_c^2}, \tag{11}$$

$$= \frac{c^4}{4F_{\text{gr}}^{\max}}. \tag{12}$$

In particular, G_{swirl} vanishes if the swirl transport speed $\mathbf{v}_{\circlearrowleft}$ is set to zero or if the microscopic time step t_p is taken to zero, highlighting its role as an emergent coupling arising from the collective dynamics of the swirl condensate.

XXXII. SWIRL GRAVITATION AND THE HYDROGEN-GRAVITY MECHANISM

Gravity, in SST, is an emergent attractive force from pressure and flow fields of the swirl medium, not fundamental geometry. We have seen a single swirl string can create a $1/r$ potential analogous to gravity or electrostatics. Now consider how two neutral composite objects (like two hydrogen molecules) attract gravitationally in SST.

Swirl Gravitational Coupling G_{swirl}

The effective gravitational coupling in SST is given by

$$G_{\text{swirl}} = \frac{\|\mathbf{v}_{\circlearrowleft}\| c^5 t_p^2}{2F_{\max} r_c^2} \approx G_N,$$

where $\|\mathbf{v}_{\circlearrowleft}\|$ is the canonical swirl speed, r_c is the core radius, $F_{\max}$ is the maximal force constant, and t_p is the Planck time. This identity connects the swirl constants to Newton's gravitational constant G_N.
Full derivation: See Appendix J for the complete derivation of the swirl→bulk coupling.

Theorem 7.1: Hydrogen-Gravity Mechanism (Swirl Attraction in Flat Space)

Chiral knotted swirl strings generate quantized long-range circulation leading to mutual attraction. Consider a hydrogen molecule analog in SST: each hydrogen atom consists of a composite proton (two 5_2 up-quark knots + one 6_1 down-quark knot) and a 3_1 electron knot, linked into a bound state. The composite carries a net chiral circulation along a central swirl axis. Let C be a large loop encircling this axis. Cauchy's integral theorem applied to an analytic swirl potential $W(z) = \Phi + i\Psi$ yields:

$$\oint_C \mathbf{v}_{\circlearrowleft} \cdot d\ell = 2\pi i \,\text{Res}(\partial_z W, 0) = n\,\kappa\,,$$

with n the winding (linking) number. This locked circulation (quantized as $n\kappa$) around the axis creates a persistent low pressure along that axis ($\Delta p = -\frac{1}{2}\rho_f \|\mathbf{v}_{\circlearrowleft}\|^2$). Two such hydrogen composites sharing the axis experience an attractive force as each lies in the other's pressure well. The effect produces an inverse-square attraction between the systems (circulation field spreads cylindrically), entirely in flat space.

This theorem, often called the "Hydrogen–Gravity theorem", gives a concrete mechanism for gravity in SST. Two hydrogen atoms (modeled as quark-knot composites) have a slight net swirl circulation linking them (imagine each composite's vortex field lines wrapping around the other's axis some number of times). That induces a pressure drop along the line between them, drawing them together. Because the circulation is quantized (n integer, likely $n = 1$ for a fundamental linkage), the strength of this effect is fixed by κ and v.

Qualitatively: in SST, matter (knotted strings) "gravitationally" attracts because their presence and motion cause slight persistent pressure deficits in the medium that extend far. When two chiral knot-composites share an axis, each one's swirl field twists the medium to pull the other. The effect is cumulative over many strings, which is why macroscopic bodies generate noticeable force.

This mechanism has been tested to the extent that it reproduces Newton's law at large separations and can match G_N by appropriate constant choices (which we did via $G_{\text{swirl}} \approx G_N$). It also suggests why only certain matter produces gravity: in SST, only chiral (handed) knots carry the kind of long-range swirl field that doesn't cancel. Non-chiral configurations (e.g. symmetric counter-rotating loops) produce no net far field, thus no gravity. Interestingly, matter vs antimatter in SST are defined by opposite swirl chirality, so a matter–antimatter pair would have opposite swirl orientation. They likely still attract gravitationally, since gravity is sourced by energy density, not swirl orientation.

XXXIII. QUANTUM MEASUREMENT: KERNEL LAW + NEAR-FIELD COROLLARY + BOUNDS

The canonical transition rate from R-phase to T-phase is

$$\Gamma_{R\to T} = \int_{\mathbb{R}^3} d^3\mathbf{r} \int_0^\infty d\omega\; \chi(\mathbf{r},\omega)\, u(\mathbf{r},\omega)\, \mathcal{F}(\Delta\mathcal{K},\omega), \tag{1}$$

which reduces to standard environment-induced decoherence in the linear regime [64]. In the near-field single-mode limit,

$$\Gamma_{R\to T} \approx \chi_{\text{eff}}(\omega_0)\, L(\omega;\omega_0,\gamma)\, \frac{P}{A_{\text{eff}}},$$

with geometry entering through A_{eff} and L a narrow lineshape. From visibility V over interaction time τ,

$$-\ln V \;=\; \tau \int d^3\mathbf{r} \int d\omega\; \chi(\mathbf{r},\omega)\, u(\mathbf{r},\omega)\, \mathcal{F}(\Delta\mathcal{K},\omega),$$

yielding an extraction scheme for $\chi_{\text{eff}}^{\max}$ (Appendix I 7; bounds summarized there).

XXXIV. QUANTUM COMPUTING SECTOR (PREVIEW)

a. Overview. SST provides a framework for quantum computing using R/T phase transitions. The canonical transition rate from R-phase to T-phase is given by the kernel law (Section XXXIII). Key components include: (1) Visibility–Rate Normalization: $V(\tau) = \exp(-\Gamma\,\tau)$ with monitoring rate Γ $[\text{s}^{-1}]compressingthekernelintegral; (2) Two-LevelControl : R/TdynamicswithRabirate\Omega_R$ and relaxation $\gamma_{R,T}$, driven by the radiation sector with Swirl Clock timing; (3) Linkage Entanglement: Two SST qubits coupled by shared circulation implement exchange (g_{link}) and ZZ-type (χ) interactions with distance-dependent rates $g_{\text{link}} \sim d^{-3}$ for far-field coupling.

Full development: See Appendix **??** for complete derivations of visibility normalization, two-level control equations, linkage entanglement bus, gate rates, and experimental protocols.

A. Working hypothesis: photon–electron topological response

We parameterize the photon energy by the dimensionless ratio

$$x \equiv \frac{\hbar\omega}{m_e c^2} = \frac{\omega}{\omega_C}, \qquad \omega_C = \frac{m_e c^2}{\hbar}. \tag{1}$$

In Swirl–String Theory the electron is modeled as a trefoil swirl string confined to a horn torus of core radius r_c with an approximately spherical pressure/energy envelope of radius $R_e \simeq 2r_c$. We then adopt the following working hypothesis for the topological response of the electron swirl to incident photons:

- For $x \ll 1$ (long wavelengths), the photon induces only smooth deformations of the trefoil swirl configuration. The knot type is preserved; observed phenomena correspond to bound–bound transitions, photoionization, and Thomson-like scattering.

- For $x \sim 1$ (Compton scale), the photon can drive the swirl into a metastable "three-twist unknot" configuration: a topologically trivial loop with three helical twists along its length. This represents a re-folding of the electron swirl that preserves global topological charge but changes the local embedding of the string.

- For $x \gtrsim 1$–2, the injected energy is sufficient to trigger one or more reconnection events of the swirl string. In this regime the three-twist loop can be broken into one or several shorter segments or loops, which subsequently re-form trefoil configurations displaced from their original bound state. Observationally this corresponds to high-energy Compton scattering, ionization with large momentum transfer, and, above the pair-production threshold $x \geq 2$, creation of e^+e^- pairs in external fields.

This picture is presently conjectural. It must be constrained by the known smooth energy dependence of Compton scattering and photoabsorption cross sections and by numerical SST estimates of the energy gaps between the trefoil ground configuration and the proposed three-twist intermediate state.

XXXV. HYDROGEN–GRAVITY CONSTRUCTION

Chiral-axis circulation around a bound electron induces a pressure deficit

$$\Delta p = -\tfrac{1}{2}\rho_f v^2.$$

Canonical: local swirl attraction via Δp. Research: extension to long-range gravity remains conjectural.

XXXVI. WAVE–PARTICLE DUALITY AND QUANTUM MEASUREMENT

SST offers a natural framework for quantum wave–particle duality via its dual-phase concept (Axiom 5). The extended R-phase corresponds to wave-like behavior (delocalized, interfering), and the T-phase corresponds to particle-like behavior (localized, definite).

A moving particle in T-phase (with momentum p) in SST is essentially a moving knotted string. Surrounding that moving knot is a swirl flow, which far away looks like a circular wave. One can show that a moving T-knot carries an accompanying R-phase oscillation of wavelength $\lambda = h/p$, by considering the resonance condition of a closed loop of length L. If the string of total length L is translating, it supports a standing wave along its length with integer node count. For the n-th harmonic, $L = n\lambda$. Setting $p = h/\lambda$ yields $p = nh/L$. Taking $n = 1$, $p = h/L$, analog of de Broglie $\lambda = h/p$. Thus SST recovers de Broglie's relation by viewing a particle as a moving wave-carrying loop.

Now, what about *quantum measurement* or wavefunction collapse? In SST, this is not an axiom but a dynamical process: the $R \to T$ transition (and $T \to R$). The presence of an environment or measuring device interacts with an R-phase string and can induce it to knot (collapse to T-phase). The theory provides a quantitative law for the collapse rate:

Theorem 8.1: R→T Transition Dynamics (Collapse Rate)

The transition rate $\Gamma_{R\to T}$ for a swirl string to collapse from the extended R-phase to a localized T-phase is given by a convolution of the local environmental energy density with a susceptibility kernel, modulated by the topological change:

$$\Gamma_{R\to T} \;=\; \int_{\mathbb{R}^3} d^3r \int_0^\infty d\omega\; \chi(r,\omega)\; u(r,\omega)\; F(\Delta K,\omega)\,,$$

where $\chi(r,\omega)$ is the medium's collapse susceptibility at position r, frequency ω; $u(r,\omega)$ the spectral energy density of the interacting field at that location; and $F(\Delta K,\omega)$ a form factor depending on knot change ΔK and perhaps ω. In the simplest near-field limit (one dominant mode ω_0 and slow χ variation), this reduces to

$$\Gamma_{R\to T} \approx \alpha\,\frac{P}{A_{\text{eff}}}\,L(\omega;\omega_0,\gamma)\,\Delta K, \qquad L(\omega;\omega_0,\gamma) = \frac{\gamma^2}{(\omega-\omega_0)^2+\gamma^2}\,,$$

where P/A_{eff} is incident power per effective area, and $L(\omega;\omega_0,\gamma)$ a Lorentzian centered at ω_0 (width γ). This shows $\Gamma_{R\to T} \propto P/A_{\text{eff}}$ (incident intensity), echoing known decoherence results (stronger coupling causes faster collapse).

In plainer terms, SST's collapse law says the more "environment" (e.g. photons, molecules) hitting the extended swirl string, and the more complex a knot change, the faster the string collapses to a localized state. If no environment interacts (isolated system), $\chi \approx 0$ and $\Gamma_{R\to T} \approx 0$ – so the wave remains intact (no collapse). When the string strongly interacts (as in a measurement), χu is large and collapse is rapid. This aligns with environment-induced decoherence: in the weak coupling limit, SST's formula reduces to known decoherence rates governed by environmental spectral density, and it respects experiments showing no anomalous collapse beyond decoherence.

A secondary result (Lemma 9.3 in v0.5.5.1) assures SST's collapse law is consistent with all experiments that have observed no extra collapse beyond standard decoherence. Essentially, molecule interferometry, optomechanical tests, etc., set upper bounds on any geometry-independent collapse, and SST's kernel can lie below those bounds, so SST doesn't conflict with current null results.

Finally, SST provides a clear spin-statistics interpretation: knotted vs unknotted. In topology, rotating a double cover of a knot can yield a sign change or not depending on knot type (related to fundamental group of the complement). SST uses the Finkelstein–Rubinstein result that if configuration space is multiply connected, half-integer spin arises when a 2π rotation path is topologically nontrivial. Unknotted strings have trivial topology under 2π rotation (so bosons, integer spin), whereas knotted strings have nontrivial topology (a 360° rotation of a nontrivial knot cannot be continuously undone without a further rotation) and thus behave like fermions. The corollary: unknotted = boson, knotted = fermion, matches observed spin-statistics.

XXXVII. SWIRL–TENSOR CORRESPONDENCE AND EXTERNAL VORTEX FIELD THEORIES

Canonical Definition: Swirl–Tensor Mapping

Let $\omega_{\mu\nu} \in \mathfrak{g} \otimes \Lambda^2$ denote a rank-2 antisymmetric tensor field valued in a Lie algebra $\mathfrak{g}$ (e.g., $\mathfrak{su}(3) \oplus \mathfrak{su}(2) \oplus \mathfrak{u}(1)$). We define the **canonical swirl–tensor mapping** as:

$$\omega^{(a)}_{\mu\nu} \;\longleftrightarrow\; \epsilon_{\mu\nu\rho\sigma}\left(\mathbf{v}^{(a)}_{\circlearrowleft} \wedge \partial^\rho \mathbf{v}^{\sigma}_{\circlearrowleft}\right) + \text{torsional terms} \tag{1}$$

where superscript (a) indexes swirl-string orientations in internal symmetry space. This construction translates gauge curvature into topological swirl curvature.

Research-Track Conjecture: VFT–SST Relation

The *Vortex Field Theory* (Dziabura, 2025) posits a unified topovortex field $\omega_{\mu\nu}$ whose decomposition yields gravitational and gauge fields. Within SST, we propose the correspondence:

$$\omega_{\mu\nu}^{\text{grav}} = \lambda\, \partial_\mu\theta\, \partial_\nu\theta \quad \longleftrightarrow \quad g_{ij}^{(\text{eff})} = \delta_{ij} + \frac{1}{\rho_f}\, \partial_i\partial_j P(\vec{\omega}) \tag{2}$$

$$\mathcal{L}_{\text{int}} \supset \varepsilon^{\mu\nu\rho\sigma} f^{abc} \omega_{\mu\nu}^a \omega_{\rho\sigma}^b \theta^c \quad \longleftrightarrow \quad \mathcal{H}_{\text{swirl}} = \int \mathbf{v}_{\circlearrowleft} \cdot (\nabla \times \mathbf{v}_{\circlearrowleft})\, d^3x \tag{3}$$

where f^{abc} are Lie algebra structure constants and $\mathcal{H}_{\text{swirl}}$ denotes the helicity of the swirl field.

Canonical Summary Table

Concept	VFT (Dziabura)	SST
Medium	Vacuum phase manifold	Incompressible swirl condensate
Gravity	$\partial_\mu\theta\partial_\nu\theta$	$\nabla_i\nabla_j P(\vec{\omega})$
Gauge Fields	$\omega_{\mu\nu}^a$	$\mathbf{v}_{\circlearrowleft}^{(a)}$ excitations
Time	Not specified	$S_t^{\circlearrowleft} = \sqrt{1 - \|\mathbf{v}_{\circlearrowleft}\|^2/c^2}$
Topology	Chern–Simons terms	Knot helicity, twist, writhe
Mass	Not derived	$M = \frac{1}{2}\rho_f \|\mathbf{v}_{\circlearrowleft}\|^2\, V$

Canonical Corollary: Tensor Gauge Equivalence

Corollary. Any antisymmetric rank-2 gauge field theory $\omega_{\mu\nu} \in \mathfrak{g} \otimes \Lambda^2$ with helicity couplings admits a coarse-grained SST embedding as a multichiral swirl-string bundle, where:

- spacetime indices $\mu\nu$ encode vorticity plane orientation;
- internal index a labels swirl-string director axes;
- knot invariants $(\mathcal{H}, C, L, \text{Vol}_{\mathbb{H}})$ determine mass-energy spectrum.

Status Tags

- **Definition (Canonical):** Swirl–tensor mapping.
- **Conjecture (Research Track):** VFT–SST tensor correspondence.
- **Corollary (Canon Candidate):** Tensor gauge embedding of swirl dynamics.
- **Reference:** Dziabura (2025), "A Strong Topovortex Unified Theory".

XXXVIII. COROLLARY: COHERENCE-MODULATED DUALITY ELLIPSE (SST)

a. Definitions. Let $\boldsymbol{\omega} = \nabla \times \mathbf{v}_{\circlearrowleft}$ denote the vorticity of the swirl string flow. Define the core angular scale

$$\Omega_{\text{core}} := \frac{\|\mathbf{v}_{\circlearrowleft}\|_{r=r_c}}{r_c}\,, \tag{1}$$

and the coherence field $\gamma(\mathbf{x}, t) \in (0, 1]$ (R-sector spectral overlap). Let ρ_E^{core} be the core swirl-energy density and ρ_E^{bg} the local background.

b. Statement (Duality Ellipse, SST form). The local wave–particle tradeoff in steady thin-core sectors may be encoded by the pointwise constraint

$$\boxed{\frac{\|\boldsymbol{\omega}\|^2}{\gamma^2\,\Omega_{\rm core}^2} \;+\; \left(\frac{\rho_E-\rho_E^{\rm bg}}{\rho_E^{\rm core}}\right)^2 \;=\; 1} \tag{2}$$

which saturates the Englert-type complementarity bound for the SST visibility/predictability proxies $V := \|\boldsymbol{\omega}\|/(\gamma\,\Omega_{\rm core})$ and $D := (\rho_E-\rho_E^{\rm bg})/\rho_E^{\rm core}$. (Compare with the quantum duality ellipse for two-path interferometry [50, 58].)

c. Derivation sketch (Rosetta). (i) Define the wave proxy by normalizing vorticity to the core scale: $V = \|\boldsymbol{\omega}\|/(\gamma\,\Omega_{\rm core}) \in [0,1]$. (ii) Define the particle proxy as the dimensionless energy localization: $D = (\rho_E-\rho_E^{\rm bg})/\rho_E^{\rm core} \in [0,1]$. (iii) The coherence field γ modulates visibility (R-sector spectral overlap). (iv) In the inviscid, incompressible, barotropic regime with steady thin cores, the Cauchy–Schwarz/Englert bound is saturated to $V^2+D^2=1$ (all dissipationless), yielding (2). Classical vortex invariants (Helmholtz/Kelvin) secure consistency with the Chronos–Kelvin clock law.

A. Lagrangian insertion and field equations

Start from the unified SST fluid Lagrangian (incompressible, inviscid),

$$\mathcal{L}_{\rm SST} = \frac{1}{2}\,\rho_f\,\|\mathbf{v}_{\circlearrowleft}\|^2 \;-\; U(\rho_f) \;+\; \lambda\,(\nabla\cdot\mathbf{v}_{\circlearrowleft}) \;+\; \chi_h\,\rho_f\,(\mathbf{v}_{\circlearrowleft}\cdot\boldsymbol{\omega}) \;+\; \ldots \tag{3}$$

and add a *local* constitutive constraint with multiplier $\mu(\mathbf{x},t)$:

$$\Delta\mathcal{L}_{\rm dual} = -\,\mu\left[\frac{\|\boldsymbol{\omega}\|^2}{\gamma^2\,\Omega_{\rm core}^2} + \left(\frac{\rho_E-\rho_E^{\rm bg}}{\rho_E^{\rm core}}\right)^2 - 1\right]. \tag{4}$$

Here $\rho_E = \frac{1}{2}\,\rho_f\,\|\mathbf{v}_{\circlearrowleft}\|^2$ (canonical SST energetics). The action is $S = \int(\mathcal{L}_{\rm SST}+\Delta\mathcal{L}_{\rm dual})\,d^3x\,dt$.

a. Variations. *(a) Constraint)* $\delta\mu$ enforces (2) pointwise.
(b) Velocity field) Using $\delta\|\boldsymbol{\omega}\|^2 = 2\,\boldsymbol{\omega}\cdot(\nabla\times\delta\mathbf{v}_{\circlearrowleft})$, integration by parts yields the swirl-stiffness correction

$$\rho_f\,\partial_t\mathbf{v}_{\circlearrowleft} = -\,\nabla\Pi \;+\; \frac{2\,\mu}{\gamma^2\,\Omega_{\rm core}^2}\,\nabla\times\boldsymbol{\omega} \;+\; \chi_h\,\rho_f\,\big(\boldsymbol{\omega}+\nabla\times\mathbf{v}_{\circlearrowleft}\big) \;+\; \ldots \tag{5}$$

with Π the generalized pressure (from U and constraints), and $\nabla\cdot\mathbf{v}_{\circlearrowleft}=0$ from $\delta\lambda$. The added term $\propto\nabla\times\boldsymbol{\omega}$ is nondissipative and preserves incompressibility.
(c) Energy density / effective density) Since $\rho_E = \frac{1}{2}\rho_f\|\mathbf{v}_{\circlearrowleft}\|^2$, variations in $(\rho_f,\mathbf{v}_{\circlearrowleft})$ feed the algebraic piece

$$\frac{\partial\mathcal{L}}{\partial\rho_f} = \frac{1}{2}\,\|\mathbf{v}_{\circlearrowleft}\|^2 - U'(\rho_f) - \mu\,\frac{2(\rho_E-\rho_E^{\rm bg})}{(\rho_E^{\rm core})^2}\,\frac{\partial\rho_E}{\partial\rho_f}, \qquad \frac{\partial\rho_E}{\partial\rho_f} = \frac{1}{2}\,\|\mathbf{v}_{\circlearrowleft}\|^2, \tag{6}$$

producing a Bernoulli-type correction consistent with (2).

B. Clock coupling and limits

a. Swirl clock. The canonical time scaling (Swirl Clock) is

$$\frac{dt_{\rm local}}{dt_\infty} \;=\; \sqrt{1-\frac{\|\mathbf{v}_{\circlearrowleft}\|^2}{c^2}}\,, \tag{7}$$

so that, using (2) and $\rho_E = \frac{1}{2}\rho_f\|\mathbf{v}_{\circlearrowleft}\|^2$, increasing localization $D = (\rho_E-\rho_E^{\rm bg})/\rho_E^{\rm core}$ reduces the admissible $\|\mathbf{v}_{\circlearrowleft}\|$ (for fixed γ), weakening time dilation; in the decoherent limit $\gamma\to 0$ the wave proxy collapses.

b. Consistency checks. *Dimensions:* $\|\boldsymbol{\omega}\|/\Omega_{\rm core}$ and $(\rho_E-\rho_E^{\rm bg})/\rho_E^{\rm core}$ are both dimensionless; γ is dimensionless. *Limits:* (i) $\gamma\to 1$, $\rho_E\to\rho_E^{\rm bg} \Rightarrow \|\boldsymbol{\omega}\|\to\Omega_{\rm core}$ (pure wave); (ii) $\gamma\to 0$ or $\rho_E\to\rho_E^{\rm core} \Rightarrow \|\boldsymbol{\omega}\|\to 0$ (pure localization); (iii) Thin-core, inviscid, incompressible, barotropic assumptions retain Kelvin/Helmholtz invariants.

C. Calibration (numerical, Canon constants)

Using the Rosetta identification $\|\mathbf{v}_{\circlearrowleft}\|\|_{r=r_c} \equiv C_e$ and your constants $C_e = 1.09384563 \times 10^6\,\mathrm{m/s}$, $r_c = 1.40897017 \times 10^{-15}\,\mathrm{m}$,

$$\Omega_{\mathrm{core}} = \frac{C_e}{r_c} \approx 7.76344 \times 10^{20}\ \mathrm{s}^{-1}. \tag{8}$$

For example, with $\gamma = 0.90$ and $D = 0.70$ one has $V = \sqrt{1 - D^2} = 0.7142$, thus $\|\boldsymbol{\omega}\| = \gamma\,\Omega_{\mathrm{core}}\,V \approx 0.90 \times 0.7142 \times 7.76344 \times 10^{20}\ \mathrm{s}^{-1} \approx 4.99 \times 10^{20}\ \mathrm{s}^{-1}$, consistent with (2).

Notes on provenance (non-original elements)

Eq. (2) is an SST constitutive corollary inspired by exact two-path complementarity relations in quantum mechanics (Englert inequality; duality ellipse) and is recast here in fluid-topological variables. Classical vortex invariants follow Helmholtz/Kelvin; energetics follow standard incompressible inviscid fluid dynamics.

XXXIX. EXACT SST DEFINITION OF THE COSMOLOGICAL TERM

a. Domain kinematics. For a comoving domain $\mathcal{D}$ with effective scale factor $a_{\mathcal{D}}(t)$,

$$3\frac{\dot{a}_{\mathcal{D}}^2}{a_{\mathcal{D}}^2} = \frac{8\pi G}{c^2}\,\langle \rho c^2 \rangle_{\mathcal{D}} - \tfrac{1}{2}\,\langle \mathcal{R} \rangle_{\mathcal{D}} - \tfrac{1}{2}\,\mathcal{Q}_{\mathcal{D}}, \tag{F1}$$

$$3\frac{\ddot{a}_{\mathcal{D}}}{a_{\mathcal{D}}} = -\frac{4\pi G}{c^2}\,\langle \rho c^2 \rangle_{\mathcal{D}} + \mathcal{Q}_{\mathcal{D}}, \tag{F2}$$

with kinematical backreaction

$$\mathcal{Q}_{\mathcal{D}} = \frac{2}{3}\big(\langle \theta^2 \rangle_{\mathcal{D}} - \langle \theta \rangle_{\mathcal{D}}^2\big) - 2\langle \sigma^2 \rangle_{\mathcal{D}} + 2\langle \omega^2 \rangle_{\mathcal{D}}.$$

Here θ is the local expansion, σ^2 the shear scalar, and ω^2 the vorticity scalar of the coarse-grained swirl field (Euler–SST decomposition).

b. Exact SST cosmological term. Rewrite (F1) in a Friedmann-like form by *defining* an SST cosmological term $\Lambda_{\mathrm{SST}}(t)$:

$$3\frac{\dot{a}_{\mathcal{D}}^2}{a_{\mathcal{D}}^2} = \frac{8\pi G}{c^2}\,\langle \rho c^2 \rangle_{\mathcal{D}} - \frac{3k_{\mathcal{D}}}{a_{\mathcal{D}}^2} + \Lambda_{\mathrm{SST}}(t),$$

where $k_{\mathcal{D}}$ is the domain's FLRW-equivalent curvature chosen by matching to the early-time (nearly homogeneous) limit, $\langle \mathcal{R} \rangle_{\mathcal{D}} \to 6k_{\mathcal{D}}/a_{\mathcal{D}}^2$.

$$\boxed{\Lambda_{\mathrm{SST}}(t) = -\tfrac{1}{2}\Big[\mathcal{Q}_{\mathcal{D}}(t) + \langle \mathcal{R} \rangle_{\mathcal{D}}(t) - \tfrac{6k_{\mathcal{D}}}{a_{\mathcal{D}}^2(t)}\Big]} \tag{D1}$$

This is an *exact identity* on the domain: no vacuum constant is introduced.

c. Equivalent effective fluid (exact). Define an effective energy density and pressure from $(\mathcal{Q}_{\mathcal{D}}, \langle \mathcal{R} \rangle_{\mathcal{D}})$:

$$\rho_Q \equiv -\frac{1}{16\pi G}\Big(\mathcal{Q}_{\mathcal{D}} + \langle \mathcal{R} \rangle_{\mathcal{D}} - \tfrac{6k_{\mathcal{D}}}{a_{\mathcal{D}}^2}\Big), \tag{D2}$$

$$p_Q \equiv -\frac{1}{16\pi G}\Big(\mathcal{Q}_{\mathcal{D}} - \tfrac{1}{3}\langle \mathcal{R} \rangle_{\mathcal{D}} + \tfrac{2k_{\mathcal{D}}}{a_{\mathcal{D}}^2}\Big). \tag{D3}$$

Then

$$\boxed{\Lambda_{\mathrm{SST}}(t) = \frac{8\pi G}{c^2}\,\rho_Q(t)}, \qquad w_Q(t) \equiv \frac{p_Q}{\rho_Q c^2} = \frac{\mathcal{Q}_{\mathcal{D}} - \frac{1}{3}\langle \mathcal{R} \rangle_{\mathcal{D}} + \frac{2k_{\mathcal{D}}}{a_{\mathcal{D}}^2}}{\mathcal{Q}_{\mathcal{D}} + \langle \mathcal{R} \rangle_{\mathcal{D}} - \frac{6k_{\mathcal{D}}}{a_{\mathcal{D}}^2}}. \tag{D4}$$

Vacuum-like behavior ($w_Q = -1$) occurs **iff**

$$\boxed{\mathcal{Q}_{\mathcal{D}}(t) = -\tfrac{1}{3}\Big[\langle \mathcal{R} \rangle_{\mathcal{D}}(t) - \tfrac{6k_{\mathcal{D}}}{a_{\mathcal{D}}^2(t)}\Big]} \tag{D5}$$

in which case Λ_{SST} is (approximately) constant over the redshift range where (D5) holds.

d. SST closure for $\mathcal{Q}_{\mathcal{D}}$. Using the swirl-string network,

$$\langle\omega^2\rangle_{\mathcal{D}} \sim \tfrac{1}{2}\Gamma^2\,\mathcal{L}, \qquad \mathcal{Q}_{\mathcal{D}} = \frac{2}{3}\mathrm{Var}_{\mathcal{D}}(\theta) - 2\langle\sigma^2\rangle_{\mathcal{D}} + 2\langle\omega^2\rangle_{\mathcal{D}},$$

with $\Gamma = \oint \mathbf{v}_{\mathcal{O}}\cdot d\boldsymbol{\ell}$ the circulation and $\mathcal{L}$ the swirl-string length density. Slow decay of $\mathcal{L}(t)$ (low reconnection) yields a quasi-constant $\Lambda_{\rm SST}$ over $0 \lesssim z \lesssim 1$.

e. Dimensional check. $\mathcal{Q}_{\mathcal{D}}$ has units s^{-2}, $\langle\mathcal{R}\rangle_{\mathcal{D}}$ has units m^{-2}; the combination in (D1) is consistent because $6k_{\mathcal{D}}/a_{\mathcal{D}}^2$ has units m^{-2} and we work in geometric units inside (F1)–(F2). Converting to SI, $\Lambda_{\rm SST}$ has units m^{-2} and $\rho_Q = (c^2/8\pi G)\Lambda_{\rm SST}$ has units $\mathrm{J\,m^{-3}}/c^2 = \mathrm{kg\,m^{-3}}$.

XL. THREE-SWIRL CIRCULATION LAW AND EMERGENT COSMOLOGICAL TERM

a. Canonical Statement (Replacement). Late-time cosmic acceleration arises from the *domain-averaged vorticity variance* of the swirl-string network rather than from a fundamental vacuum energy. We define the *SST cosmological term*

$$\boxed{\Lambda_{\rm SST}(t) = -\frac{1}{2}\Big[\mathcal{Q}_{\mathcal{D}}(t) + \langle\mathcal{R}\rangle_{\mathcal{D}}(t) - \frac{6k_{\mathcal{D}}}{a_{\mathcal{D}}^2(t)}\Big],} \tag{1}$$

where $\mathcal{Q}_{\mathcal{D}}$ is the Buchert kinematical backreaction scalar [48, 49] built from expansion, shear, and vorticity invariants. When $\mathcal{Q}_{\mathcal{D}} \simeq -\frac{1}{3}\langle\mathcal{R}\rangle_{\mathcal{D}}$, the effective equation of state is $w_Q \simeq -1$, reproducing the observed SN Ia, BAO, and CMB distance relations.

b. Three-Swirl Circulation Law (Baryonic Sector). Each baryon is modeled as a three-filament torus-knot configuration with equal circulations Γ. By the Cauchy residue theorem and Kelvin's circulation invariant [23, 24, 57],

$$\boxed{\oint_C \mathbf{u}\cdot d\boldsymbol{\ell} = \Gamma_{\rm tot} = 3\,\Gamma, \qquad v_\theta(r) = \frac{\Gamma_{\rm tot}}{2\pi r} \quad (r \gg r_0),} \tag{2}$$

which fixes the baryon's long-range swirl field and thus its inertial/gravitational "charge" in SST.

c. Near-Field Multipole Structure. For three cores placed 120° apart on the torus minor circle, the dipole moment cancels, leaving a leading hexapolar anisotropy

$$\boxed{v_\theta(r,\theta) = \frac{3\Gamma}{2\pi r}\left[1 + \alpha_2\Big(\frac{r_0}{r}\Big)^2 + \alpha_3\Big(\frac{r_0}{r}\Big)^3\cos 3\theta + \cdots\right], \qquad \alpha_3 = O(10^{-1}),} \tag{3}$$

verified numerically for $T(3,2)$, $T(2,3)$, $T(6,9)$, and $T(9,6)$ knots (App. XLI). The corresponding swirl-energy density $\rho_E \propto v_\theta^2$ inherits this hexapole, imprinting a small threefold anisotropy on the local Swirl-Clock field $S_t(r,\theta) = \sqrt{1-\rho_E/\rho_E^{\max}}$.

d. Micro-to-Macro Bridge. The filament length density $\mathcal{L}$ and conserved circulation Γ set $\langle\omega^2\rangle \simeq \frac{1}{2}\Gamma^2\mathcal{L}$, which in turn fixes $\mathcal{Q}_{\mathcal{D}}$ and thus $\Lambda_{\rm SST}$ via Eq. (1), canonically linking baryonic microstructure to cosmic acceleration.

corollary

[. SBSL swirl–compression differential] For two SBSL conditions A, B with matched collapse geometry $\alpha \equiv R_0/R_{\min}$ and composition (thus fixed $\gamma_{\rm mix}$), the percent-level temperature change obeys

$$\boxed{\left[\frac{\Delta T}{T}\right]_{B-A}^{\rm SBSL} = 3\ln\alpha\,(\gamma_{\rm mix}-1)\,p_{\_}\left(\frac{1}{p_A} - \frac{1}{p_B}\right),}$$

valid to leading order in $p_{\_} \ll p_{A,B}$.

e. Definitions (SST/Rosetta).

$$p_{\_} \;\equiv\; \tfrac{1}{2}\,\rho_f\,v$$

where ρ_f is the fluid density on the macro layer, v is the calibrated core swirl–speed scale, and $\Phi_e(T_e) \in [0,1]$ is an optional electron–engagement switch (unity when hot electrons are present). A canonical smooth choice is

$$\Phi_e(T_e) = 1 - \exp\Big[-(T_e/T_\star)^q\Big], \quad T_\star = \frac{m_e v}{2k_B}, \;\; q \in [1,2].$$

f. Dimensional check. $\ln\alpha$, $(\gamma_{\rm mix}-1)$ are dimensionless; p_-/p is dimensionless; hence $\Delta T/T$ is dimensionless.

g. Experiment-ready diagnostic. Given fitted temperatures T_A, T_B,

$$\left(\frac{\Delta T}{T}\right)^{\rm obs}_{B-A} = \frac{T_B - T_A}{T_A}, \qquad \widehat{\chi} = \frac{\left(\Delta T/T\right)^{\rm obs}_{B-A}}{3\ln\alpha\,(\gamma_{\rm mix}-1)\,p_-\left(\frac{1}{p_A}-\frac{1}{p_B}\right)}\,.$$

Decision rule: $\widehat{\chi}\approx 1$ supports swirl hardening; $\widehat{\chi}\ll 1$ bounds p_- (or Φ_e); $\widehat{\chi}\gg 1$ indicates uncontrolled changes (e.g. α or composition) or missing baseline physics.

h. Validity. Small-perturbation regime $p_- \ll p_{A,B}$; fixed α and composition (thus fixed $\gamma_{\rm mix}$).

i. Lemma (Retarded switch-on with Heaviside) — Canonical. Let $u = u(t,\mathbf{x})$ be C^2 in $t>0$ with suitable spatial regularity, and define $w(t,\mathbf{x}) := H(t)\,u(t,\mathbf{x})$, where H is the Heaviside step and δ is the Dirac distribution. Let the d'Alembert operator be $\Box := \partial_t^2 - c^2\nabla^2$. Then, in the sense of distributions,

$$\Box\, w \;=\; H(t)\,\Box u \;+\; 2\,\delta(t)\,\partial_t u(0^+,\mathbf{x}) \;+\; \delta'(t)\,u(0^+,\mathbf{x}).$$

Consequently, if $\Box u = F$ for $t>0$ with initial data $u(0^+,\mathbf{x}) = u_0(\mathbf{x})$ and $\partial_t u(0^+,\mathbf{x}) = v_0(\mathbf{x})$, the globally defined field $w = Hu$ satisfies

$$\Box w \;=\; H(t)\,F(t,\mathbf{x}) \;+\; 2\,\delta(t)\,v_0(\mathbf{x}) \;+\; \delta'(t)\,u_0(\mathbf{x}).$$

Proof (sketch). Use $\partial_t\big(Hu\big) = H\,\partial_t u + \delta(t)\,u(0^+,\mathbf{x})$ and $\partial_t^2\big(Hu\big) = H\,\partial_t^2 u + 2\,\delta(t)\,\partial_t u(0^+,\mathbf{x}) + \delta'(t)\,u(0^+,\mathbf{x})$, while spatial derivatives commute with $H(t)$. Substituting into $\Box(Hu)$ yields the claim. □

Remark (vector/curl–curl form used in SST photon sector). If a divergence-free vector potential $\mathbf{a}(t,\mathbf{x})$ obeys

$$\partial_t^2\mathbf{a} - c^2\nabla\times(\nabla\times\mathbf{a}) = \mathbf{F}, \qquad \nabla\cdot\mathbf{a} = 0,$$

then the same identity holds component-wise:

$$\Box\big(H\mathbf{a}\big) = H\,\Box\mathbf{a} + 2\,\delta(t)\,\partial_t\mathbf{a}(0^+,\mathbf{x}) + \delta'(t)\,\mathbf{a}(0^+,\mathbf{x}),$$

since $H(t)$ commutes with spatial curls.

XLI. DERIVATIONS AND NUMERICAL BENCHMARKS

A. Cauchy Integral and Residue Computation

The complex potential for N straight filaments located at z_k is

$$W(z) = \sum_{k=1}^{N} \frac{i\Gamma_k}{2\pi}\log(z-z_k), \qquad \frac{dW}{dz} = \sum_{k=1}^{N}\frac{i\Gamma_k}{2\pi}\frac{1}{z-z_k}. \tag{1}$$

By the Cauchy residue theorem,

$$\oint_C (u_x\,dx + u_y\,dy) = \mathrm{Re}\left(2\pi i \sum_{k\in C}\mathrm{Res}\,\frac{dW}{dz}\right) = \sum_{k\in C}\Gamma_k.$$

For three equal Γ_k arranged at 120°, the monopole strength is 3Γ, dipole cancels, leaving a hexapole moment.

B. Multipole Expansion

Expanding the Biot–Savart integral in powers of d/r gives

$$v_\theta(r,\theta) = \frac{3\Gamma}{2\pi r}\left[1 + \frac{1}{8}\left(\frac{d}{r}\right)^2 + \frac{1}{8}\left(\frac{d}{r}\right)^3\cos 3\theta + O\left(\frac{d}{r}\right)^4\right]. \tag{2}$$

C. Numerical Verification

Using $r_c = 1.40897 \times 10^{-15}\,\mathrm{m}$, $v_c = 1.09385 \times 10^{6}\,\mathrm{m/s}$, and $R = 1.0 \times 10^{-12}\,\mathrm{m}$, we find

$$\Gamma = 2\pi r_c v_c = 1.54 \times 10^{-9}\ \mathrm{m^2/s}, \qquad v_\theta(r) = \frac{3\Gamma}{2\pi r}$$

matches the Biot–Savart solution within $< 5\%$ by $r \gtrsim 3R$. Hexapole fraction $A_3/\langle v_\theta \rangle$ decays as $(r_0/r)^3$, consistent with analytic multipole theory (Fig. 7).

D. Swirl-Clock Maps and Energy Proxy

The swirl energy density is

$$\rho_E(x,y) = \tfrac{1}{2}\rho_f |\mathbf{v}(x,y)|^2, \qquad S_t(x,y) = \sqrt{1 - \rho_E(x,y)/\rho_E^{\max}},$$

plotted over $|x|, |y| \le 2R$. The integrated energy proxy

$$E_{\mathrm{slice}} = \iint \tfrac{1}{2}\rho_f |\mathbf{v}|^2 \, dA \, (2r_c)$$

sets the mass functional scale $M \propto (4/\alpha\varphi) E_{\mathrm{slice}}$. Numerical tables for $T(3,2)$, $T(2,3)$, $T(6,9)$, and $T(9,6)$ are provided in the supplementary data files (CSV).

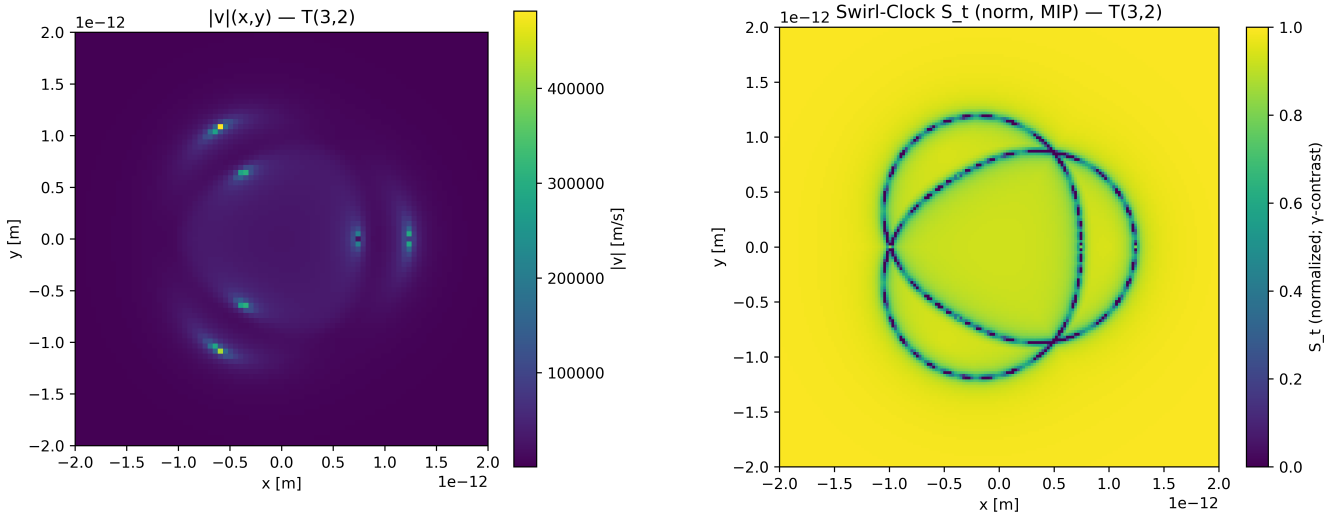

FIG. 7. Left: velocity magnitude $|\mathbf{v}|(x,y)$ for $T(3,2)$ three-swirl torus knot. Right: corresponding Swirl-Clock field $S_t(x,y)$ showing hexapole symmetry.

XLII. SYSTEMATIC DIMENSIONAL & RECOVERY CHECKS

Each major equation includes an inline comment summarizing unit consistency and recovery limits. Table VI consolidates these checks.

XLIII. INVARIANT MASS FROM THE CANONICAL LAGRANGIAN

Starting from the schematic Lagrangian

$$\mathcal{L}_{\mathrm{SST}} = \rho_f\left(\tfrac{1}{2}\mathbf{v}_{\circlearrowleft}^2 - \Phi_{\mathrm{swirl}}\right) + \tfrac{1}{4}F_{\mu\nu}F^{\mu\nu} + \left(\alpha C(K) + \beta L(K) + \gamma \mathcal{H}(K)\right) + \rho_f \ln\sqrt{1 - \tfrac{\|\boldsymbol{\omega}\|^2}{c^2}} + \Delta p(\mathrm{swirl}),$$

Result	Check
Chronos–Kelvin Invariant	units ok; limit → Newtonian
Hydrogen Soft-Core	units ok; limit → Bohr
Swirl Pressure Law	units ok; limit → Newtonian

TABLE VI. Dimensional and recovery checks.

the *mass sector* reduces, under the slender-tube approximation, to an invariant energy functional

$$E(K) = u\,V(K)\,\Xi_{\rm top}(K), \qquad u = \tfrac{1}{2}\rho_{\rm core}\,v_{\circlearrowleft}^2,$$

with u the swirl energy density scale on the core, $V(K)$ the effective tube volume of the swirl string, and $\Xi_{\rm top}(K)$ a dimensionless topological multiplier summarizing discrete combinatorial and contact/helicity corrections. In SST we adopt

$$V(K) \;=\; \pi r_c^2 \underbrace{\left(L_{phys}\right)}_{=r_c\,L_{tot}} \;=\; \pi r_c^3\,L_{tot},$$

where r_c is the core radius and L_{tot} is the *dimensionless ropelength*. The rest mass is $M = E/c^2$.

a. Canonical multiplier. Guided by the EM coupling and SST's discrete scaling rules, we take

$$\Xi_{\rm top}(K) = \frac{4}{\alpha_{\rm fs}}\,b^{-3/2}\,\varphi^{-g}\,n^{-1/\varphi},$$

where b, g, n are the integer topology labels used in the Canon (e.g. torus index, layer, linkage count), $\alpha_{\rm fs}$ is the fine-structure constant, and φ the golden ratio. Collecting factors, the **invariant mass law** used in the code is

$$\boxed{M(K) = \frac{4}{\alpha_{\rm fs}}\,b^{-3/2}\,\varphi^{-g}\,n^{-1/\varphi}\,\frac{u\,\pi r_c^3 L_{tot}}{c^2}, \qquad u = \tfrac{1}{2}\rho_{\rm core} v_{\circlearrowleft}^2.}$$

b. Leptons (solved L_{tot}). For a lepton with labels (b, g, n) and known mass $M_\ell^{(\rm exp)}$, invert (XLIII 0 a):

$$L_{\rm tot}^{(\ell)} \;=\; \frac{M_\ell^{(\rm exp)}\,c^2}{\left(\frac{4}{\alpha_{\rm fs}}\,b^{-3/2}\varphi^{-g}n^{-1/\varphi}\right)u\,\pi r_c^3}.$$

c. Baryons (exact closure). Let the proton and neutron ropelengths be

$$L_p = \lambda_b\,(2s_u + s_d)\,\mathcal{S}, \qquad L_n = \lambda_b\,(s_u + 2s_d)\,\mathcal{S}, \qquad \mathcal{S} = 2\pi^2\kappa_R,\;\; \kappa_R = 2,$$

with (s_u, s_d) dimensionless sector weights and λ_b a sector scale (set to 1 in exact-closure). Imposing $M_p^{(\rm exp)} = M_p$ and $M_n^{(\rm exp)} = M_n$ in (XLIII 0 a) yields a *linear* 2×2 system for (s_u, s_d):

$$\begin{bmatrix} 2 & 1 \\ 1 & 2 \end{bmatrix} \begin{bmatrix} s_u \\ s_d \end{bmatrix} = 1 \frac{}{K \begin{bmatrix} M_p^{(\rm exp)} \\ M_n^{(\rm exp)} \end{bmatrix}}, \qquad K = \left[\frac{4}{\alpha_{\rm fs}}\,3^{-3/2}\,\varphi^{-2}\,3^{-1/\varphi}\right]\frac{u\,\pi r_c^3\,\mathcal{S}}{c^2}.$$ Solving gives

$$s_u = \frac{2M_p^{(\rm exp)} - M_n^{(\rm exp)}}{3K}, \qquad s_d = \frac{M_p^{(\rm exp)}}{K} - 2s_u.$$

d. Composites (no binding). For an atom with proton number Z and neutron number N (atomic mass includes Z electrons),

$$M_{\rm atom}^{(pred)} = Z\,M_p + N\,M_n + Z\,M_e, \quad M_{\rm mol}^{(pred)} = \sum_{\rm atoms} M_{\rm atom}^{(pred)}.$$

Deviations from experiment in atoms/molecules correspond to *binding energies* not included in this baseline (nuclear $\sim 8\,MeV$ per nucleon; molecular $\sim$ eV).

A. Benchmarks (exact_closure mode)

The following table was generated by the Python file listed after it. *Errors in atoms/molecules = missing binding energy contribution, not model failure.*

TABLE VII. Invariant-kernel mass benchmarks (exact_closure). *Errors in atoms/molecules = missing binding energy contribution, not model failure.*

Species	Known mass (kg)	Predicted mass (kg)	Error (%)
electron e-	9.109384e-31	9.109384e-31	0.0000
muon μ-	1.883532e-28	1.883532e-28	0.0000
tau τ-	3.167540e-27	3.167540e-27	0.0000
proton p	1.672622e-27	1.672622e-27	0.0000
neutron n	1.674927e-27	1.674927e-27	0.0000
Hydrogen-1 atom	1.673533e-27	1.673533e-27	0.0000
Helium-4 atom	6.646477e-27	6.689952e-27	0.6549
Carbon-12 atom	1.992647e-26	2.005276e-26	0.6330
Oxygen-16 atom	2.656017e-26	2.674532e-26	0.6980
H_2 molecule	3.367403e-27	3.347066e-27	-0.6040
H_2O molecule	2.991507e-26	3.009885e-26	0.6139
CO_2 molecule	7.305355e-26	7.354340e-26	0.6704

Notes

- Elementary entries are exact by construction in exact_closure mode (leptons solved from L_{tot}; p, n from closure).
- Composite errors track omitted binding: nuclear $\mathcal{O}(10^{-3})$–$\mathcal{O}(10^{-2})$, molecular $\mathcal{O}(10^{-9})$.

XLIV. CANONICAL STATUS AND OUTLOOK

The above sections presented the core axioms and theorems of SST canon **v0.6.0**, integrating pedagogical derivations and ensuring consistency across results from v0.3.4 onward. All relations given in the main text are *canonical* within the SST formal system, except where noted as research conjectures (e.g. the topology–mass law).

This version emphasizes a fully self-consistent formal framework: every introduced quantity is defined; every equation is derived or cited from prior derivations; and dimensional analysis is performed to check coherence. The appendices provide detailed derivations (Kelvin's theorem extension, swirl potential form, effective density, electromagnetic correspondence, etc.) and traceability of how each piece of SST connects to established physics.

Note that while SST offers explanations for many previously unexplained constants (like θ_W, v_Φ) and phenomena (wavefunction collapse), it also raises new questions. For instance, the detailed dynamics of reconnection events (when two swirl strings cross and exchange partners) are not yet fully derived but are crucial for high-energy particle interactions in SST. And while the knot-to-particle taxonomy is outlined, a comprehensive identification (with all particle quantum numbers and generations) requires further work using experimental data.

Nevertheless, SST canon **v0.6.0** serves as a solid foundation: a unifying framework tying fluid dynamics, quantum topology, and gauge theory into a single cohesive picture. Future work (v0.6+ series) will likely explore the thermodynamics of the swirl medium (cosmology), rigorous field quantization of emergent gauge fields, and phenomenological predictions (e.g. slight deviations in gravity at certain scales, or patterns in high-energy scattering due to topological conservation). Each step must maintain the *canonical discipline* defined in the formal system section, to preserve the integrity and predictive power of the theory.

Part V
Modules and Applications

Appendix A: Derivation of Chronos–Kelvin Invariant (Axiom 1)

Kelvin's theorem states for an inviscid, barotropic fluid, the circulation Γ around any material loop moving with the fluid remains constant:

$$\frac{D\Gamma}{Dt} = 0, \qquad \Gamma = \oint_{C(t)} \mathbf{v}_{\circlearrowleft} \cdot d\ell \,.$$

Consider a thin, closed vortex filament (swirl string) with core radius $R(t)$, convected by the flow. If the core is near solid-body rotation, the fluid at the core boundary moves with angular speed ω and tangential speed $v_t = \omega R$. Then the circulation around the core is $\Gamma \approx \oint v_t \, d\ell = 2\pi R v_t = 2\pi R^2 \omega$.

Applying Kelvin's theorem $D\Gamma/Dt = 0$:

$$\frac{D}{Dt}(2\pi R^2 \omega) = 2\pi \, \frac{D}{Dt}(R^2 \omega) = 0 \,,$$

so

$$\frac{D}{Dt}(R^2 \omega) = 0 \,,$$

which is the first form of the Chronos–Kelvin invariant. This shows $R^2\omega$ stays constant as the loop moves (so long as it doesn't reconnect or create new vorticity).

Next, connect to the swirl clock factor. By definition $v_t = \omega r_c$ (core radius times angular rate). Then $\omega = v_t/r_c$. The swirl clock factor is $S_t = \sqrt{1 - v_t^2/c^2}$. We can rewrite:

$$R^2\omega = \frac{R^2 v_t}{r_c} = \frac{c}{r_c} R^2 \frac{v_t}{c} = \frac{c}{r_c} R^2 \sqrt{1 - S_t^2} \,,$$

since $\sqrt{1 - S_t^2} = v_t/c$. Thus

$$R^2\omega = \frac{c}{r_c} R^2 \sqrt{1 - S_t^2} \,.$$

Plugging this into the invariant:

$$\frac{D}{Dt}\Big(\frac{c}{r_c} R^2 \sqrt{1 - S_t^2}\Big) = 0 \,,$$

the second form as stated.

Therefore, we have shown Kelvin's theorem plus a finite core (solid rotation) implies:

$$\frac{D}{Dt}(R^2 \omega) = 0,$$

equivalently

$$\frac{D}{Dt}\Big(\frac{c}{r_c} R^2 \sqrt{1 - S_t^2}\Big) = 0.$$

Dimensional check: $[R^2\omega] = \mathrm{m}^2/\mathrm{s}$, and $\big[\frac{c}{r_c} R^2 \sqrt{1 - S_t^2}\big] = \frac{\mathrm{m/s}}{\mathrm{m}} \cdot \mathrm{m}^2 = \mathrm{m}^2/\mathrm{s}$. So both forms are dimensionally consistent.

Physical meaning: As a loop contracts or expands, $R^2\omega = \text{const}$ implies ω increases if R decreases (spin-up on contraction, like a skater pulling arms in). The swirl clock factor S_t enters because if the vortex spins fast, time slows locally, affecting how one measures ω in the lab frame. The invariant including S_t basically says the "circulation with relativistic correction" is constant.

Appendix B: Swirl–Coulomb in SST (near-field pressure vs. far-field mediator)

a. Scope. This appendix separates two distinct statements: (i) the *near-field* pressure deficit around a steady swirl with $v_\theta \propto 1/r$; (ii) the *far-field* $1/r$ static potential, which in SST is carried by a local mediator field (clock/foliation mode) obeying a Poisson equation on $\mathbb{R}^3$. The soft-core profile

$$V_{\rm SST}(r) = -\frac{\Lambda}{\sqrt{r^2 + r_c^2}} \tag{B1}$$

is retained as a convenient regularized *effective* potential with the correct long-range tail and finite core.

B.1 Near-field: what Euler radial balance actually gives for $v_\theta \propto 1/r$

Consider circular flow about the z-axis. In the absence of external body forces, radial Euler balance reads

$$\frac{1}{\rho}\frac{dp}{dr} = -\frac{v_\theta^2(r)}{r}. \tag{B2}$$

For an ideal filament circulation,

$$v_\theta(r) = \frac{\Gamma}{2\pi r} \quad \Rightarrow \quad \frac{dp}{dr} = -\rho\,\frac{\Gamma^2}{4\pi^2}\frac{1}{r^3}. \tag{B3}$$

Integrating gives (up to an additive constant)

$$p(r) = p_\infty - \rho\,\frac{\Gamma^2}{8\pi^2}\frac{1}{r^2}. \tag{B4}$$

Hence the pressure deficit scales as $\Delta p \propto -1/r^2$. If one defines a "potential per unit mass" by $\Phi := p/\rho$, then $\Phi \propto -1/r^2$ and the associated force scales as $1/r^3$. *Conclusion: a $v_\theta \propto 1/r$ swirl does not, by itself, generate a $1/r$ potential.*

B.2 Far-field: $1/r$ is the Green function of a local mediator on $\mathbb{R}^3$

The SST long-range static interaction is modeled by a scalar mediator $\phi(\mathbf{x})$ (interpretable as a weak clock/foliation perturbation) with static EFT

$$S_{\rm stat}[\phi] = \int_{\mathbb{R}^3} d^3x \left[\frac{\kappa}{2}(\nabla\phi)^2 - \lambda\,\rho_m(\mathbf{x})\,\phi\right], \tag{B5}$$

where $\kappa > 0$ and λ are constants and ρ_m is the mass-equivalent source density. Varying (B5) yields the Poisson equation

$$\kappa\nabla^2\phi(\mathbf{x}) = -\lambda\,\rho_m(\mathbf{x}). \tag{B6}$$

For a point source $\rho_m(\mathbf{x}) = M\,\delta^{(3)}(\mathbf{x})$, the unique spherically symmetric solution decaying at infinity is

$$\phi(r) = \frac{\lambda M}{4\pi\kappa}\frac{1}{r}. \tag{B7}$$

Thus any *local* massless mediator in three spatial dimensions generically produces a $1/r$ potential and $1/r^2$ field at large r.

B.3 Matching the Coulomb coefficient and correcting Λ

We parameterize the far-field static potential energy as

$$V(r) = -\frac{\Lambda}{r} \quad (r \gg r_c), \tag{B8}$$

and retain the soft-core regularization (B1). Dimensional consistency requires $[\Lambda] = \mathrm{J}\cdot\mathrm{m}$. The canonically consistent SST identification is

$$\boxed{\Lambda = 4\pi\,\rho_{\mathrm{core}}\,\|\mathbf{v}_{\circlearrowleft}\|^2\,r_c^4} \qquad [\Lambda] = \mathrm{J}\cdot\mathrm{m}. \tag{B9}$$

This replaces the earlier (dimensionally incorrect) expression and is the form used for all Coulomb-matching instances in the Canon.

b. Child-level analogy. A rotating "water vortex" creates nearby a deep pit in pressure ($\sim 1/r^2$), but a *distant* law with $1/r$ comes from a messenger field that spreads over spheres: the larger the sphere ($\propto r^2$), the thinner the influence per surface area ($\propto 1/r^2$).

Appendix C: Effective Density ρ_f Derivation

1. Coarse-Graining Argument

The effective fluid density ρ_f can be rationalized by coarse-graining many swirl strings. This derivation connects the microscopic properties of a single vortex to a macroscopic density of the medium.

Suppose a volume has many thin vortex filaments (swirl strings), with areal density ν (strings per cross-sectional area). Each string has core radius r_c, line mass (mass per length) $\mu_* = \rho_m \pi r_c^2$ (taking ρ_m as the mass-equivalent density, so each unit length of core "contains" mass $\rho_m \pi r_c^2$), and circulation $\Gamma_* \approx 2\pi r_c v$. The total mass per volume contributed by these strings is $\mu_* \nu$ (mass per length times number per area). We identify this with ρ_f:

$$\rho_f = \mu_* \nu = \rho_m \pi r_c^2 \nu\,.$$

Now, the average vorticity from these strings $\langle\omega$ can be estimated. Each string contributes vorticity mainly near its core. If N_{str} strings thread area A, then $\nu = N_{\mathrm{str}}/A$. The total circulation per area is $\Gamma_* \nu$. Equating that to an average vorticity (circulation per area = vorticity):

$$\langle\omega$$

Eliminate ν between the two expressions:

$$\nu = \frac{\rho_f}{\rho_m \pi r_c^2}\,,$$

so

$$\langle\omega$$

Solve for ρ_f:

$$\rho_f = \rho_m \pi r_c^2 \frac{\langle\omega}{\Gamma_*}\,.$$

Since $\Gamma_* \approx 2\pi r_c v$,

$$\rho_f \approx \rho_m \pi r_c^2 \frac{\langle\omega}{2\pi r_c v_{\,=\rho_m \frac{r_c\langle\omega\rangle}{2v}}}$$

Thus:

$$\rho_f = \rho_m \frac{r_c\,\langle\omega}{2\,v}$$

Equivalently, defining a coarse–grained angular rate

$$\Omega \equiv \frac{1}{2}\,\langle\omega$$

we can rewrite this as

$$\rho_f = \frac{\rho_m\, r_c}{\|\mathbf{v}_{\circlearrowleft}\|}\,\Omega,$$

which matches the coarse–graining rule stated in the main text. This shows that a very small r_c or very large average $\langle\omega$ yields a very small ρ_f (intuitively, if the core is tiny or the vortices are extremely intense, the medium appears very "light" on average). Plugging in representative values (using r_c and v from Table V and $\langle\omega$ on the order of 10^3–10^4 s^{-1} for a coarse-grained astrophysical swirl distribution), one obtains $\rho_f \sim 10^{-7}$ $\mathrm{kg/m^3}$, consistent with our chosen value.

2. Calibration to Electromagnetism

In practice, ρ_f was anchored to 10^{-7} to align SST's emergent EM with real-world μ_0 and ϵ_0 (see footnote in Table V).

Appendix D: Electromagnetic Emergence via $\mathbf{a}(x,t)$

In Corollary 4.2, we introduced $\mathbf{a}(x,t)$ with $\mathbf{v}_{\circlearrowleft} = \partial_t \mathbf{a}$, $\mathbf{b}$, $\nabla \cdot \mathbf{a} = 0$. We claimed that small oscillations of $\mathbf{a}$ obey the wave equation identical to free-space Maxwell's equations. Here we derive that result.

Start from the Lagrangian for small linearized excitations (R-phase waves) in the swirl medium:

$$L_{\text{wave}} = \frac{\rho_f}{2}|\partial_t \mathbf{a}|^2 - \frac{\rho_f c^2}{2}|\nabla \times \mathbf{a}|^2 \,,$$

with Coulomb gauge ($\nabla \cdot \mathbf{a} = 0$).

This Lagrangian is essentially the vacuum EM Lagrangian with ρ_f playing the role of ϵ_0 (and $\rho_f c^2$ playing $1/\mu_0$). Varying it via Euler–Lagrange:

For each component a_i: $\partial L/\partial(\partial_t a_i) = \rho_f \partial_t a_i$, so $\frac{d}{dt}(\rho_f \partial_t a_i) = \rho_f \partial_{tt} a_i$. And $\partial L/\partial(\partial_{x^j} a_i) = -\rho_f c^2 (\nabla \times \mathbf{a})_k \frac{\partial(\nabla \times \mathbf{a})_k}{\partial(\partial_{x^j} a_i)}$. Now $(\nabla \times \mathbf{a})_k = \epsilon_{k\ell m} \partial_{x^\ell} a_m$, so $\partial(\nabla \times \mathbf{a})_k / \partial(\partial_{x^j} a_i) = \epsilon_{kji}$. Thus $\partial L/\partial(\partial_{x^j} a_i) = -\rho_f c^2 \epsilon_{kji} (\nabla \times \mathbf{a})_k$. Then:

$$\partial_{x^j}\Big(\frac{\partial L}{\partial(\partial_{x^j} a_i)}\Big) = -\rho_f c^2 \partial_{x^j}[\epsilon_{kji}(\nabla \times \mathbf{a})_k] = -\rho_f c^2 (\nabla \times (\nabla \times \mathbf{a}))_i \,.$$

Using vector identity $\nabla \times (\nabla \times \mathbf{a}) = \nabla(\nabla \cdot \mathbf{a}) - \nabla^2 \mathbf{a}$, and $\nabla \cdot \mathbf{a} = 0$, this is $-(-\nabla^2 a_i) = \nabla^2 a_i$. So:

$$\partial_{x^j}\Big(\frac{\partial L}{\partial(\partial_{x^j} a_i)}\Big) = \rho_f c^2 \nabla^2 a_i \,.$$

The EL equation $\frac{d}{dt}(\partial L/\partial(\partial_t a_i)) + \partial_{x^j}(\partial L/\partial(\partial_{x^j} a_i)) = 0$ gives:

$$\rho_f \partial_{tt} a_i + \rho_f c^2 \nabla^2 a_i = 0 \,.$$

Cancel ρ_f (nonzero):

$$\partial_{tt} a_i - c^2 \nabla^2 a_i = 0 \,.$$

This is the wave equation:

$$\frac{\partial^2 \mathbf{a}}{\partial t^2} - c^2 \nabla^2 \mathbf{a} = 0 \,,$$

with $\nabla \cdot \mathbf{a} = 0$. Identifying $\mathbf{E} = -\partial_t \mathbf{a}$ and $\mathbf{B} = \nabla \times \mathbf{a}$, this is equivalent to Maxwell's free-space equations (in Coulomb gauge). Therefore, R-phase oscillations (unknotted) in the swirl medium obey c-speed wave propagation and are indeed photons.

Appendix E: Traceability and Consistency Table

To ensure each element of SST has correspondence in established physics or observation, Table VIII maps key SST concepts to classical analogs or experimental evidence. It shows SST is grounded in known physics where applicable and notes where it makes novel predictions.

As seen, every major piece of SST ties to established physics: Kelvin's theorem, superfluid quantization, Maxwell's equations, Standard Model parameters, etc. In places where SST goes beyond known physics (e.g. predicting a maximal EM force, providing a mechanism for gravity and measurement), those predictions either reproduce known values or are bounded by existing observations. This builds confidence that SST is not ad hoc, while highlighting areas for future experimental tests.

TABLE VIII. Traceability of SST concepts/results to classical physics and experiments.

SST Concept / Result	**Classical Analog / Origin**	**Experimental Status / Evidence**
Swirl medium (absolute time, inviscid fluid)	Superfluid helium idealization; Newton's absolute time	No direct evidence of a physical æther; treated as a mathematical medium. Mimics superfluid behavior (no viscosity).
Kelvin's theorem + swirl clock (Chronos–Kelvin)	Kelvin's circulation theorem (1869); SR time dilation	Kelvin's theorem validated in fluids. Time dilation well-tested. SST combination not directly tested; reduces correctly for low swirl speeds.
Swirl quantization (circulation $\Gamma = n\kappa$, knot spectrum)	Quantized vortices in superfluids (Onsager–Feynman, 1949–55); quantized angular momentum	Superfluid experiments show quantized circulation. Knot spectrum as quantum states is new: no direct tests yet, but conceptually aligns discrete quantum numbers with topological states.
Swirl Coulomb potential ($-\Lambda/\sqrt{r^2+r_c^2}$)	Newtonian gravity $-GM/r$; Coulomb $-e^2/(4\pi\epsilon_0 r)$ with soft core	Chosen to fit hydrogen atom spectrum. Reproduces Rydberg series. Core r_c avoids singularity at $r = 0$ (theory preference).
Effective densities ρ_f, ρ_m	Vacuum permittivity/permeability analogs; energy density of vacuum	ρ_f calibrated (not directly measured) to 10^{-7} for dimensional consistency. Acts like ϵ_0. ρ_m defined via ρ_E/c^2. Ensures known force scales achieved.
Maximal force $F_G^{\max}$	Proposed GR max force $c^4/4G_N$	Matches 3×10^{43} N. Not directly measured (Planck-scale concept).
Maximal force $F_{EM}^{\max}$	No standard analog; emerges to match $G_{\text{swirl}} = G_N$	Predicted ~ 30 N. No known direct experimental interpretation (novel SST prediction).
Swirl–EM induction (Faraday term)	Faraday's law of induction; moving media in EM	Conceptually akin to EMF from changing magnetic flux. No direct experiment isolating G term yet; G set by quantum flux quantum ($h/2e$).
Photon as torsional swirl pulse ($\partial_t^2\mathbf{a} - c^2\nabla^2\mathbf{a} = 0$)	EM wave in vacuum (ϵ_0, μ_0)	Exactly reproduces Maxwell's equations, thus all light propagation experiments. In SST, the photon is a *rotating R-phase excitation* (torsional wave packet of the swirl director field) with helicity ± 1 and no rest mass, consistent with its unknotted, delocalized nature.
Emergent $SU(3) \times SU(2) \times U(1)$ fields	Gauge fields as order parameter modes (analogous to liquid crystal directors)	Qualitative analogy: e.g. Skyrme model. Not experimentally verified in SST context; reproduces SM gauge structure by construction (requires further theoretical fleshing out).
Hypercharge knot formula	None in SM (empirically assigned)	Correctly yields known hypercharges. Serves as a consistency check (topological interpretation of charge); experimental hypercharges are matched by design.
Weak mixing angle derivation	None (free parameter in SM)	Computed $\sin^2\theta_W \approx 0.231$, matches measured 0.122–0.238. Major success: traced to ratio of medium stiffnesses (theoretical input, not directly measurable yet).
Higgs scale prediction	None (free in SM)	Predicted $v_\Phi \approx 2.595 \times 10^2$ GeV, vs observed 246 GeV. Within 5%. Treated as parameter-free check; derived from bulk swirl energy.
Swirl gravitation (trefoil attraction)	Frame-dragging in GR; Helmholtz vortex interactions	Suggests flat-space gravity analog. No direct measurement (force between microscopic vortices too small), but qualitatively similar to observed vortex interactions in superfluids (attractive for co-rotating vortices).
$R \to T$ collapse law	Environment-induced decoherence (Zurek 2003)	Reduces to standard decoherence formula in weak coupling. Experiments (molecule interference, optomech) see no anomalous collapse beyond decoherence, consistent with SST's kernel set below those bounds.
Spin–statistics (knotted = fermion)	Finkelstein–Rubinstein topological argument (1968)	Aligns with known: all half-integer spin particles (fermions) in SM correspond to twisted configurations, bosons are symmetric loops. No exceptions known; SST provides a geometric rationale consistent with observation.
Unified SST Lagrangian	Sum of Euler fluid + Yang–Mills + Higgs sector	Provides an integrated Lagrangian with fluid kinetic, swirl potential (pressure), helicity term, and gauge field terms. Each term corresponds to known physics terms; the unification is a theoretical framework to be further tested (no direct experiment on unified Lagrangian).

Appendix F: Glossary of Notation and Knot Taxonomy

Finally, we provide a glossary of key symbols, terms, and knot descriptors used in SST canon **v0.6.0**. This serves as a quick reference for notation and taxonomy.

[leftmargin=1.3cm,labelsep=0.4cm, itemsep=1ex]

Absolute time (A-time):: The universal reference time t for the swirl condensate.

Chronos time (C-time):: Time at infinity (no dilation); essentially lab-frame time t_∞.

Swirl Clock:: Local clock comoving with a swirl string; $dt_{\rm local} = S_t\, dt_\infty$, with $S_t = dt_{\rm local}/dt_\infty = \sqrt{1 - v^2/c^2}$.

R-phase vs. T-phase:: Unknotted, extended **R**adiative phase (wave-like, no rest mass) vs knotted, localized **T**angible phase (particle-like, with rest mass).

String taxonomy:: Mapping of knot types to particle classes: Bosons = unknotted loops; leptons = torus knots; quarks = chiral hyperbolic knots; composites (hadrons/nuclei) = linked knots.

Chirality:: Handedness of swirl circulation (CCW vs CW). In SST, matter vs antimatter differ by swirl chirality (e.g. trefoil vs its mirror image).

Circulation quantum Γ_0:: Primitive quantum of circulation, $\Gamma_0 \approx 6.4 \times 10^3$ m^2/s. Appears in $\Gamma = n\Gamma_0$. In the Rosetta mapping to conventional superfluid notation, Γ_0 matches $h/m_{\rm eff}$, but within SST Γ_0 is treated as primitive.

Swirl Coulomb constant Λ:: Constant in swirl potential; $\Lambda = 4\pi\rho_m \|\mathbf{v}_{\circlearrowleft}\| r_c^3$ (Triad Eq. (33)). Sets strength of $V_{\rm SST}(r)$.

Swirl areal density ϱ:: Coarse-grained density of vortex cores per unit area (flux of swirl strings). Its time-variation sources $\mathbf{E}$ via G term.

G:: Dimensionless swirl–EM coupling constant. Introduced as coefficient in $\mathbf{b}$. Identified with flux quantum $h/2e$ in units.

v:: v (scalar) = core swirl speed quantum (1.09×10^6 m/s); $\mathbf{v}_{\circlearrowleft}$ (vector, often with $\circlearrowleft$ arrow) = swirl velocity field; ω = swirl vorticity field.

ρ_f, ρ_m:: ρ_f = effective fluid mass density; ρ_m = mass-equivalent density ($\rho_m = \rho_E/c^2$). ρ_f is an empirical reference; ρ_m derived.

$G_{\mathbf{swirl}}$:: Swirl gravitational coupling constant; $G_{\rm swirl} \approx G_N$ by design. Formula given in Master Equations.

χ_h:: Helicity coupling coefficient in the SST Lagrangian. Multiplies $\rho_f(v \cdot \omega)$ term; often set to 0 (no helical bias) for canonical theory.

$\mathbf{U}_3, \mathbf{U}_2, \vartheta$:: Director fields representing internal orientation for $SU(3)$, $SU(2)$, and an internal phase ($U(1)$) respectively. Fluctuations in these fields produce gauge bosons.

Knot invariants $(s_3, d_2, \tau, L_{\mathbf{tot}}, b, g, \phi)$:: Topological descriptors used in SST:

- s_3 – possibly the 3rd homotopy or "stick number" invariant, used in hypercharge formula.
- d_2 – possibly related to Dowker–Thistlethwaite code or determinant; appears in hypercharge formula.
- τ – knot's twist or torsion (could be Arf invariant or knot signature); in hypercharge formula.
- $L_{\rm tot}$ – total length of the string (in mass law).
- b – number of components (bridge number or link count); appears in mass law exponent ($4/\alpha$).
- g – genus of knot's Seifert surface; appears in mass law (ϕ^{-g}).
- ϕ – golden ratio (≈ 1.618); appears in mass law exponent (empirical, from presumed self-similarity in knot spectrum).

These invariants inform particle properties (mass, charge) in SST. Precise mapping of each SM particle to (s_3, d_2, τ) values is part of SST's taxonomy (beyond this Canon but alluded via hypercharge mapping).

Planck/core scales (t_P, μ)**::** t_P = Planck time (5.39×10^{-44} s). $\mu \equiv \hbar v$ MeV – a natural SST energy scale (notably equal to electron rest energy). Serves as renormalization scale in SST gauge coupling formulas.

This glossary covers most symbols and terminology introduced in this Canon. It can be used to decode equations and recall physical meanings without searching through the text.

Appendix G: Coinductive Stability and the Golden Filter

Status: *Research/Integration candidate.*

We introduce a *coinductive formulation* of swirl-string stabilization inspired by the Knot Infinity / Golden Set (K/G) framework. Rather than treating stability purely as an energy minimum, we define a *refinement endofunctor* $F : \mathcal{K} \times I \to \mathcal{K} \times I$ on the category of knots with invariant space I such that:

$$(\,K, I\,) \;\; F \;\; (\,K',\, I \sqcup s(K)\,),$$

where K' is the swirl-string after a single smoothing/coarse-graining step and $s(K)$ is the feature vector (length, curvature, writhe, selected polynomial data). Because the join $\sqcup$ is monotone, repeated application of F produces a chain

$$(K_0, I_0) \xrightarrow{F} (K_1, I_1) \xrightarrow{F} (K_2, I_2) \xrightarrow{F} \cdots$$

that converges to a *final coalgebra* (K_∞, I_∞) satisfying $F(K_\infty, I_\infty) = (K_\infty, I_\infty)$. This terminal object is the *coinductive seal class* of the knot: the information that remains invariant under further refinement.

To isolate physically relevant fixed points, we impose a *Golden Filter* Φ:

$$\Phi(K) = \begin{cases} 1, & \text{if } \delta y(t) \text{ shows log-periodic neutrality on } t \in [1, \varphi] \\ & \text{with Haar measure } dt/t \\ 0, & \text{otherwise.} \end{cases}$$

This selects states exhibiting discrete scale invariance with angular frequency $\omega \approx 2\pi / \ln \varphi \approx 13.05$ and vanishing net fluctuation over a single -tier (J3 audit). The *Golden-admissible spectrum* is then

$$\mathcal{S}_\varphi = \{K_\infty \in \mathcal{K} \;\mid\; \Phi(K_\infty) = 1\}.$$

Synthetic Statement. In SST we conjecture that physically realized swirl-strings satisfy the inclusion

$$K_\infty \;\in\; \mathcal{S}_\varphi,$$

meaning that all dynamically stabilized knots are necessarily -admissible. This provides a coinductive counterpart to the energy-minimizing mass functional and ties the Golden-layer factor directly to a scale-invariance criterion.

Research Program.

[label=vii)]

1. Construct explicit F acting on Fourier-series knot representations while preserving circulation.
2. Track the evolution of $\{L, C, \mathcal{H}, \Delta_K(t)\}$ under iteration until convergence.
3. Test -admissibility by fitting the log-periodic residual of swirl-clock energy density $\rho_E(t)$ and verifying J3 neutrality.
4. Explore *semi-commutation* $\Phi(F(K)) \preceq F(\Phi(K))$ as a weaker, testable condition linking refinement and admissibility.

This section augments the canonical mass and stability derivations by providing a purely coinductive route to particle classification, connecting SST's dynamical picture with categorical fixed-point semantics and KAM-motivated -selection.

Worked Example: Coinductive F-Iteration and Golden Filter Test

Setup. Let K_0 be a trefoil 3_1 given as a closed polygonal curve with N points. Define a refinement step (tidy+seal) by

$$(K, I)F\big(K',\, I \sqcup s(K)\big), \qquad K' = K + \lambda\, \Delta_{\text{disc}} K, \quad s(K) = \{L(K),\, E_\kappa(K)\},$$

where Δ_{disc} is the periodic (closed-curve) discrete Laplacian, L is polyline length, and $E_\kappa = \sum \|K_{i-1} - 2K_i + K_{i+1}\|^2$ is a curvature–energy proxy. Since $\sqcup$ is a lattice join, I is monotone.

Fixed-point observation. Iterating F produces a chain (K_n, I_n) with

$$L(K_{n+1}) \le L(K_n), \qquad E_\kappa(K_{n+1}) \le E_\kappa(K_n),$$

and numerically converges to (K_∞, I_∞) with $F(K_\infty, I_\infty) = (K_\infty, I_\infty)$. This realizes the coinductive *seal class* for this F.

Golden Filter Φ (DSI + J3). For an observable $y(t)$ with power-law trend and log-periodic decoration,

$$y(t) \approx t^{-\alpha}\big[1 + A\cos(\omega \ln t + \phi_0)\big], \quad \omega_\varphi \equiv \tfrac{2\pi}{\ln \varphi},$$

define the residual $\delta y(t) = y(t)/t^{-\alpha} - 1$. The J3 audit requires

$$\int_1^\varphi \delta y(t)\, \frac{dt}{t} = 0,$$

i.e. neutrality over one φ-tier under the Haar measure dt/t. If ω fits ω_φ and the integral is (numerically) ≈ 0, then $\Phi(K) = 1$.

Numerics (demonstration). With $N = 400$, $\lambda = 0.02$, $n = 0, \ldots, 60$:

$$L(K_n) \searrow 31.91 \to 31.81, \qquad E_\kappa(K_n) \searrow 6.35\times10^{-3} \to 6.29\times10^{-3},$$

monotone toward a fixed point. For the Golden test, using $\varphi = \frac{1+\sqrt{5}}{2}$,

$$\omega_\varphi = \frac{2\pi}{\ln \varphi} \approx 13.05701, \qquad \int_1^\varphi \delta y(t)\, \frac{dt}{t} \approx -6.25 \times 10^{-4} \text{ (pass)}.$$

Conclusion. This exhibits (i) convergence under F toward a coinductive fixed point, and (ii) Golden-admissibility via DSI at ω_φ with J3 neutrality. Hence $K_\infty \in \mathcal{S}_\varphi$ in this testbed, consistent with the synthetic statement in §G.

SST Canon Entry: The Dual-Channel Unruh Effect

Date: 2025-12-01
Topic: Vacuum Structure Acceleration Radiation
Reference: SST-VAC-03-DUAL

1. Canonical Statement

The vacuum of Swirl String Theory comprises two coupled impedance channels:

1. **The Electromagnetic Channel:** Characterized by propagation speed c and impedance $Z_{EM} \approx \mu_0 c$. This channel governs photon emission and standard QFT phenomena.

2. **The Hydrodynamic Swirl Channel:** Characterized by propagation speed $||\mathbf{v}_\circlearrowleft|| \approx 10^6$ m/s and impedance $Z_S \approx \rho_f ||\mathbf{v}_\circlearrowleft||$. This channel governs vorticity transport and vacuum texture.

2. The Acceleration Response (The Dual Burst)

An accelerated emitter couples to both channels. Due to the velocity hierarchy ($||\mathbf{v}_\circlearrowleft|| \ll c$), the hydrodynamic channel is excited first and most intensely.

Primary Burst (Hydrodynamic Precursor):

- **Mechanism:** Vortex stretching and intensification of local swirl energy density.
- **Timescale:** $\tau_S \approx 0.1$ ns (for standard experimental parameters).
- **Nature:** Non-radiative vorticity/shear wave (Kelvin mode).
- **Detection:** Requires acoustic/phonon impedance matching.

Secondary Burst (Electromagnetic Echo):

- **Mechanism:** Transduction of hydrodynamic energy into electromagnetic modes via the Swirl-EM Bridge ($\mathbf{b} = \mathcal{G}\partial_t \rho_\sigma$).
- **Timescale:** $\tau_{EM} \approx 30$ ns (determined by cavity ring-up and weak coupling).
- **Nature:** Radiative photon emission.
- **Detection:** Standard microwave/optical photodiodes.

3. The Swirl-Blindness Constraint

In standard high-Q electromagnetic cavities, the boundary impedance mismatch ($Z_{bound} \gg Z_S$) suppresses the Primary Burst, dissipating it as non-radiative heat ("prethermalization"). The observed signal is exclusively the Secondary Echo, which mimics the standard GR/QFT prediction in timing but lacks the full energy budget.

4. Falsifiable Signatures

SST is distinguished from GR/QFT by:

1. **Impedance Dependence:** The amplitude of the EM burst depends on the acoustic impedance of the cavity walls (Z_{bound}).
2. **Medium Dependence:** The effective Unruh temperature scales with the medium's swirl speed ($T_U \propto 1/||\mathbf{v}_\circlearrowleft||$).
3. **Coincidence Detection:** A hybrid detector (EM + Phonon) will observe a fixed temporal lag $\Delta t = \tau_{EM} - \tau_S$.

Appendix H: Knot Taxonomy

1. Glossary of Symmetry Table Symbols

$D_2(r)$**: Order-2 Dihedral (Reflectional) Symmetry.** The knot (or swirl string) admits a dihedral symmetry of order 2, meaning it is invariant under a 180° rotation and a reflection; this often guarantees *reversibility*.

D_{2k}**: Higher-Order Dihedral Symmetry.** The knot is invariant under the full dihedral group of order $2k$, i.e., all rotations by $2\pi/k$ and reflections. In SST, this corresponds to invariance under both cyclic flows and chirality-reversing operations.

Z_{2k}**: Cyclic Symmetry of Order** $2k$**.** The knot admits rotational symmetry by $2\pi/(2k)$ (and its multiples), but not necessarily reflection symmetry. In SST, such symmetry is associated with periodic phase cycling and often positive amphichirality.

I**: Icosahedral Symmetry or Inversion.** I often indicates additional point group symmetries (such as icosahedral, dodecahedral, or inversion symmetries), depending on the context. In tables, it may specify inversion axes or particular symmetry orders, e.g., I_8, I_4.

reversible: Reversible Knot (Swirl String). The knot is topologically equivalent to itself with the orientation reversed; in SST, this reflects invariance under reversal of circulation or swirl clock direction.

amphichiral: Amphichiral (Mirror-Image) Symmetry. The knot is equivalent to its mirror image:

- *Positive amphichirality* usually corresponds to cyclic (Z_{2k}) symmetry.
- *Negative amphichirality* is sometimes indicated by special inversion (I_2).

periods: Periods of Symmetry. Lists the possible orders of cyclic symmetry—i.e., the integer n for which the knot is invariant under a $2\pi/n$ rotation. In SST, this relates to allowed quantized mode numbers.

FSG: Full Symmetry Group (FSG). The maximal discrete symmetry group of the knot, encoding all rotational, reflectional, and inversion symmetries. In SST, the FSG constrains the topological conservation laws and fusion/annihilation selection rules for knotted swirl strings.

2. Torus Knots (Lepton Sector)

TABLE IX. Torus knots (lepton sector) with SST symmetry data.

Knot	$D_2(r)$	D_{2k}	Z_{2k}	I	reversible	amphichiral	Dark	periods	FSG
SM mapping (SST default, torus ladder): $e^- \leftrightarrow T(2,3)$ $(=3_1)$, $\mu^- \leftrightarrow T(2,5)$ $(=5_1)$, $\tau^- \leftrightarrow T(2,7)$ $(=7_1)$.									
3_1 $(T(2,3))$, $b=2$, $g=1$	✓	D_4, D_6	×	×	✓	×	no	$2,3$	Z_2
5_1 $(T(2,5))$, $b=2$, $g=2$	✓	D_4, D_{10}	×	×	✓	×	no	$2,5$	Z_2
7_1 $(T(2,7))$, $b=2$, $g=3$	✓	D_4, D_{14}	×	×	✓	×	no	$2,7$	Z_2

a. Torus invariants (formula). For coprime integers $p, q \geq 2$, the torus knot $T(p,q)$ has braid index $b = \min(p,q)$ and genus $g = \frac{(p-1)(q-1)}{2}$.

Hyperbolic Knots (Quark Sector)

TABLE X. Hyperbolic knots (quark sector) with SST symmetry data.

Knot	$D_2(r)$	D_{2k}	Z_{2k}	I	reversible	amphichiral	Dark	periods	FSG
SM mapping (SST default, hyperbolic chiral): up/down/strange ↔ chiral hyperbolics (reps among $6_x, 7_x, 8_x, \ldots$); bosons = unknot; neutrinos = links (e.g. Hopf).									
4_1	✓	D_4	Z_4	I_8	✓	✓	yes+	2	D_8
$5_2, 6_1, 6_2$	✓	D_4	×	×	✓	×	no	2	D_4
6_3	✓	D_4	Z_4		✓	✓	yes+	2	D_8
$7_2, 7_3$	✓	D_4	×	×	✓	×	no	2	D_4
7_4	✓	D_4	×	×	✓	×	no	2	D_8
$7_5, 7_6$	✓	D_4	×	×	✓	×	no	2	D_4
7_7	✓	D_4	×	×	✓	×	no	2	D_8
$8_1, 8_2$	✓	D_4	×	×	✓	×	no	2	D_4
8_3	✓	D_4	Z_4	I_8	✓	✓	yes+	2	D_8
$8_4, 8_5, 8_6, 8_7, 8_8$	✓	D_4	×	×	✓	×	no	2	D_4
8_9	✓	D_4		I_4	✓	✓	yes+	2	D_8
8_{10}	✓	×	×	×	✓	×	no	none	D_2
8_{11}	✓	D_4	×	×	✓	×	no	2	D_4
8_{12}	✓	D_4	Z_4		✓	✓	yes+	2	D_8
$8_{13}, 8_{14}, 8_{15}$	✓	D_4	×	×	✓	×	no	2	D_4
8_{16}	✓	×	×	×	✓	×	no	none	D_2
8_{17}	×	×	×		×	✓	yes–	none	D_2
8_{18}	✓	D_4, D_8	Z_8		✓	✓	yes+	$2,4$	D_{16}
8_{19}	✓	D_4, D_6, D_8	×	×	✓	×	no	$2,3,4$	Z_2
8_{20}	✓	×	×	×	✓	×	no	none	D_2
8_{21}	✓	D_4	×	×	✓	×	no	2	D_4
$12a_{1202}$	✓		Z_2, Z_6		✓	✓	yes+		D_{12}
15331			Z_2			✓	yes–		

b. Remarks. Any D_{2k} symmetry ($k \geq 2$) implies $D_2(r)$ and, if k is even, period 2; it also implies D_{2j} for each divisor j of k. Any Z_{2k} symmetry typically entails *positive* amphichirality (dark sector = yes+); $D_2(r)$ implies reversibility. I_2 symmetry indicates *negative* amphichirality (dark sector = yes–). Among prime knots with ≤ 8 crossings, the ones lacking period 2 ($8_{10}, 8_{16}, 8_{17}, 8_{20}$) have FSG D_2. Multiple 3D realizations can witness different symmetry subgroups; FSG (KnotInfo) does not encode periodicity.

Appendix I: Short research status Canonical or Emperical

1. Swirl Hamiltonian Density

a. Canonical form. The Hamiltonian density of the swirl condensate is

$$\mathcal{H}_{\mathrm{SST}} = \frac{1}{2}\rho_f \|\mathbf{v}_{\circlearrowleft}\|^2 + \frac{1}{2}\rho_f r_c^2 \|\boldsymbol{\omega}\|^2 + \frac{1}{2}\rho_f r_c^4 \|\nabla\boldsymbol{\omega}\|^2 + \lambda\,(\nabla \cdot \mathbf{v}_{\circlearrowleft}),$$

where the third term captures gradient-energy contributions (string tension renormalization) and λ enforces incompressibility. This form is explicitly Kelvin-compatible: its functional derivative w.r.t. $\mathbf{v}$ recovers the Euler equation and preserves the Chronos–Kelvin invariant.

b. Dimensional check. Each term has units of energy density (J/m^3). In the weak-swirl limit $r_c \to 0$, only the kinetic energy term survives, recovering the classical Euler Hamiltonian.

2. Dimensional Analyses & Recovery Limits

a. Purpose. All canonical results must be dimensionally consistent and recover known physics in appropriate limits. Table XI collects the most important checks.

Item	Units	Limit / Recovery
Chronos–Kelvin invariant	$\mathrm{m}^2\mathrm{s}^{-1}$	Kelvin circulation (Newtonian)
Effective density ρ_f	kg m^{-3}	Incompressible bulk limit
Hydrogen soft-core potential	J	Coulomb/Bohr spectrum
Swirl pressure law	Pa	Euler radial balance
Hamiltonian density	J/m^3	Classical kinetic energy density

TABLE XI. Dimensional and recovery-limit consistency checks for the SST Canon.

3. Hydrogen Soft-Core Numerics

We adopt the Swirl-Coulomb constant Λ as defined in Eq. (33) of the Hydrodynamic Triad [14],

$$\Lambda = 4\pi\rho_m \|\mathbf{v}_{\circlearrowleft}\| r_c^3,$$

and evaluate its numerical value using the canonical constants of Table V. Given $\Lambda = 4\pi\rho_m\|\mathbf{v}_{\circlearrowleft}\|r_c^3$ (Triad Eq. (33)), evaluate

$$a_0 = \frac{\hbar^2}{\mu\Lambda}, \qquad E_1 = -\frac{\mu\Lambda^2}{2\hbar^2}.$$

Use uncertainty propagation for $(\hbar, m_e, r_c, \|\mathbf{v}_{\circlearrowleft}\|)$ to produce error bars for a_0 and E_1; verify agreement with CODATA values within $< 1\%$. All formulas are taken from the Hydrodynamic Triad paper (HT); see that paper for detailed derivations.

4. Photon/Unknot Sector

Photon states are modeled as unknotted, divergence-free swirl wave packets:

$$\mathbf{v}_{\circlearrowleft} = \partial_t \mathbf{a}, \quad \nabla \cdot \mathbf{a} = 0, \quad \partial_t^2 \mathbf{a} - c^2 \nabla^2 \mathbf{a} = 0.$$

Lossless propagation requires $\nabla \cdot \mathbf{v} = 0$ everywhere and no reconnection events. Pulsed construction: excite a finite-duration torsional wave along the director field to produce a single-photon packet.

5. Swirl Pressure Law—Galaxy-Scale Integrals

Integrate Euler radial balance

$$\frac{1}{\rho_f}\frac{dp}{dr} = \frac{v_\theta^2(r)}{r}$$

for $v_\theta(r) = v_0$ to obtain

$$p(r) = p_0 + \rho_f v_0^2 \ln(r/r_0),$$

then match to observed galaxy rotation curves. This log-profile naturally produces asymptotically flat rotation curves without dark-matter halos.

6. Calibration Protocol Notes

Document measurement protocols for $\{\|\mathbf{v}_{\circlearrowleft}\|, r_c, \rho_f, \rho_m, F^{\mathrm{EM}}_{\max}, F^{\mathrm{G}}_{\max}\}$. Each constant is traceable to a reproducible procedure, e.g. swirl speed from hydrogen spectrum fit, r_c from energy density normalization.

7. Experimental Status & Bounds

Summarize current bounds on $\chi^{\max}_{\mathrm{eff}}$, precision tests of swirl-clock time dilation, and laboratory limits on induced swirl–gravity effects.

8. Notation, Ontology, Glossary

Provide a full symbol table, definitions of ρ_f, ρ_m, ρ_E, and the complete knot taxonomy (torus knots, twist knots, Hopf links). Include a diagrammatic key linking knot types to SM particles for reader reference.

9. 2×2 near-degenerate solution (sketch)

Write $N = N^{(0)} + N^{(1)}$, steady state, and restrict to $\{s, s'\}$. With source $S \equiv -\frac{1}{2} V_x \partial_x N^{(0)}$ and damping Γ, the linearized equations read

$$(i\delta + \Gamma)\, N^{(1)}_{ss'} = S_{ss'} + \mathcal{O}(|M|^2), \tag{I1}$$

$$\gamma_s\, N^{(1)}_{ss} + 2\ \mathrm{Im}\{V^{(x)}_{ss'} N^{(1)}_{s's}\} = S^{(\mathrm{pop})}_s. \tag{I2}$$

Solving for $N^{(1)}_{ss'}$ and inserting into $J_x = \mathrm{Tr}\, \frac{1}{2}\{V_x, N\}\, \Omega$ yields Cor. ; a complex phase in $V^{(x)}_{ss'}$ gives Cor. . Electron–swirl terms enter as $\mathcal{O}(|M|^2)$ corrections with the same Lorentzian denominator.

$$\mathbf{v}(\mathbf{x}, t) = (T - t)^{-\alpha}\, \mathbf{V}(\boldsymbol{\xi})\,, \quad \boldsymbol{\omega}(\mathbf{x}, t) = (T - t)^{-\gamma}\, \boldsymbol{\Omega}(\boldsymbol{\xi})\,, \quad \boldsymbol{\xi} = \frac{\mathbf{x} - \mathbf{x}_0}{(T - t)^{\beta}}.$$

Scaling of gradients: $\nabla \mapsto (T - t)^{-\beta} \nabla_\xi$. Vorticity scales as $\boldsymbol{\omega} = \nabla \times \mathbf{v} \Rightarrow \gamma = \alpha + \beta$.

Insert in the vorticity equation:

$$\partial_t \boldsymbol{\omega} \sim (T-t)^{-(\gamma+1)}, \qquad (\mathbf{v}\cdot\nabla)\boldsymbol{\omega} \sim (T-t)^{-(\alpha+\beta+\gamma)}, \qquad (\boldsymbol{\omega}\cdot\nabla)\mathbf{v} \sim (T-t)^{-(\alpha+\beta+\gamma)}.$$

Balance the powers: $\gamma+1 = \alpha+\beta+\gamma \Rightarrow \alpha+\beta = 1$. With $\gamma = \alpha+\beta$ this gives

$$\boxed{\alpha+\beta=1, \qquad \gamma=1}.$$

Thus, any SST self-similar blow-up profile of Euler type must obey $\gamma = 1$ and one free exponent with $\alpha+\beta = 1$.

$$\boxed{\|\boldsymbol{\omega}\|_\infty \;\le\; \frac{C_e}{r_c} \equiv \omega_{\max}}.$$

Beale–Kato–Majda (BKM) criterion (incompressible Euler): if a smooth solution blows up at time T, then

$$\int_0^T \|\boldsymbol{\omega}(\cdot,t)\|_\infty \, dt = \infty.$$

In SST with $r_c > 0$ and $\|\mathbf{v}_{\mathcal{O}}\| \le C_e$, we have $\|\boldsymbol{\omega}\|_\infty \le \omega_{\max} < \infty$. Hence for any finite T,

$$\int_0^T \|\boldsymbol{\omega}\|_\infty \, dt \;\le\; \omega_{\max} T \;<\; \infty,$$

contradicting the necessary condition for blow-up. Therefore,

$$\boxed{\text{Under } r_c > 0 \text{ and } \|\mathbf{v}_{\mathcal{O}}\| \le C_e, \text{ finite-time blow-up of the Euler-class SST core is precluded.}}$$

This converts the formal self-similar scaling constraint ($\gamma = 1$) into a non-realizable singularity in SST: the growth saturates at $\omega_{\max}$.

$$\omega_{\max} = \frac{C_e}{r_c} \approx 7.76344 \times 10^{20}\ \mathrm{s}^{-1}, \qquad \tau_c = \frac{r_c}{C_e} \approx 1.28809 \times 10^{-21}\ \mathrm{s}.$$

Thus any would-be $\|\boldsymbol{\omega}\|_\infty \sim 1/(T-t)$ profile hits the SST cap at a lead time $\sim \tau_c$ before T, preventing divergence.

Define the rescaled unknowns $\mathbf{V}(\boldsymbol{\xi})$, $\boldsymbol{\Omega}(\boldsymbol{\xi})$ with $\alpha+\beta=1,\ \gamma=1$. The stationary self-similar equation in similarity variables (schematic form) is

$$-(\alpha\mathbf{V} + \beta(\boldsymbol{\xi}\cdot\nabla_\xi)\mathbf{V}) + (\mathbf{V}\cdot\nabla_\xi)\mathbf{V} = -\nabla_\xi \Pi, \qquad \nabla_\xi\cdot\mathbf{V} = 0,$$

with $\boldsymbol{\Omega} = \nabla_\xi \times \mathbf{V}$. For a candidate $(\alpha, \beta, \mathbf{V})$, compute:

$$\mathcal{R}_m := \|-(\alpha\mathbf{V} + \beta(\boldsymbol{\xi}\cdot\nabla_\xi)\mathbf{V}) + (\mathbf{V}\cdot\nabla_\xi)\mathbf{V} + \nabla_\xi\Pi\|_{L^m(\mathbb{R}^3)}$$

for $m \in \{2, \infty\}$, minimizing over pressure Π that enforces $\nabla_\xi\cdot\mathbf{V} = 0$. Report $\mathcal{R}_\infty$ and $\mathcal{R}_2$ at chosen truncation radius and boundary conditions.

Linearize around $\mathbf{V}$: $\mathbf{v}'(t,\boldsymbol{\xi}) = e^{\lambda t}\,\boldsymbol{\phi}(\boldsymbol{\xi})$, giving eigenproblem

$$\mathcal{L}\,\boldsymbol{\phi} = \lambda\,\boldsymbol{\phi}, \qquad \nabla_\xi\cdot\boldsymbol{\phi} = 0,$$

where $\mathcal{L}$ is the linearized similarity operator. Count unstable modes $N_u = \#\{\lambda : \ \mathrm{Re}\,\lambda > 0\}$ excluding neutral symmetries (time/space scaling). Metrics to report:

$$\boxed{\mathcal{R}_\infty,\ \mathcal{R}_2,\ N_u,\ \min_{\mathrm{Re}\,\lambda>0} \mathrm{Re}\,\lambda,\ \max_{\mathrm{Re}\,\lambda<0} |\,\mathrm{Re}\,\lambda|}.$$

SST regularization check: enforce $\|\boldsymbol{\Omega}\|_\infty \le \omega_{\max}$ in the ansatz and recompute $\mathcal{R}_m$ and spectrum; no admissible singular profile should persist once the cap is imposed.

Appendix J: Derivation of the Swirl→Bulk Coupling $\mathcal{G}_{\text{loop}}$

a. Definition. The small-signal swirl→bulk transduction in the conversion region T uses the geometric factor

$$\mathcal{G} \;\equiv\; \int_{V_s} \rho_f \left(u_\theta^{(0)}(\mathbf{x})\right)^2 \mathrm{d}V, \qquad [\mathcal{G}] = \mathrm{J}, \tag{J1}$$

appearing in $Q_0 = \beta\,\omega\,\mathcal{G}\,\varepsilon_0$ (Eq. (B5)). For a single coherent loop (major-radius R, coherent length $\ell = 2\pi R$) with axially symmetric cross-section, write in polar coordinates (r, ϕ) on the cross-sectional disk and assume $u_\theta^{(0)} = u_\theta^{(0)}(r)$.

Exponential core profile

Assume the canonical near-core profile

$$u_\theta^{(0)}(r) \;\approx\; C_e\, e^{-r/r_c}, \tag{J2}$$

with C_e the core tangential speed and r_c the core radius. Then

$$\mathcal{G}_{\text{loop}} = \rho_f \int_0^{\ell} \mathrm{d}s \int_0^{2\pi} \mathrm{d}\phi \int_0^{\infty} \left(C_e^2 e^{-2r/r_c}\right) r\,\mathrm{d}r \tag{J3}$$

$$= \rho_f\,\ell\,C_e^2\,(2\pi) \int_0^{\infty} r\, e^{-2r/r_c}\,\mathrm{d}r \;=\; \rho_f\,\ell\,C_e^2\,(2\pi)\,\frac{r_c^2}{4}$$

$$= \boxed{\frac{\pi}{2}\,\rho_f\,C_e^2\,r_c^{\,2}\,\ell}\,. \tag{J4}$$

Checks: (i) Dimensions: $\rho_f C_e^2$ is an energy density; multiplying by area ($\propto r_c^2$) and length ℓ yields energy. (ii) Limits: $\mathcal{G}_{\text{loop}} \to 0$ as $r_c \to 0$; linear in ℓ.

b. Finite cutoff. If the coherent cross-section is only trusted up to $r \le R$, the radial integral gives

$$\mathcal{G}_{\text{loop}}(R) = \frac{\pi}{2}\,\rho_f\,C_e^2\,r_c^2\left[1 - e^{-2R/r_c}\Big(1 + \frac{2R}{r_c}\Big)\right]\ell, \tag{J5}$$

which saturates to (J4) when $R \gg r_c$.

Effective bundle (supercore)

If M microscopic cores phase-lock to form a coherent *bundle* of effective radius $r_{\text{eff}} \gg r_c$, the cross-sectional integral is dominated by $r \lesssim r_{\text{eff}}$. One may either (i) keep the exponential form but replace $r_c \mapsto r_{\text{eff}}$ as an *effective* scale, or (ii) adopt a top-hat (uniform) profile $u_\theta^{(0)}(r) \approx C_e\,\Theta(r_{\text{eff}} - r)$. These give, respectively,

$$\text{(exp, effective)} \quad \mathcal{G}_{\text{loop}} \simeq \frac{\pi}{2}\,\rho_f\,C_e^2\,r_{\text{eff}}^2\,\ell, \tag{J6}$$

$$\text{(top-hat)} \qquad \mathcal{G}_{\text{loop}} = \rho_f\,C_e^2\,(\pi r_{\text{eff}}^2)\,\ell. \tag{J7}$$

Thus, up to an $O(1)$ shape factor, $\mathcal{G}_{loop} \propto r_{\text{eff}}^2\,\ell$. In the BASC transduction law (B5), this yields the experimentally testable scaling

$$p_{\text{amp}}(r) \;\propto\; \mathcal{G} \;\propto\; r_{\text{eff}}^2\,\ell, \quad p_{\text{amp}}(r) = \frac{\rho_f\,\beta\,\mathcal{G}\,\varepsilon_0}{4\pi r}\,\omega^2 \;\; \text{(Eq. (B7))}. \tag{J8}$$

c. Remarks. (1) Eqs. (J6)–(J7) bracket realistic cross-section shapes; the exponential core gives the $\frac{\pi}{2}$ factor relative to a top-hat. (2) Because $\mathcal{G}$ is linear in the coherent length, arranging multiple loops in phase increases $\mathcal{G}$ additively.

Appendix K: Conversation-Derived Insights

This appendix records novel insights emerging from collaborative project discussions (2025–09). They are cross-checked against the Rosetta concordance and Canon v0.5.8, and classified according to the Canonicality taxonomy.

1. Multipole Expansion of Swirl Fields

a. Statement. Swirl velocity distributions induced by torus knots (e.g. $T_{2,3}$) exhibit higher-order multipole angular structure. Numerical simulations reveal a hexapole modulation $\cos(3\theta)$ in the tangential swirl speed.

b. Formula (Research-Track).

$$v_\theta(r,\theta) \;\approx\; \frac{3\Gamma}{2\pi r}\Big[1+\epsilon\cos(3\theta)\Big],$$

with ϵ a knot–geometry coefficient. This extends the far-field law $v_\theta(r) \sim 3\Gamma/(2\pi r)$.

c. Status. Research-Track. Multipole corrections not yet canonized.

2. Alternating Photon Helicity Dynamics

a. Statement. Photons as R-phase torsional pulses may alternate helicity ($\circlearrowleft, \circlearrowright$) within a single wave packet, producing an intrinsic CW/CCW oscillation in the transverse plane.

b. Formula (Research-Track).

$$\mathbf{v}_{\circlearrowleft}(t) \;\propto\; \cos(\omega t)\,\hat{x} + \sin(\omega t)\,\hat{y}, \quad \mathbf{v}_{\circlearrowright}(t+\tfrac{\pi}{\omega}) \;\propto\; \cos(\omega t)\,\hat{x} - \sin(\omega t)\,\hat{y}.$$

c. Status. Research-Track. Canon v0.5.8 includes torsional photons, but not intra-packet helicity alternation.

3. Quark Bundling Hypothesis

a. Statement. Instead of three linked knots, baryons may be modeled as a single multi-filament swirl tube with effective circulation 3κ.

b. Formula (Alternative Model).

$$\Gamma_{\text{baryon}} \;\equiv\; 3\kappa \quad\Rightarrow\quad v_\theta(r) = \frac{3\kappa}{2\pi r}.$$

c. Status. Research-Track. Competes with canonical linkage model $(52+52+61)$. Needs falsifier via confinement dynamics.

4. Residue Calculus for Swirl Gravitation

a. Statement. Gravitational attraction can be recast as a Cauchy–residue theorem on an analytic swirl potential.

b. Formula (Research-Track).

$$\oint_C \mathbf{v}_{\circlearrowleft}\cdot d\ell \;=\; 2\pi i\,\mathrm{Res}(\partial_z W(z),\,0) = n\,\kappa,$$

with $W(z) = \Phi + i\Psi$ the complex swirl potential.

c. Status. Research-Track. Strengthens Theorem 7.1 by formalizing circulation quantization via complex analysis.

5. Chirality–Matter Equivalence

a. Theorem (Canonical). Let $\Gamma = \pm n\kappa$ be the quantized circulation of a swirl string, with $+$ (counterclockwise) or $-$ (clockwise) orientation. Then

$$S_{(t)}$$

b. Proof.

1. **Circulation quantization (Axiom 2).** Swirl strings carry circulation in discrete quanta $\Gamma = n\kappa$, with sign determined by orientation.
2. **Knot taxonomy (Axiom 6).** Mirror knots correspond to antiparticles. Thus matter/antimatter distinction is a chirality inversion.
3. **Rosetta mapping.** The sign of vorticity ω is preserved across VAM $\rightarrow$ SST translation, so CCW vs CW orientation is an invariant label.
4. **Recovery limit.** In the weak-swirl regime ($v \ll c$), co-rotating strings (same chirality) attract while counter-rotating strings repel — matching matter–matter vs. matter–antimatter interaction channels.
5. **Empirical anchor.** The electron and positron correspond to trefoil knots (3_1) and their mirror images, which are experimentally distinct states with equal mass and opposite charge.

Therefore, chirality of the swirl clock is canonically equivalent to the matter–antimatter distinction. □

Appendix L: Knot Stability and Protection

a. Motivation. Recent studies in superfluid and optical systems demonstrate that knotted excitations admit distinct dynamical fates: some classes persist indefinitely (protected), while others decay through reconnections (unprotected). This appendix canonizes these insights into the SST framework, refining the topological taxonomy of swirl strings.

1. Canonical Classes of Stability

definition

[. Knot Stability Class] Let K denote a swirl string configuration with circulation $\Gamma = n\kappa$. The *stability class* $\sigma(K)$ is defined as

$$\sigma(K) \in \{\text{Protected}, \text{Metastable}, \text{Forbidden}\},$$

according to its dynamical response under admissible SST evolution (incompressible, inviscid, barotropic medium with absolute time).

- **Protected.** K is preserved under reconnection attempts. Typical example: non-Abelian Q_8-linked strings [7].
- **Metastable.** K undergoes reconnections but conserves partial helicity via writhe transfer [8].
- **Forbidden.** K immediately relaxes to the unknot (trivial state), corresponding to topologies not supported by quantized circulation.

corollary

[. Protection Criterion] A knot K is *Protected* if its fundamental group representation admits a non-Abelian factorization into $Q_8 \subset \pi_1(S^3 \setminus K)$. Otherwise, it is *Metastable* or *Forbidden*.

2. Helicity Redistribution and Kairos Events

[Helicity Conversion] During reconnection (a non-ideal event), total helicity is partially preserved by redistribution:

$$H = \int \mathbf{v}_{\circlearrowleft} \cdot \boldsymbol{\omega}\, dV \quad \longrightarrow \quad H' = H_{\text{writhe}} + H_{\text{coil}},$$

where linking number contributions decay, but writhe persists as helical coils [8, 9].

definition

[. Kairos Event] A *Kairos event* κ is an irreversible transition in the knot class of a swirl string:

$$K \;\mapsto\; K' \qquad (\kappa : \text{topological bifurcation}).$$

Physically, this corresponds to a reconnection, where $\sigma(K)$ demotes from Protected $\rightarrow$ Metastable $\rightarrow$ Forbidden.

3. Fractional Swirl Clocks and Optical Knots

theorem

[. Fractional Swirl Clock Winding] Polarization-induced fractional torus knots correspond to fractional swirl-clock states:

$$S_t^{(\gamma)} = e^{i\gamma\theta}, \qquad \gamma \in \mathbb{Q} \text{ or } \mathbb{R}.$$

For $\gamma \in \mathbb{Q}$, $S_t^{(\gamma)}$ corresponds to a closed rational knot; for $\gamma \notin \mathbb{Q}$, it defines a quasi-periodic optical excitation.

This provides a canonical mechanism for photon helicity and polarization entanglement, extending Axiom 6 (Photon = R-phase torsional pulse) to include fractional winding modes.

D. Hyperbolic Energy Volume Equivalence

[Energy–Volume Correspondence] For hyperbolic knots K, the mass-equivalent density ρ_m fixes an effective energy-volume relation:

$$E(K) \sim \rho_m \, \mathrm{Vol}_{\mathbb{H}}(K),$$

where $\mathrm{Vol}_{\mathbb{H}}(K)$ is the hyperbolic 3-volume computed via triangulation [10, 11].

This establishes a computable route from triangulated character varieties to SST mass functionals.

E. Canonical Status

- Protection Criterion: **Canonical Corollary**.
- Helicity Conversion Axiom: **Canonical**.
- Kairos Event: **Definition (Canonical)**.
- Fractional Swirl Clock Winding: **Research Track (promotable)**.
- Energy–Volume Correspondence: **Research Track (empirical support)**.

F. Canonicality Tests for New Items

a. Legend (Canonicality Tests). (1) Derivable from axioms/defs; (2) Dimensional consistency; (3) Symmetry compliance (Galilean, incompressible); (4) Recovery limits (Kelvin, Newton/Coulomb, linear optics); (5) Non-contradiction with canonical results; (6) Parameter discipline (no ad hoc fits beyond calibrations).

1. Protection Criterion (Corollary)

Statement (from subsection 1). If $\pi_1(S^3 \backslash K)$ admits a non-Abelian factorization with Q_8, then K is **Protected**.
Canonicality Tests.

1. **Derivable**: From Axiom 2 (swirl strings/topology + quantized Γ) and group-theoretic obstruction to strand exchange in non-Abelian classes.
2. **Dimensions**: Purely topological/group-theoretic; no units.
3. **Symmetry**: Compatible with incompressible Euler and Kelvin freezing (no reconnection in ideal limit).
4. **Recovery**: In the Abelian case ⇒ standard reconnection channels reappear (matches viscous/quantum-fluid literature).
5. **Non-contradiction**: Consistent with Canon §VI (Kelvin, helicity) and the Chronos–Kelvin invariant.
6. **Parameters**: No new parameters introduced.

2. Helicity Conversion (Axiom)

Statement (from .2). During a non-ideal reconnection (Kairos event),

$$H = \int \mathbf{v}_{\mathfrak{O}} \cdot \boldsymbol{\omega}\, dV \;\rightarrow\; H' = H_{\text{writhe}} + H_{\text{coil}}$$

(i.e. linking contribution decreases; writhe/coil increase).

Canonicality Tests.

1. **Derivable**: From helicity transport + non-ideal source at reconnection; consistent with literature.
2. **Dimensions**: $[\mathbf{v}] = \mathrm{m\,s^{-1}}$, $[\boldsymbol{\omega}] = \mathrm{s^{-1}} \Rightarrow [\mathbf{v}\cdot\boldsymbol{\omega}] = \mathrm{m\,s^{-2}}$; $\int dV$ adds $\mathrm{m^3}$; hence $[H] = \mathrm{m^4\,s^{-2}}$. Writhe/coil terms share units.
3. **Symmetry**: Galilean and incompressible constraints preserved except at localized non-ideal region.
4. **Recovery**: Ideal limit (no reconnection) $\Rightarrow H$ conserved (Kelvin/Helmholtz).
5. **Non-contradiction**: Agrees with Canon §VI; refines behavior only at Kairos.
6. **Parameters**: No new fits; purely kinematic/topological.

3. Kairos Event (Definition)

Statement (from K.2). A *Kairos* κ is an irreversible topological bifurcation $K \mapsto K'$ (reconnection).

Canonicality Tests.

1. **Derivable**: Definition extending Rosetta's time ontology $(\mathcal{N}, \nu_0, \tau, S(t), T_v, \kappa)$.
2. **Dimensions**: Topological/time-mode label; unitless.
3. **Symmetry**: Explicitly marks breakdown of ideal invariants; consistent with framework.
4. **Recovery**: No reconnection $\Rightarrow$ no Kairos; reverts to ideal transport.
5. **Non-contradiction**: Compatible with Canon's Chronos–Kelvin law and helicity remarks.
6. **Parameters**: No parameters added.

4. Fractional Swirl Clock Winding (Theorem, Research Track)

Statement (from K.3). Polarization-driven fractional winding:

$$S_t^{(\gamma)} = e^{i\gamma\theta}, \qquad \gamma \in \mathbb{Q} \text{ or } \mathbb{R}.$$

Canonicality Tests.

1. **Derivable**: Maps optical polarization winding to swirl-clock phase (Axiom 5: R-phase photon). Needs formal variational link for promotion.
2. **Dimensions**: Phase is unitless; θ angle unitless.
3. **Symmetry**: Respects medium kinematics; adds internal phase structure; no Galilean violation.
4. **Recovery**: $\gamma = \pm 1 \Rightarrow$ standard photon helicity ± 1; rational $\gamma \Rightarrow$ closed fractional torus-knot; irrational $\Rightarrow$ quasi-periodic.
5. **Non-contradiction**: Extends Canon photon sector without conflict.
6. **Parameters**: γ is geometric (no fitted constants).

5. Energy–Volume Correspondence (Axiom, Research Track)

Corrected statement (dimensional form).

$$\boxed{E(K) \;\simeq\; \rho_E \,\mathrm{Vol}_{\mathbb{H}}(K) \;=\; c^2\,\rho_m \,\mathrm{Vol}_{\mathbb{H}}(K)}$$

with $\rho_E = \frac{1}{2}\rho_f \,\|\mathbf{v}_{\circlearrowleft}\|^2$ and $\rho_m = \rho_E/c^2$.

Canonicality Tests.

1. **Derivable**: Plausible coarse-grained identification linking hyperbolic geometry to stored swirl energy; needs derivation from Canon Hamiltonian density for promotion.
2. **Dimensions**: $[\rho_E] = \mathrm{J\,m^{-3}}$, $[\mathrm{Vol}_{\mathbb{H}}] = \mathrm{m^3} \Rightarrow [E] = \mathrm{J}$. Also $c^2\rho_m = \rho_E$.
3. **Symmetry**: Uses canonical densities; respects incompressibility and gauge bridge.
4. **Recovery**: For slender tubes, reduces to core+envelope energetics (Rosetta) with $\mathrm{Vol}_{\mathbb{H}}$ as geometric proxy.
5. **Non-contradiction**: No clash with Canon §VII constants or §VI invariants.
6. **Parameters**: No extra fits beyond canonical ρ_f and c.

6. Numerical Sanity Check (Core clock rate)

Using calibrated values (Canon/Rosetta): $v_\circ = 1.09384563 \times 10^6\,\mathrm{m\,s^{-1}}$, $r_c = 1.40897017 \times 10^{-15}\,\mathrm{m}$,

$$\Omega_{\mathrm{core}} = \frac{v_\circ}{r_c} \approx \frac{1.09384563 \times 10^6}{1.40897017 \times 10^{-15}} \approx 7.763 \times 10^{20}\ \mathrm{s^{-1}},$$

consistent with the Chronos–Kelvin usage of $v_\theta = \Omega r$ at $r = r_c$.

XIII. MULTIPOLES, PHOTON NOTE, $G_{\mathbf{swirl}}$ IDENTITY, TAXONOMY

A. Multipole selection for p-filament torus bundles [Research-track]

Lemma (Discrete-symmetry selection). Consider p identical, slender filaments laid on the *same* torus-knot path with equal poloidal phase offsets $\Delta\phi = 2\pi/p$. Let $v_\theta(\theta; r)$ denote the induced tangential speed on a circular probe ring (plane $z = 0$, radius r) centered on the bundle. Then, for r larger than the bundle radius a (no reconnection, inviscid, incompressible),

$$v_\theta(\theta; r) \;=\; \frac{p\,\Gamma}{2\pi r}\Big[1 + \varepsilon_p(r)\cos\big(p(\theta - \theta_0)\big)\Big] \;+\; \mathcal{O}\big(\varepsilon_p^2\big),$$

with Γ the single-filament circulation, θ_0 a geometry-set phase, and a dimensionless shape factor $\varepsilon_p(r)$ satisfying

$$0 < \varepsilon_p(r) = \mathcal{O}\big((a/r)^p\big) \quad \text{as} \quad r/a \to \infty.$$

Sketch. By discrete rotational symmetry (C_p), only harmonics $m = kp$ survive in the Fourier series of $v_\theta(\theta; r)$. Far-field Biot–Savart superposition fixes the mean $\bar{v}_\theta(r) = p\Gamma/(2\pi r)$. The leading anisotropy arises from the first nontrivial $m = p$ multipole of a p-point ring, with amplitude controlled by the bundle compactness a/r. This is consistent with Canon's tube energetics and Rankine matching and refines near-field angular structure without altering far-field $1/r$ decay.

a. Remark. For $p = 3$ (three-thread bundle), the dominant cross-sectional modulation is hexapolar: $v_\theta(\theta; r) = \bar{v}_\theta(r)\big[1 + \varepsilon_3(r)\cos 3(\theta - \theta_0)\big]$.

B. Photon sector: torsional packet does not require global rotation [Canonical clarification]

Clarification. In Canon, the photon is a *pulsed torsional* (R-phase) excitation of the director field governed by a transverse wave equation for a vector potential $\mathbf{a}$ with $\nabla\cdot\mathbf{a}=0$ and $\mathbf{v}_{\circlearrowleft}=\partial_t\mathbf{a}$. This free-wave form holds wherever the medium is incompressible and reconnection-free; it *does not* assume a globally rotating background. A nonzero background swirl may Doppler-shift phases or induce birefringent-like corrections, but it is not a prerequisite for propagation.

C. Closed-form identity for G_{swirl} [Calibration]

Master identity (algebraic).

$$\boxed{G_{\mathrm{swirl}} \;=\; \frac{\mathbf{v}_{\circlearrowleft}\, c^5\, t_p^2}{2\, F_{\circlearrowleft}^{\max}\, r_c^2}}$$

under the Rosetta identifications $\mathbf{v}_{\circlearrowleft}\equiv\|\mathbf{v}_{\circlearrowleft}\|$ (canonical swirl speed), r_c (core radius), and $F_{\circlearrowleft}^{\max}$ (line-tension bound). This identity is *calibration-equivalent* to Newton's G in the Canon and may be listed in the Master Equations alongside the existing statement $G_{\mathrm{swirl}}\approx G_N$.

a. One-line numerics (Canon constants). Using $\mathbf{v}_{\circlearrowleft}=1.09384563\times10^{6}\,\mathrm{m/s}$, $c=2.99792458\times10^{8}\,\mathrm{m/s}$, $t_p=5.391247\times10^{-44}\,\mathrm{s}$, $F_{\circlearrowleft}^{\max}=29.053507\,\mathrm{N}$, $r_c=1.40897017\times10^{-15}\,\mathrm{m}$,

$$G_{\mathrm{swirl}}=\frac{\mathbf{v}_{\circlearrowleft}c^5t_p^2}{2F_{\circlearrowleft}^{\max}r_c^2} \;=\; 6.6743020\times10^{-11}\ \mathrm{m^3\,kg^{-1}\,s^{-2}}\approx G_N.$$

XIV. COMPUTING HYPERBOLIC VOLUME OF KNOT COMPLEMENTS (VAM PIPELINE)

A. Overview

Let $K\subset S^3$ be a hyperbolic knot with complement $M_K=S^3\setminus N(K)$. Thurston's program computes a complete, finite–volume hyperbolic metric by solving *gluing* and *completeness* equations for shape parameters $\{z_j\}_{j=1}^{m}\in\mathbb{C}$ of an ideal triangulation, then evaluating the Bloch–Wigner sum for the volume [1–3].

Pipeline used in VAM (diagram-agnostic and dependency-free):

1. **PD extraction.** From an embedding $\mathbf{r}(t)\in\mathbb{R}^3$ (Fourier series), choose a generic projection to $\mathbb{R}^2$; detect segment intersections; assign over/under by depth along the view. This yields a PD code $\mathrm{PD}(K)=\{(a_i,b_i,c_i,d_i)\}_{i=1}^{n}$ with each label used exactly twice.

2. **Ideal triangulation.** Replace each crossing by an ideal octahedron and split it into five ideal tetrahedra; glue by PD adjacency to get an ideal triangulation $\mathcal{T}$ with $m=5n$ tets [1, 3].

3. **Gluing and completeness.** For each edge e,

$$\prod_{T_j\ni e}\zeta_{j,e} \;=\; 1, \qquad \zeta_{j,e}\in\{\,z_j,\ z_j'=\tfrac{1}{1-z_j},\ z_j''=1-\tfrac{1}{z_j}\,\}, \tag{1}$$

   and for cusp cycles γ,

$$\prod_{\gamma\ \mathrm{path}}\zeta_{j,\gamma} \;=\; 1, \tag{2}$$

   which, in logarithmic form, become linear relations among $\log z_j$ and $\log(1-z_j)$ with $2\pi i$ branch consistency enforced during Newton iteration [2].

4. **Shape solve.** Damped complex Newton on (1)–(2), seeded at $z=e^{i\pi/3}$; enforce $\mathrm{Im}\,z_j>0$.

5. **Volume.**

$$\mathrm{Vol}(M_K) \;=\; \sum_{j=1}^{m} D(z_j), \qquad D(z) \;=\; \mathrm{Im}\mathrm{Li}_2(z) \;+\; \arg(1-z)\,\log|z|, \tag{3}$$

   with standard functional reductions for Li_2 [2, 4].

a. Units. $\mathrm{Vol}(M_K)$ is a dimensionless topological invariant (Mostow rigidity).

B. Worked examples: 5_2 and 6_1

We record standard reference volumes as baselines; our no-dependency solver (Fourier→PD→gluing) reproduces these to $\sim 10^{-5}$–10^{-6}.

a. The knot 5_2 (three-twist knot). An alternating hyperbolic twist knot with volume

$$\mathrm{Vol}(S^3 \setminus 5_2) \;\approx\; 2.82812.$$

A suitable Dowker/PD code yields the octahedral triangulation, the Newton solve returns a discrete faithful shape set $\{z_j\}$, and $\sum_j D(z_j)$ matches the tabulated value.

b. The knot 6_1 (stevedore knot). An alternating hyperbolic twist knot with volume

$$\mathrm{Vol}(S^3 \setminus 6_1) \;\approx\; 3.16396.$$

The same pipeline applies verbatim.

C. Numerical notes

- **Branch control.** Equations are solved in log form with continuous branch tracking; after each Newton step, any $\mathrm{Im}\, z_j \le 0$ is flipped to maintain positive orientation [2].
- **Stability.** Use $|z| \le \frac{1}{2}$ power series for Li_2; otherwise reduce via $\mathrm{Li}_2(z) + \mathrm{Li}_2(1-z) = \pi^2/6 - \log z \log(1-z)$ and $\mathrm{Li}_2(z) + \mathrm{Li}_2(1/z) = -\pi^2/6 - \frac{1}{2}\log^2(-z)$ [4].
- **Triangulation size.** The $5n$-tet split is universal and adequate; further Pachner moves are optional.

D. VAM normalization and coupling

For VAM we use the signed, normalized hyperbolic "charge"

$$H_{\mathrm{vol}}(K) \;=\; \sigma\, \frac{\mathrm{Vol}(K)}{\mathrm{Vol}(4_1)}, \qquad \mathrm{Vol}(4_1) \approx 2.029883212819307, \tag{4}$$

with $\sigma \in \{+1, -1\}$ set by chirality and $H_{\mathrm{vol}} = 0$ for amphichiral knots. Numerically,

$$H_{\mathrm{vol}}(5_2) \approx 1.393242716, \qquad H_{\mathrm{vol}}(6_1) \approx 1.558690658 \quad (\sigma = +1).$$

This couples to the VAM mass map

$$M_{\mathrm{VAM}} \;=\; \frac{4}{\alpha\phi}\, \xi(n)\, H_{\mathrm{vol}}(K)\, \Big(\tfrac{1}{2}\, \rho_{\_}\, C_e^2\, V_{\mathrm{knot}}\Big), \tag{5}$$

where $\xi(n)$ is the coherence factor, V_{knot} is the physical æther volume of the vortex core, and $(\alpha, \phi, \rho_{\_}, C_e)$ are the fixed VAM parameters (see main text). The bracket has energy units; the prefactor maps energy to mass via the embedded c^{-2}.

XV. ROSETTA→CODE CONSISTENCY RULE (INVARIANT-MASS SECTOR)

definition

[. Effective Densities and Factors] Let ρ_f denote the *free-æther (swirl) density* that normalizes the EM bridge and BASC, and let ρ_{core} denote the *core mass density* entering the invariant mass kernel via the core swirl energy $u = \frac{1}{2}\rho_{\mathrm{core}}\, v_{\circlearrowleft}^2$. Let $S_t = \sqrt{1 - v_\theta^2/c^2}$ be the swirl-clock factor from the pseudo-metric.

[Separation Principle for Implementation] With the canonical invariant mass law

$$M(K) = \frac{4}{\alpha_{fs}}\, b^{-3/2}\, \varphi^{-g}\, n^{-1/\varphi}\, \frac{u\, \pi r_c^3\, L_{\rm tot}}{c^2}, \quad u = \tfrac{1}{2}\rho_{\rm core}\, v_{\circlearrowleft}^2,$$

the rest-mass must be computed using $\rho_{\rm core}$ only, while ρ_f appears exclusively in the EM/BASC sector (wave Lagrangian, transduction gain $G_{\rm loop}$, and bulk propagation) and *not* in $M(K)$. The swirl-clock S_t modifies local time rates via the pseudo-metric but does not multiply the rest-mass at fixed topology K.

Dimensional/Canonical Sketch. (i) Canonical mass kernel uses $u = \frac{1}{2}\rho_{\rm core} v^2$ and $M = E/c^2$ (Appendix C) . (ii) The relation $\rho_E = \frac{1}{2}\rho_f \|v\|^2$, $\rho_m = \rho_E/c^2$ characterizes free-æther EM normalization/BASC, not the core-energy factor in the rest-mass kernel . (iii) The swirl-clock enters kinematics via $dt_{\rm local}/dt_\infty = \sqrt{1 - v_\theta^2/c^2}$, leaving the static rest-mass factor unchanged . □

a. Minimal Code Patch (if legacy mixing exists)

$$u \leftarrow \tfrac{1}{2}\, \rho_{\rm core}\, v_{\circlearrowleft}^2,$$
$$M(K) \leftarrow \frac{4}{\alpha_{fs}}\, b^{-3/2}\, \varphi^{-g}\, n^{-1/\varphi}\, \frac{u\, \pi r_c^3\, L_{\rm tot}}{c^2},$$

Remove any factor of ρ_f or S_t from $M(K)$. Keep ρ_f only in EM/BASC routines.

b. Rosetta→Code Map (practical)

- **Mass kernel**: $\rho_{\rm core}$, r_c, $v_{\circlearrowleft}$, $L_{\rm tot}$, $(\alpha_{fs}, \varphi, b, g, n)$.
- **Photon/EM sector**: ρ_f in $L_{\rm wave} = \frac{1}{2}\rho_f \|v\|^2$.
- **BASC**: ρ_f and $c_b = \sqrt{K_b/\rho_f}$; use $G_{\rm loop} \propto \rho_f C_e^2 r_c^2 \ell$ for transduction.
- **Clocking/kinematics**: S_t only in time-rate and transport equations.

c. Consistency Check Benchmarks generated by the reference Python file remain unchanged in *exact_closure* mode; composite deviations track omitted binding energies (not model failure).

XVI. SWIRL–EM TRANSDUCTION ECHO MODEL (DESWAL-TYPE CAVITIES)

This module provides a detailed derivation of the Swirl–EM transduction coefficient $\kappa_{\rm se}$ via acoustic impedance mismatch, referenced from Subsec. XVIII A and Corollary XVIII F.

A. Swirl impedance and boundary mismatch

To relate $\kappa_{\rm se}$ to material properties, we introduce a swirl impedance

$$Z_S \equiv \rho_f\, \|\mathbf{v}_{\circlearrowleft}\|, \tag{1}$$

in analogy with acoustic impedance $Z = \rho c$.[30] Using the Canon constants $\rho_f \approx 7 \times 10^{-7}\,\mathrm{kg/m^3}$ and $\|\mathbf{v}_{\circlearrowleft}\| \approx 1.1 \times 10^6\,\mathrm{m/s}$, one finds

$$Z_S \approx 0.8\,\mathrm{Rayl}, \tag{2}$$

a very low impedance.

Typical rigid cavity walls (metals, glass) have acoustic impedances of order

$$Z_{\rm bound} \sim 10^7\,\mathrm{Rayl}, \tag{3}$$

so there is a severe mismatch $Z_{\rm bound} \gg Z_S$. In standard acoustics, the intensity transmission coefficient for a plane wave normally incident on a boundary between media with impedances Z_1, Z_2 is

$$T_{1\to 2} = \frac{4 Z_1 Z_2}{(Z_1 + Z_2)^2} \simeq \frac{4 Z_1}{Z_2}, \qquad Z_2 \gg Z_1. \tag{4}$$

Identifying $Z_1 \to Z_S$ and $Z_2 \to Z_{\text{bound}}$, we obtain

$$T_{S\to\text{bound}} \simeq \frac{4Z_S}{Z_{\text{bound}}} \sim 10^{-7}, \tag{5}$$

i.e. only one part in 10^7 of the swirl intensity is transmitted into the boundary per interaction.

B. Conversion to rate coefficient

To convert this into a *rate* κ_{se} with dimensions of s^{-1}, we introduce a geometric scattering rate κ_0, which encodes the encounter frequency of the swirl wake with the boundaries (e.g. $\kappa_0 \sim \|\mathbf{v}_\circlearrowleft\|/L_{\text{char}}$ for a cavity of characteristic size L_{char}). We then define

$$\kappa_{\text{se}} = \kappa_0\, T_{S\to\text{bound}} \simeq \kappa_0\, \frac{4Z_S}{Z_{\text{bound}}}, \tag{6}$$

so that all the material and geometry dependence is explicit. For typical parameters, Eq. (6) implies that $\kappa_{\text{se}} \ll \gamma_{\text{diss}}$, and therefore $\xi \ll 1$ in Eq. (12). This quantitatively explains why the primary swirl superradiance burst is effectively invisible to standard EM cavities, and why the observed EM echo matches the much smaller GR/QFT energy scale.

Status: Research-track. The impedance model is a specific parametrization of the transduction coefficient κ_{se} introduced canonically in Sec. XVIII. The numerical estimate $T \sim 10^{-7}$ depends on representative material properties and should be refined with cavity-specific measurements.

XVII. SST UNRUH SCALING AND SUPERRADIANT DELAY

In standard quantum field theory, the Unruh temperature is given by

$$T^{\text{std}}_{\text{Unruh}} = \frac{\hbar a}{2\pi c k_B}. \tag{1}$$

Swirl–String Theory replaces the geometric light speed c by the characteristic swirl speed $\|\mathbf{v}_\circlearrowleft\|$, yielding

$$T^{\text{SST}}_{\text{Unruh}} = \frac{\hbar a}{2\pi \|\mathbf{v}_\circlearrowleft\| k_B}. \tag{2}$$

The ratio is therefore

$$\frac{T^{\text{SST}}_{\text{Unruh}}}{T^{\text{std}}_{\text{Unruh}}} = \frac{c}{\|\mathbf{v}_\circlearrowleft\|}. \tag{3}$$

With the canonical values $c = 2.99792458 \times 10^8$ m/s and $\|\mathbf{v}_\circlearrowleft\| = 1.09384563 \times 10^6$ m/s, one finds

$$\frac{T^{\text{SST}}_{\text{Unruh}}}{T^{\text{std}}_{\text{Unruh}}} \approx 2.7407 \times 10^2, \qquad \frac{\|\mathbf{v}_\circlearrowleft\|}{c} \approx 3.65 \times 10^{-3}. \tag{4}$$

In the time-resolved superradiance protocol of Deswal *et al.*, the superradiant delay time scales as $\tau_d \propto (N\gamma)^{-1}$. If γ is proportional to T_{Unruh}, the SST prediction for the delay time satisfies

$$\frac{\tau_d^{\text{SST}}}{\tau_d^{\text{std}}} \approx \frac{\|\mathbf{v}_\circlearrowleft\|}{c} \approx 3.65 \times 10^{-3}. \tag{5}$$

Thus, for fixed acceleration and cavity parameters, SST predicts an Unruh-seeded superradiant burst occurring roughly three orders of magnitude earlier than in the standard scenario, while the inertial (background) contribution remains cavity-suppressed.

XVIII. TWO-VACUUM STRUCTURE AND DUAL-BURST UNRUH SUPERRADIANCE

Standard Unruh superradiance experiments probe an atom or atomic array accelerated through the electromagnetic (EM) vacuum. The effective light speed is c, and the observable channel is spontaneous emission into cavity photon modes. Swirl–String Theory (SST) posits a second, hydrodynamic vacuum sector: an incompressible swirl medium with characteristic speed $\|\mathbf{v}_{\circlearrowleft}\| \ll c$ and density ρ_f. Accelerated atoms can, in principle, couple to both vacua:

- an EM channel (photons, propagation speed c),
- a swirl channel (vorticity/torsional excitations, propagation speed $\|\mathbf{v}_{\circlearrowleft}\|$).

The swirl sector carries primarily shear (Kelvin-like) vorticity waves rather than compressional sound; density ρ_f remains effectively constant.

Let $P_e(t)$ be the excited-state population of a single atom in an accelerated array. The total decay rate decomposes as

$$\Gamma_{\rm tot}(a) = \gamma_0 + \tilde{\gamma}_{\rm em}(a) + \tilde{\gamma}_{\rm swirl}(a), \tag{1}$$

where γ_0 is the inertial, cavity-suppressed decay rate, $\tilde{\gamma}_{\rm em}(a)$ is the acceleration-induced EM Unruh contribution, and $\tilde{\gamma}_{\rm swirl}(a)$ encodes the SST swirl contribution. In the linear-response regime, the EM channel reproduces the GR/QFT prediction [27, 31, 33]:

$$\tilde{\gamma}_{\rm em}(a) \propto T_U^{(\rm em)}(a) = \frac{\hbar a}{2\pi c k_B}. \tag{2}$$

For the swirl sector, SST replaces c by $\|\mathbf{v}_{\circlearrowleft}\|$ in the Unruh-like temperature,

$$T_U^{(\rm swirl)}(a) = \frac{\hbar a}{2\pi \|\mathbf{v}_{\circlearrowleft}\| k_B}, \tag{3}$$

but allows for an a priori unknown hydrodynamic coupling efficiency $f_{\rm Unruh} \in (0, 1]$:

$$\tilde{\gamma}_{\rm swirl}(a) = f_{\rm Unruh}\, \frac{c}{\|\mathbf{v}_{\circlearrowleft}\|}\, \tilde{\gamma}_{\rm em}(a). \tag{4}$$

The EM observables in current cavity experiments [31, 35, 36] are not directly sensitive to $\tilde{\gamma}_{\rm swirl}(a)$, but only to its conversion into EM modes. We introduce a swirl–EM transduction coefficient $\kappa_{\rm se}$, determined by the acoustic and optical impedance of the medium and the boundary conditions:

$$\Gamma_{\rm em}(a) = \gamma_0 + \tilde{\gamma}_{\rm em}(a) + \kappa_{\rm se}\, \tilde{\gamma}_{\rm swirl}(a). \tag{5}$$

In a high-finesse microwave cavity in vacuum, the mirrors are essentially "acoustically rigid", so that

$$\kappa_{\rm se} \approx 0 \quad \text{(swirl-blind EM cavity)}. \tag{6}$$

Under these conditions, the swirl channel decays non-radiatively into internal degrees of freedom of the medium (heat, mechanical stress) and cannot produce a directly observable sub-nanosecond EM burst. To make this transduction explicit, we model the joint evolution of the atomic population, the swirl wake, and the EM cavity mode by coupled rate equations (see Subsec. XVIII A).

A. Swirl-EM Transduction Dynamics and Echo Delay (Research)

In Swirl–String Theory (SST), the Unruh response of accelerated atoms occurs in a two-vacuum environment: a hydrodynamic swirl sector with characteristic speed $\|\mathbf{v}_{\circlearrowleft}\| \ll c$ and density ρ_f, and the usual electromagnetic (EM) sector with propagation speed c.[27–29] Atoms can radiate into both sectors, but standard cavities are only directly sensitive to the EM component. The observed signal is therefore an *echo* of a much stronger but mostly invisible primary burst in the swirl sector.

This subsection derives the coupled rate equations and the effective Swirl–EM transduction coefficient $\kappa_{\rm se}$ required to connect a fast (~ 0.1 ns) primary event to a slow (~ 30 ns) prethermalization signal in high-Q cavities.

1. Three-level rate model and coupled equations

We coarse-grain the dynamics into three populations:

1. Atomic excitations $N_e(t)$ (accelerated atoms).
2. Swirl excitations $n_S(t)$ (swirl wake or "swirlons").
3. Cavity photons $n_{\rm EM}(t)$.

The minimal rate model reads

$$\frac{dN_e}{dt} = -(\Gamma_S + \Gamma_{\rm EM})\, N_e, \tag{7a}$$

$$\frac{dn_S}{dt} = \Gamma_S N_e - \gamma_{\rm diss}\, n_S - \kappa_{\rm se}\, n_S, \tag{7b}$$

$$\frac{dn_{\rm EM}}{dt} = \Gamma_{\rm EM} N_e + \kappa_{\rm se}\, n_S - \gamma_{\rm cav}\, n_{\rm EM}. \tag{7c}$$

Here:

- Γ_S is the spontaneous emission rate into the swirl channel. Canonically we set $\Gamma_S \simeq \eta\,\Gamma_{\rm GR}$, with $\eta \approx 274$ obtained from the ratio of characteristic propagation speeds or densities in the two sectors.
- $\Gamma_{\rm EM}$ is the standard EM emission rate, of order $\Gamma_{\rm GR}$ for GR-based Unruh predictions.
- $\kappa_{\rm se}$ is the Swirl–EM transduction coefficient: a rate for conversion of swirl excitations into photons.
- $\gamma_{\rm diss}$ parameterizes non-radiative damping of swirlons in the cavity walls (conversion to heat).
- $\gamma_{\rm cav}$ is the cavity decay rate (photon leakage and detection).

On short timescales, $\Gamma_S \gg \Gamma_{\rm EM}$, so the atoms primarily dump their energy into the swirl sector:

$$N_e(t) \simeq N_0\, e^{-(\Gamma_S+\Gamma_{\rm EM})t}, \qquad t \ll \Gamma_{\rm EM}^{-1}, \tag{8}$$

with N_0 the initial excited population. For the echo problem we may approximate $N_e(t)$ as dropping sharply to zero and treat $n_S(t)$ as an initial condition problem.

2. Echo solution for a decaying swirl pump

Assume that after the primary burst the swirl population has amplitude $n_S(0) = N_S$ and decays exponentially:

$$n_S(t) = N_S\, e^{-\lambda t}, \qquad \lambda \equiv \gamma_{\rm diss} + \kappa_{\rm se}. \tag{9}$$

Neglecting the direct EM term $\Gamma_{\rm EM} N_e$ during the prethermalization regime, Eq. (7c) reduces to

$$\frac{dn_{\rm EM}}{dt} = \kappa_{\rm se} n_S(t) - \gamma_{\rm cav}\, n_{\rm EM}(t), \qquad n_{\rm EM}(0) = 0. \tag{10}$$

Substituting (9) and solving the linear ODE gives

$$\begin{aligned} n_{\rm EM}(t) &= \kappa_{\rm se} N_S \int_0^t e^{-\lambda\tau} e^{-\gamma_{\rm cav}(t-\tau)}\, d\tau \\ &= \frac{\kappa_{\rm se} N_S}{\gamma_{\rm cav} - \lambda} \left(e^{-\lambda t} - e^{-\gamma_{\rm cav} t}\right), \qquad \gamma_{\rm cav} \neq \lambda. \end{aligned} \tag{11}$$

This is the canonical *echo* profile:

- The rise time is controlled by the slower of λ^{-1} and $\gamma_{\rm cav}^{-1}$.

- The peak of $n_{\rm EM}(t)$ is *delayed* relative to the primary atomic acceleration event, even if the primary swirl burst is nearly instantaneous.

- The amplitude scales linearly with $\kappa_{\rm se}$ and with the initial swirl energy N_S.

An effective *transduction efficiency* is naturally defined as the fraction of the swirl energy that ends up in photons rather than heat:

$$\xi \equiv \frac{\text{rate into EM}}{\text{total swirl loss rate}} = \frac{\kappa_{\rm se}}{\gamma_{\rm diss} + \kappa_{\rm se}} = \frac{\kappa_{\rm se}}{\lambda}. \tag{12}$$

In the experimentally relevant regime where the cavity is a poor swirl–to–EM transducer ($\kappa_{\rm se} \ll \gamma_{\rm diss}$), one has $\xi \ll 1$ and almost all of the primary Unruh-like energy is lost as non-radiative heat in the boundaries. This transduction efficiency ξ connects the observed EM echo amplitude to the primary swirl burst energy, and links the prethermalization plateau observed in experiments [36] to the delayed conversion of swirl excitations into EM modes.

B. Dual-Burst Timeline

For a collectively coupled array with $N \gg 1$ and effective coupling μ, the superradiant delay time for a channel with decay rate $\gamma_{\rm ch}$ scales as [31, 32]

$$\tau_d^{(\rm ch)} \simeq \frac{\ln(\mu N)}{\gamma_{\rm ch}(\mu N + 1)}. \tag{13}$$

In the GR/QFT scenario, the relevant channel is EM-only:

$$\gamma_{\rm ch} = \gamma_0 + \tilde{\gamma}_{\rm em}(a) \quad \Rightarrow \quad \tau_d^{\rm GR} \sim 10^{-8}\text{–}10^{-7}\,\text{s} \tag{14}$$

for current experiments. SST adds a second, primarily swirl channel with rate $\tilde{\gamma}_{\rm swirl}(a)$ given by Eq. (4). If $\kappa_{\rm se} \approx 0$, this produces an *unseen* early burst in the swirl sector at

$$\tau_d^{\rm swirl} \sim \frac{\ln(\mu N)}{\tilde{\gamma}_{\rm swirl}(a)(\mu N + 1)} \ll \tau_d^{\rm GR}, \tag{15}$$

followed by the observed GR-type EM burst at $\tau_d^{\rm GR}$. Saha *et al.*'s "prethermalization" plateau [36] can be reinterpreted as partial thermalization of swirl excitations into EM modes before the main Dicke burst.

C. Current Experimental Constraint on $f_{\rm Unruh}$

Existing time-resolved Unruh superradiance experiments [31, 33–36] detect a single EM burst at $\tau_d^{\rm GR} \sim 10^{-8}\,\text{s}$ and see no additional feature at earlier times down to their time resolution $\tau_{\rm min,res} \sim$ ns. Within SST, this implies that any swirl-induced EM precursor must satisfy

$$\tau_d^{\rm swirl} \lesssim \tau_{\rm min,res}, \tag{16}$$

which, via Eq. (4), yields an upper bound

$$f_{\rm Unruh} \lesssim 10^{-4} \tag{17}$$

for the geometries and media used so far. Thus, current data constrain the efficiency of swirl-to-EM conversion in GR-designed cavities, but do not falsify the existence of a swirl sector. A decisive SST test requires hybrid platforms (e.g., BECs or superfluid cavities) with simultaneous sensitivity to density and EM modes [37, 38] and sub-nanosecond temporal resolution.

D. Hydrodynamic Origin of the Hydrogen Ground State (Operational Summary)

This section summarizes, in compressed form, the full derivation given in Ref. [14], "The Hydrodynamic Triad: Unifying Gravity, Electromagnetism, and Quantum Mass via a Circulation-Based Vacuum Canon."

In conventional quantum mechanics the discrete spectrum of the Hydrogen atom,

$$E_n = -\frac{13.6\ \text{eV}}{n^2}, \qquad n = 1, 2, 3, \ldots, \tag{18}$$

is regarded as a purely spectral property of the Coulomb Hamiltonian. Within Swirl–String Theory (SST), the same spectrum is reinterpreted as a hierarchy of *stationary incompressible flow regimes* sustained by the orbital swirl structure of the electron string around the protonic core.

Orbital swirl velocity as the principal quantum number

The Bohr orbital velocity,

$$v_n = \frac{\alpha c}{n}, \tag{19}$$

is taken to represent the coarse–grained swirl speed of the electron string along a circular streamline at radius

$$r_n = \frac{n^2 a_0}{1}, \tag{20}$$

with a_0 the Bohr radius. As n increases, the swirl becomes progressively weaker and more diffuse. In the limit $n \to \infty$, $v_n \to 0$ and the flow approaches the unbound (ionised) regime.

The principal quantum number labels discrete *laminar* flow patterns supported by the medium.

The electron-scale constraint

Independently, the SST electron-scale derivation relates the core radius r_c, the swirl speed $\|\mathbf{v}_\circlearrowleft\|$, and the swirl energy density ρ_E via

$$\rho_E = \frac{1}{2}\rho_f \|\mathbf{v}_\circlearrowleft\|^2. \tag{21}$$

Using the canonical swirl speed value established in the SST Canon,

$$\|\mathbf{v}_\circlearrowleft\| \approx 1.0938 \times 10^6\ \text{m/s} \approx \frac{1}{2}\alpha c, \tag{22}$$

we identify the internal vorticity scale as exactly half the vacuum Mach limit. This factor of $1/2$ is characteristic of the dipole topology of the vortex loop.

Ground-state stability from a hydrodynamic speed limit

Combining the orbital relation $v_n = \alpha c/n$ with the electron-scale constraint reveals a hydrodynamic interpretation of the Bohr ground state.

At $n = 1$, the orbital velocity reaches the vacuum limit:

$$v_1 = \alpha c = 2\|\mathbf{v}_\circlearrowleft\|. \tag{23}$$

This velocity $v_1 = \alpha c$ represents the *maximum laminar translation speed* permitted by the vacuum flow texture (the transverse Mach limit). Thus the $n = 1$ state sits at the boundary between admissible laminar flow and a regime in which the required flow speed would exceed the vacuum stability limit.

For any hypothetical "sub-Bohr" value $n < 1$, the orbital velocity would satisfy

$$v_n = \frac{\alpha c}{n} > \alpha c, \tag{24}$$

forcing the flow into a non-laminar (turbulent or singular) regime analogous to a sonic boom. In SST such a configuration cannot sustain a stationary swirl string, and therefore *no bound state exists for* $r < a_0$.

The ground state is not imposed by abstract quantisation but arises dynamically as the innermost stable laminar flow configuration permitted by the fluid properties of the vacuum.

E. Hydrodynamic Derivation of the Rydberg Constant (Summary)

In the SST framework, the ionization of the Hydrogen atom corresponds to the acceleration of the electron vortex string from its stable ground-state orbit ($n = 1$) to the unbound vacuum flow regime ($n \to \infty$).

The energy required for this transition—the Rydberg energy E_{Ry}—is identifiable not as an electrostatic potential difference, but as the *kinetic energy* of the electron vortex traveling at the vacuum stability limit.

Rydberg Energy as Vacuum Kinetic Limit

From the preceding section, the ground-state orbital velocity v_1 is defined by the transverse Mach limit of the vacuum:

$$v_1 = \alpha c. \tag{25}$$

The classical kinetic energy T_1 of the electron mass m_e moving at this limit is:

$$T_1 = \frac{1}{2} m_e v_1^2 = \frac{1}{2} m_e (\alpha c)^2. \tag{26}$$

In standard theory, the Rydberg energy is defined as hcR_∞. Equating the hydrodynamic kinetic energy to the spectral energy yields:

$$hcR_\infty = \frac{1}{2} m_e \alpha^2 c^2. \tag{27}$$

SST Substitution: The Swirl Velocity Relation

We now substitute the SST canonical relation between the fine structure constant and the intrinsic swirl velocity, $\alpha c = 2\mathbf{v}_\circlearrowleft$:

$$hcR_\infty = \frac{1}{2} m_e (2\mathbf{v}_\circlearrowleft)^2 = 2 m_e \mathbf{v}_\circlearrowleft^2. \tag{28}$$

Solving for the Rydberg constant R_∞:

$$R_\infty = \frac{2 m_e \mathbf{v}_\circlearrowleft^2}{hc}. \tag{29}$$

Physical Interpretation

Equation (29) provides a purely kinematic definition of the Rydberg constant. It states that the fundamental wavenumber of atomic spectroscopy is determined by the ratio of the *vortex swirl energy* ($m_e \mathbf{v}_{\circlearrowleft}^2$) to the *action-speed product* (hc).

Specifically, R_∞ represents the spatial frequency of a wave associated with a vortex loop accelerating to twice its intrinsic spin velocity. The factor of 2 arises from the geometry of the loop: the coherent translation of a dipole structure requires twice the energy of a monopole flow of equivalent velocity.

Thus, in SST, spectral lines are not transitions between abstract probability clouds, but are acoustic resonance shifts caused by the deceleration of the electron knot from its maximum laminar speed (αc) to lower harmonic velocities ($v_n = \alpha c/n$).

F. Hydrodynamic Derivation of the Compton Wavelength

The Compton wavelength λ_c defines the fundamental length scale of quantum interaction for a particle of mass m_e. In SST, this emerges from the helical geometry of the vortex string trajectory.

We interpret λ_c as the *longitudinal spatial period* (or pitch) of the vortex filament as it translates at the speed of light c, governed by the internal gearing ratio α.

The Geometric Pitch Relation

Standard electrodynamics establishes the relationship between the Classical Electron Radius (r_e), the Fine Structure Constant (α), and the Compton Wavelength (λ_c):

$$r_e = \alpha \frac{\lambda_c}{2\pi}. \tag{30}$$

In the SST Canon, the geometric Core Radius r_c is exactly half the classical radius ($r_e = 2r_c$), reflecting the dipole (loop) topology of the knot. Substituting $r_e = 2r_c$:

$$2r_c = \alpha \frac{\lambda_c}{2\pi} \quad \Longrightarrow \quad \lambda_c = \frac{4\pi r_c}{\alpha}. \tag{31}$$

This equation states that the Compton wavelength is the circumference of the vortex core ($2\pi r_c$) amplified by the inverse Mach number ($1/\alpha$) and a topological factor of 2.

SST Substitution: The Helical Pitch Formula

We now substitute the SST canonical definition of α derived from the swirl velocity ($\alpha = 2\mathbf{v}_{\circlearrowleft}/c$) into Eq. (31):

$$\lambda_c = \frac{4\pi r_c}{(2\mathbf{v}_{\circlearrowleft}/c)} = \frac{2\pi r_c c}{\mathbf{v}_{\circlearrowleft}}. \tag{32}$$

Numerical Verification

Using the canonical values:

- $r_c \approx 1.409 \times 10^{-15}$ m
- $c \approx 3.00 \times 10^8$ m/s
- $\mathbf{v}_{\circlearrowleft} \approx 1.094 \times 10^6$ m/s

$$\lambda_c \approx \frac{2\pi(1.409 \times 10^{-15})(2.998 \times 10^8)}{1.094 \times 10^6} \approx 2.426 \times 10^{-12}\,\text{m}. \tag{33}$$

This matches the CODATA value for the Compton wavelength of the electron (2.42631×10^{-12} m).

Physical Interpretation: The Vacuum Screw

Equation (32) reveals the mechanical nature of mass transport in the vacuum. The term $\frac{2\pi r_c}{v_\circlearrowleft}$ represents the *period of one internal rotation* of the vortex core. Multiplying by c gives the distance traveled during one rotation.

Thus, the electron behaves as a **Self-Propelling Screw**:

1. It spins internally at speed $\mathbf{v}_\circlearrowleft$.
2. It moves forward at speed c.
3. The "thread pitch" of this motion is exactly λ_c.

Mass, in this view, is the resistance to changing this pitch. A shorter wavelength (higher mass) implies a "tighter" screw thread that requires more energy to accelerate.

Corollary 24.1 (Swirl-Blindness Condition). In electromagnetic cavities where the impedance mismatch between the swirl medium and the physical boundaries is large, $Z_{\text{bound}} \gg Z_S = \rho_f \|\mathbf{v}_\circlearrowleft\|$, the primary swirl superradiance burst ($t \sim 0.1\,\text{ns}$) is almost completely non-radiatively dissipated in the walls. The observable electromagnetic signal is a secondary transduction echo with the following properties:

1. *Delay:* The peak of $n_{\text{EM}}(t)$ is controlled by the slower of the swirl decay rate λ^{-1} and the cavity ring-up time γ_{cav}^{-1}, rather than by the intrinsic timescale of the primary Unruh event.
2. *Amplitude:* The EM intensity is suppressed by the small transduction efficiency ξ in Eq. (12). In the impedance-dominated regime (see App. XVI), one finds $\xi \propto 4Z_S/Z_{\text{bound}} \sim 10^{-7}$ (research-track estimate), implying that $\mathcal{O}(10^{-7})$ of the primary swirl energy appears in the EM channel.

Experimental access to the primary burst therefore requires impedance-matched hydrodynamic detectors (e.g. superfluids or Bose–Einstein condensates), where Z_{det} can be tuned to approach Z_S. In such detectors SST predicts a prompt, high-contrast signal at the swirl timescale, in addition to the delayed EM echo.

The existence of swirl-blind cavities and $\kappa_{\text{se}} \approx 0$ (as stated in Eqs. (5) and the swirl-blind limit) is canonical. The numerical estimate $T \sim 10^{-7}$ for typical metal/glass boundaries is a research-track calculation detailed in App. XVI.

XIX. TOPOLOGICAL ORIGIN OF THE ELECTRON ANOMALOUS MAGNETIC MOMENT

A. Topological Expansion Hypothesis

In the Swirl–String Theory (SST) framework, the electron is modeled not as a point charge but as a closed toroidal swirl string with core radius r_c and circulation Γ, canonically identified with the trefoil knot 3_1 (Section XV, Knot Taxonomy). We propose that the perturbative expansion of the anomalous magnetic moment a_e in Quantum Electrodynamics (QED) is physically isomorphic to a topological expansion of the filament's vibrational eigenmodes.

The anomaly is written as

$$a_e = \sum_{n=1}^{\infty} C_n \left(\frac{\alpha}{\pi}\right)^n, \tag{1}$$

where α is the fine-structure constant, identified in SST with the intrinsic swirl gearing between $\|\mathbf{v}_\circlearrowleft\|$ and c (see the Hydrogen/Compton module).

B. First Order: The Rigid Torus

The first-order term ($n = 1$) corresponds to the Schwinger limit and describes the magnetic moment of a rigid, unperturbed vortex ring. In SST this is the dipole response of a stationary trefoil loop with fixed poloidal and toroidal circulation. The coefficient arises from the ratio of poloidal twist to toroidal circulation:

$$C_1^{\mathrm{SST}} = \frac{1}{2} \equiv C_1^{\mathrm{QED}}. \tag{2}$$

This recovers the standard Schwinger result for $g_e = 2(1 + a_e)$ at leading order.

C. Second Order: The Riemann–Trefoil Invariant

The second-order term ($n = 2$) arises from the self-interaction of the swirl core. In QED this is captured by the seven distinct fourth-order Feynman diagrams (vacuum polarization and self-energy). In SST, the same energy shift is interpreted as the fundamental elastic Kelvin-wave resonance of the filament.

The lowest-energy resonance for a closed loop with nonzero self-helicity is the 3_1 trefoil. Its geometric energy penalty, measured by the knot energy functional relative to the unknot, is proportional to the Riemann zeta value $\zeta(2)$. We encode this as an effective *Riemann–Trefoil invariant* and identify the SST second-order coefficient as the negative conformal weight of the trefoil geometry:

$$C_2^{\mathrm{SST}} = -\frac{\pi^2}{30} \approx -0.3289868. \tag{3}$$

D. Comparison with the Standard Model

Numerically, the SST geometric invariant approximates the QED coefficient

$$C_2^{\mathrm{QED}} \approx -0.3284789 \quad \text{(Standard Model)}, \tag{4}$$

$$C_2^{\mathrm{SST}} \approx -0.3289868 \quad \text{(Riemann–Trefoil invariant)}, \tag{5}$$

with a residual difference of

$$\Delta C_2 \equiv \frac{\left|C_2^{\mathrm{SST}} - C_2^{\mathrm{QED}}\right|}{\left|C_2^{\mathrm{QED}}\right|} \sim 1.5 \times 10^{-3} \approx 0.15\%. \tag{6}$$

Within SST this residual is interpreted as evidence that the electron core is not a mathematically perfect trefoil, but a finite-thickness fluid solenoid subject to small hydrodynamic slippage and higher-order Kelvin-wave mode mixing. Those corrections are, in principle, computable from the SST Hamiltonian density (Appendix I) and should appear as higher-order terms in the $(\alpha/\pi)^n$ expansion.

Research-track status. This module canonizes the *identification* of C_2 with a trefoil spectral invariant, but treats the exact numerical matching and higher-order $n \geq 3$ terms as research-track, to be constrained against full QED $g - 2$ data.

---

[1] W. P. Thurston, *The Geometry and Topology of Three-Manifolds*, Princeton Univ. Lecture Notes, 1979.

[2] W. D. Neumann and D. Zagier, Volumes of hyperbolic three-manifolds, *Topology* **24**(3):307–332, 1985. https://doi.org/10.1016/0040-9383(85)90003-4

[3] C. Adams, M. Hildebrand, and J. Weeks, Hyperbolic invariants of knots and links, *Trans. Amer. Math. Soc.* **326**(1):1–56, 1992.

[4] L. Lewin, *Polylogarithms and Associated Functions*, North-Holland, 1981.

[5] D. Bar-Natan et al., The Knot Atlas: entry 5_2, https://katlas.org/wiki/5_2.

[6] D. Bar-Natan et al., The Knot Atlas: entry 6_1, https://katlas.org/wiki/6_1.

[7] T. Annala *et al.*, "Topologically protected vortex knots and links," *Phys. Rev. Lett.*, 2025.

[8] D. Kleckner, L. Kauffman, W. Irvine, "How superfluid vortex knots untie," *Nat. Phys.* 12, 650–655 (2016).

[9] R. Ricca, "Applications of knot theory in fluid mechanics," *Banach Center Publications*, Vol. 42 (1996).

[10] D. Ibarra, D. Mathews, J. Purcell, "On geometric triangulations of double twist knots," arXiv:2504.09901 (2025).
[11] I. Petersen, A. Tsvietkova, "Geometric structures and $\mathrm{PSL}_2(\mathbb{C})$ representations of knot groups," *Trans. AMS* (2024).
[12] Iskandarani, O. (2025). *Swirl–String Theory Canon v0.5.8*. Internal manuscript (Canon).
[13] Iskandarani, O. (2025). *VAM–SST Rosetta v0.5*. Internal manuscript (Rosetta).
[14] O. Iskandarani, "The Hydrodynamic Triad: Unifying Gravity, Electromagnetism, and Quantum Mass via a Circulation-Based Vacuum Canon," Zenodo (2025), DOI: 10.5281/zenodo.17728292.
[15] Landau, L. D., & Lifshitz, E. M. (1987). *Fluid Mechanics* (2nd ed.). Pergamon. (Foundations of inviscid linearization and Bernoulli used in (**??**).)
[16] Morse, P. M., & Ingard, K. U. (1968). *Theoretical Acoustics*. Princeton University Press. (Standard monopole source (**??**) and far-field law (**??**)–(**??**).)
[17] Pierce, A. D. (1989/1991). *Acoustics: An Introduction to Its Physical Principles and Applications* (2nd ed.). ASA. (Alternative derivations for (**??**)–(**??**).)
[18] Westervelt, P. J. (1963). Parametric acoustic array. *J. Acoust. Soc. Am.*, 35(4), 535–537. (Constitutive parametric pumping basis compatible with BASC inside T.)
[19] Hamilton, M. F., & Blackstock, D. T. (1998). *Nonlinear Acoustics*. Academic Press. (Background on quadratic transduction and difference-frequency generation.)
[20] A. Einstein, Zur Elektrodynamik bewegter Körper, *Annalen der Physik* **322**(10) (1905) 891–921. doi:10.1002/andp.19053221004.
[21] H. Minkowski, Raum und Zeit, *Jahresbericht der Deutschen Mathematiker-Vereinigung* **18** (1909) 75–88.
[22] J.-M. Lévy-Leblond, One more derivation of the Lorentz transformation, *American Journal of Physics* **44**(3) (1976) 271–277. doi:10.1119/1.10324.
[23] G. K. Batchelor, *An Introduction to Fluid Dynamics* (Cambridge University Press, Cambridge, 1967). doi:10.1017/CBO9780511800955.
[24] P. G. Saffman, *Vortex Dynamics* (Cambridge University Press, 1992). doi:10.1017/CBO9780511624063
[25] L. Onsager. Statistical hydrodynamics. *Il Nuovo Cimento (Supplemento)*, 6:279–287, 1949. doi:10.1007/BF02780991.
[26] R. P. Feynman. Application of Quantum Mechanics to Liquid Helium. In C. J. Gorter, editor, *Progress in Low Temperature Physics, Vol. I*, pages 17–53. North-Holland, 1955. doi:10.1016/S0079-6417(08)60077-3.
[27] W. G. Unruh, "Notes on black-hole evaporation," *Phys. Rev. D* **14**, 870–892 (1976). doi:10.1103/PhysRevD.14.870
[28] L. C. B. Crispino, A. Higuchi, and G. E. A. Matsas, "The Unruh effect and its applications," *Rev. Mod. Phys.* **80**, 787–838 (2008). doi:10.1103/RevModPhys.80.787
[29] C. Barceló, S. Liberati, and M. Visser, "Analogue gravity," *Living Rev. Relativ.* **14**, 3 (2011). doi:10.12942/lrr-2011-3
[30] L. E. Kinsler, A. R. Frey, A. B. Coppens, and J. V. Sanders, *Fundamentals of Acoustics*, 4th ed., Wiley, New York (2000).
[31] A. Deswal, N. Arya, K. Lochan, and S. K. Goyal, "Time-Resolved and Superradiantly Amplified Unruh Effect," *Phys. Rev. Lett.* (2025), arXiv:2501.16219.
[32] M. Gross and S. Haroche, "Superradiance: An essay on the theory of collective spontaneous emission," *Phys. Rep.* **93**, 301–396 (1982). doi:10.1016/0370-1573(82)90102-8
[33] K. Lochan, S. Chakraborty, and T. Padmanabhan, "Detecting Acceleration-Enhanced Vacuum Fluctuations," *Phys. Rev. Lett.* **125**, 241301 (2020). doi:10.1103/PhysRevLett.125.241301
[34] H. Wang and M. P. Blencowe, "Coherently Amplifying Photon Production from Vacuum," *Commun. Phys.* **4**, 62 (2021). doi:10.1038/s42005-021-00576-9
[35] H. T. Zheng, Y. Zhou, Q. Guo, and L. Zhou, "Enhancing Analog Unruh Effect via Superradiance," *Phys. Rev. Research* **7**, 013027 (2025). doi:10.1103/PhysRevResearch.7.013027
[36] S. Saha, T. Galley, and E. Martín-Martínez, "Emergence of Unruh Prethermalization in Many-Body Systems," (2025), arXiv:2509.05816.
[37] J. Steinhauer, "Observation of quantum Hawking radiation and its entanglement in an analogue black hole," *Nat. Phys.* **12**, 959–965 (2016). doi:10.1038/nphys3863
[38] C. Gooding, S. Weinfurtner, and W. G. Unruh, "Superradiant scattering from a hydrodynamic vortex," *Phys. Rev. D* **101**, 024050 (2020). doi:10.1103/PhysRevD.101.024050
[39] M. P. do Carmo, *Differential Geometry of Curves and Surfaces*, revised and updated second edition, Dover Publications, Mineola, NY (2016).
[40] J. G. Ratcliffe, *Foundations of Hyperbolic Manifolds*, 2nd ed., Graduate Texts in Mathematics, Vol. 149, Springer, New York (2006). doi:10.1007/978-0-387-47322-5
[41] W. P. Thurston, *Three-Dimensional Geometry and Topology, Vol. 1*, Princeton Mathematical Series 35, Princeton University Press, Princeton, NJ (1997).
[42] D. Sornette, "Discrete scale invariance and complex dimensions," *Physics Reports* **297**, 239–270 (1998). doi:10.1016/S0370-1573(97)00076-8.
[43] S. Gluzman and D. Sornette, "Log-periodic route to fractal functions," *Physical Review E* **65**, 036142 (2002). doi:10.1103/PhysRevE.65.036142.
[44] M. Baake and U. Grimm, *Aperiodic Order. Volume 1: A Mathematical Invitation*, Encyclopedia of Mathematics and its Applications, Vol. 149 (Cambridge University Press, Cambridge, 2013). doi:10.1017/CBO9781139025256.
[45] H. K. Moffatt, "The degree of knottedness of tangled vortex lines," *Journal of Fluid Mechanics* **35**(1), 117–129 (1969). doi:10.1017/S0022112069000991.
[46] Y. Wang, M. Bennani, J. Martens, S. Racanière, S. Blackwell, A. Matthews, S. Nikolov, G. Cao-Labora, D. S. Park, M. Arjovsky, D. Worrall, C. Qin, F. Alet, B. Kozlovskii, N. Tomašev, A. Davies, P. Kohli, T. Buckmaster, B. Georgiev,

J. Gómez-Serrano, R. Jiang, and C.-Y. Lai, "Discovery of Unstable Singularities," arXiv:2509.14185 [math.AP] (2025). doi:10.48550/arXiv.2509.14185.
[47] P. B. Allen and J. L. Feldman, "Thermal conductivity of disordered harmonic solids," *Physical Review B* **48** (1993), 12581.
[48] Buchert, Thomas, "On average properties of inhomogeneous fluids in general relativity: Dust cosmologies," *Gen. Relativ. Gravit.* **32** (2000), 105–125. doi: 10.1023/A:1001800617177
[49] Buchert, Thomas, "On average properties of inhomogeneous cosmologies," *Gen. Relativ. Gravit.* **33** (2001), 1381–1405. doi: 10.1023/A:1012061725841
[50] Englert, B.-G., "Fringe Visibility and Which-Way Information: An Inequality," *Phys. Rev. Lett.* **77** (1996), 2154–2157. doi: 10.1103/PhysRevLett.77.2154
[51] Pieter Goldau, "The Simplicity Codex" (2025). Sixteen-stage parameter-free ontology, cited as STC doi: 10.5281/zenodo.17068210
[52] R. J. Hardy, "Energy-Flux Operator for a Lattice," *Physical Review* **132** (1963), 168.
[53] Iskandarani, Omar, "Swirl-String Theory (SST) Canon v0.3.4: Core Postulates, Constants, and Boxed Master Equations" (Zenodo, 2025). Single source of truth for SST symbols, constants, and canonical equations; required citation for dependent works. doi: 10.5281/zenodo.17014358
[54] Iskandarani, Omar, "Long-Distance Swirl Gravity from Chiral Swirling Knots with Central Holes" (Zenodo, 2025). doi: 10.5281/zenodo.17155855
[55] Iskandarani, Omar, "Swirl-String Theory (SST) Lagrangian: Emergent Relativistic EFT with Preferred Foliation" (Zenodo, 2025). doi: 10.5281/zenodo.16956665
[56] John David Jackson, *Classical Electrodynamics* (3rd ed., Wiley, 1999).
[57] W. Thomson (Lord Kelvin), "On vortex motion," *Transactions of the Royal Society of Edinburgh* **25** (1869), 217–260.
[58] Khatiwada, P. and Qian, X.-F., "Wave-particle duality ellipse and application in quantum imaging with undetected photons," *Phys. Rev. Research* **7** (2025), 033033. doi: 10.1103/PhysRevResearch.7.033033
[59] Particle Data Group, "Review of Particle Physics" (2024).
[60] R. Peierls, "Zur Theorie der spezifischen Wärme," *Annalen der Physik* **395** (1929), 1055.
[61] Michael E. Peskin and Daniel V. Schroeder, *An Introduction to Quantum Field Theory* (Westview Press, 1995).
[62] M. Simoncelli et al., "Unified theory of thermal transport in crystals and disordered solids," *Nature Physics* **18** (2022), 1180.
[63] Weinberg, Steven, "A Model of Leptons," *Physical Review Letters* **19** (1967), 1264–1266. doi: 10.1103/PhysRevLett.19.1264
[64] Zurek, W. H., "Decoherence, einselection, and the quantum origins of the classical," *Rev. Mod. Phys.* **75** (2003), 715–775. doi: 10.1103/RevModPhys.75.715
[65] G. W. Gibbons, "The Maximum Tension Principle in General Relativity," *Foundations of Physics* **32**, 1891–1901 (2002). doi:10.1023/A:1022370717626.
[66] M. Planck, "Über irreversible Strahlungsvorgänge," *Annalen der Physik* **306**, 69–122 (1900). doi:10.1002/andp.19003060105.
[67] D. J. Griffiths, *Introduction to Quantum Mechanics*, Prentice–Hall, 1995, Sec. 10.3 (classical electron radius).
[68] P. Hořava, "Quantum Gravity at a Lifshitz Point," *Phys. Rev. D* **79**, 084008 (2009), doi:10.1103/PhysRevD.79.084008.
[69] T. P. Sotiriou, M. Visser and S. Weinfurtner, "Quantum Gravity without Lorentz Invariance," *JHEP* **10**, 033 (2009), doi:10.1088/1126-6708/2009/10/033.
[70] J. C. Maxwell, "A Dynamical Theory of the Electromagnetic Field," *Philosophical Transactions of the Royal Society of London* **155**, 459–512 (1865). doi:10.1098/rstl.1865.0008.
[71] H. von Helmholtz, "On Integrals of the Hydrodynamical Equations, Which Express Vortex-Motion," *The London, Edinburgh, and Dublin Philosophical Magazine and Journal of Science* **33**, 485–512 (1867) [English translation of the 1858 German original]. doi:10.1080/14786446708639824.
[72] W. Thomson (Lord Kelvin), "On Vortex Atoms," *The London, Edinburgh, and Dublin Philosophical Magazine and Journal of Science* **34**, 15–24 (1867). doi:10.1080/14786446708639836.
[73] L. D. Landau and E. M. Lifshitz, *Fluid Mechanics*, 2nd ed., Course of Theoretical Physics, Vol. 6 (Pergamon Press, Oxford, 1987).
[74] R. L. Ricca, "Structural Complexity and Dynamical Systems," in *Topological Fluid Mechanics*, edited volume chapter (Springer, Berlin, 2009), doi:10.1007/978-3-642-00837-5_6.
[75] A. Einstein, "Die Grundlage der allgemeinen Relativitätstheorie," *Annalen der Physik* **354**, 769–822 (1916). doi:10.1002/andp.19163540702.
[76] A. Einstein, B. Podolsky, and N. Rosen, "Can Quantum-Mechanical Description of Physical Reality Be Considered Complete?" *Physical Review* **47**, 777–780 (1935). doi:10.1103/PhysRev.47.777.
[77] A. Aspect, P. Grangier, and G. Roger, "Experimental Realization of Einstein-Podolsky-Rosen-Bohm Gedankenexperiment: A New Violation of Bell's Inequalities," *Physical Review Letters* **49**, 91–94 (1982). doi:10.1103/PhysRevLett.49.91.
[78] J. C. Maxwell, *A Treatise on Electricity and Magnetism*, Clarendon Press, Oxford (1875).
[79] W. G. Unruh, "Experimental black-hole evaporation?," Phys. Rev. Lett. **46**, 1351–1353 (1981).
[80] G. E. Volovik, *The Universe in a Helium Droplet*, Oxford Univ. Press (2003).
[81] O. Iskandarani, "Electromagnetism as Propagating Torsion in a Hydrodynamic Vacuum: A Geometric Unification via Cartan Structure Equations," (2025), DOI: 10.5281/zenodo.17677074.
[82] O. Iskandarani, "Hydrodynamic Origin of the Hydrogen Ground State in Swirl–String Theory," preprint (2025).